



**Titre:** Polymer blends as a route for controlled drug release  
Title:

**Auteur:** Pouneh Salehi  
Author:

**Date:** 2007

**Type:** Mémoire ou thèse / Dissertation or Thesis

**Référence:** Salehi, P. (2007). Polymer blends as a route for controlled drug release [Mémoire de maîtrise, École Polytechnique de Montréal]. PolyPublie.  
Citation: <https://publications.polymtl.ca/8108/>

 **Document en libre accès dans PolyPublie**  
Open Access document in PolyPublie

**URL de PolyPublie:** <https://publications.polymtl.ca/8108/>  
PolyPublie URL:

**Directeurs de  
recherche:**  
Advisors:

**Programme:** Non spécifié  
Program:

**UNIVERSITÉ DE MONTRÉAL**

**POLYMER BLENDS AS A ROUTE FOR  
CONTROLLED DRUG RELEASE**

**POUNEH SALEHI  
DÉPARTEMENT DE GÉNIE CHIMIQUE  
ÉCOLE POLYTECHNIQUE DE MONTRÉAL**

**MÉMOIRE PRÉSENTÉ EN VUE DE L'OBTENTION  
DE DIPLÔME DE MAÎTRISE ÈS SCIENCES APPLIQUÉES  
(GÉNIE CHIMIQUE)  
SEPTEMBRE 2007**



Library and  
Archives Canada

Bibliothèque et  
Archives Canada

Published Heritage  
Branch

Direction du  
Patrimoine de l'édition

395 Wellington Street  
Ottawa ON K1A 0N4  
Canada

395, rue Wellington  
Ottawa ON K1A 0N4  
Canada

*Your file    Votre référence*

*ISBN: 978-0-494-36938-8*

*Our file    Notre référence*

*ISBN: 978-0-494-36938-8*

#### NOTICE:

The author has granted a non-exclusive license allowing Library and Archives Canada to reproduce, publish, archive, preserve, conserve, communicate to the public by telecommunication or on the Internet, loan, distribute and sell theses worldwide, for commercial or non-commercial purposes, in microform, paper, electronic and/or any other formats.

The author retains copyright ownership and moral rights in this thesis. Neither the thesis nor substantial extracts from it may be printed or otherwise reproduced without the author's permission.

#### AVIS:

L'auteur a accordé une licence non exclusive permettant à la Bibliothèque et Archives Canada de reproduire, publier, archiver, sauvegarder, conserver, transmettre au public par télécommunication ou par l'Internet, prêter, distribuer et vendre des thèses partout dans le monde, à des fins commerciales ou autres, sur support microforme, papier, électronique et/ou autres formats.

L'auteur conserve la propriété du droit d'auteur et des droits moraux qui protègent cette thèse. Ni la thèse ni des extraits substantiels de celle-ci ne doivent être imprimés ou autrement reproduits sans son autorisation.

---

In compliance with the Canadian Privacy Act some supporting forms may have been removed from this thesis.

Conformément à la loi canadienne sur la protection de la vie privée, quelques formulaires secondaires ont été enlevés de cette thèse.

While these forms may be included in the document page count, their removal does not represent any loss of content from the thesis.

Bien que ces formulaires aient inclus dans la pagination, il n'y aura aucun contenu manquant.

  
**Canada**

**UNIVERSITÉ DE MONTRÉAL**

**ÉCOLE POLYTECHNIQUE DE MONTRÉAL**

Ce mémoire intitulé :

**POLYMER BLENDS AS A ROUTE FOR  
CONTROLLED DRUG RELEASE**

présenté par : SALEHI Pounch

en vue de l'obtention du diplôme de : Maîtrise ès sciences appliquées

a été dûment accepté par le jury d'examen constitué de :

M. DE CRESCENZO Gregory, Ph.D., président

M. FAVIS Basil, Ph.D., membre et directeur de recherche

M. BUREAU Martin, Ph.D., membre



## ACKNOWLEDGMENTS

In the first place I would like to express my gratitude to Dr. Basil Favis for his supervision, advice, and guidance from the very early stages of this research as well as giving me extraordinary experiences throughout the work. Above all and the most needed, he provided me with encouragement and support in various ways. I also gratefully thank Dr. Favis for devoting his precious time to read this thesis and his critical comments about it.

I gratefully acknowledge Pierre Sarazin for his advice, and crucial contribution and discussion. I am thankful for his constructive comments on my research work and time he devoted to my work.

Many thanks go to Nick Virgilio for his valuable advice in scientific discussions. I have benefited by advice and guidance from Nick. He always kindly granted me his time for training on experimental equipment and for answering my questions. Thanks also to Sepehr Ravati for the Elipsometry data.

I gratefully thank Dr. Mario Jolicoeur for helpful discussions and would like to thank Dr. Michael D. Buschmann for letting me use their equipment.

My special thanks go to Lucie Jean for her precious scientific discussions and her indispensable help on UV/Vis spectrophotometry. Without her help this research would have been much more difficult to carry out.

I also benefited from the outstanding work of the technicians of the chemical engineering department, principally Jacques Beausoleil, Carol Painchaud and Gino Robin who helped and advised me in handling my specific equipments.

I gratefully thank Christophe Mobushon and Pierre Sarazin for helping with the French translation of “RÉSUMÉ” and “CONDENSÉ EN FRANÇAIS”.

I also acknowledge all the personnel of Ecole Polytechnique de Montreal who helped me during these two years of work; professors, technicians, the research assistants, secretaries, and all my friends at Ecole.

My parents deserve special mention for their inseparable support and prayers. They provided the fundamentals of my learning and showed me the joy of intellectual pursuit ever since I was a child. Mom, Dad, Nickoo, thanks for being supportive and caring.

Words fail me to express my appreciation to my husband Hesam whose dedication, love and persistent confidence in me, has taken the load off my shoulder.

Finally, I would like to thank everybody who was important to the successful realization of thesis, as well as expressing my apology that I could not mention every one personally one by one.

## ABSTRACT

Controlled drug delivery is a growing multidisciplinary field of research that aims at developing methods to control the rate of the drug release into the body. For many years conventional drug formulations were used which involved a fast release of the active agent. With the development of more potent drugs, however, it became obvious that conventional therapeutic systems suffer from many drawbacks, including adverse side effects, fluctuation of drug levels in the body, poor drug efficacy, and poor patient compliance. The concentration, duration, and bioavailability of the pharmaceutical agents can not be controlled. Controlled release technology was anticipated to circumvent these problems. The goal of this technology is to maintain a therapeutic concentration of a drug in the body for a sustained period of time by releasing the agent in a predictable and controllable fashion. The term "*Controlled drug delivery*" covers a very wide range of techniques used to get therapeutic agents into the human body in a controlled manner. These techniques are capable of controlling the rate of drug delivery, sustaining the duration of therapeutic activity, and/or targeting the delivery of a drug to a specific tissue.

Polymers have been widely used to encapsulate drugs in the form of a reservoir or matrix in controlled release formulations. The active ingredient is either physically entrapped into the polymer matrix by an emulsification-, atomization-, or agitation-based process or it is linked to the polymer backbone via physical or chemical bonds. The drug release is typically observed to be diffusion controlled, polymer erosion controlled, or a combination of the two.

The objective of this project was to develop a novel polymer substrate satisfying the criteria of controlled release. We developed a new substrate preparation and drug encapsulation techniques, which have the potential to be applied in controlled drug delivery systems. We also studied surface modifications on polymer substrates, including internal surface modification using LBL technique and surface modification using a

closed – cell method which extends the application possibilities for our porous substrate. Three different substrates with pores of different sizes were utilized to examine how pore size may affect the drug release profile.

The method used in this study to fabricate a co-continuous porous scaffold was performed by the melt blending of two immiscible polymers. The polymer substrate for drug release experiments was made by melt-blending of 3 different model blends; HDPE/SEB, HDPE/SEBS, and PLA/PS, followed by extraction of the porogen phase (SEB, SEBS, and PS). Polymer substrates with porosities above 94% were obtained.

The prepared sample was examined using SEM, BET, MIP and IA for internal surface area, average pore diameter, and microstructure. We obtained porous HDPE from HDPE/SEB with an average pore diameter of 0.32  $\mu\text{m}$  and internal surface area of 13.72  $\text{m}^2/\text{g}$ , porous HDPE from HDPE/SEBS blend with an averaged pore diameter of 0.63  $\mu\text{m}$  and internal surface area of 8.2  $\text{m}^2/\text{g}$ , and porous PLA from PLA/PS blend with an average pore size of 1.56  $\mu\text{m}$  and internal surface area of 2.15  $\text{m}^2/\text{g}$ . BSA, a model drug, was loaded into these substrates following a vacuum-pressure protocol. Loading percentages with water of approximately 80% for HDPE substrates and 96% for PLA were obtained. BSA release tests were performed for all the samples using UV/Vis spectrophotometry. Two methods modification were used to improve the BSA release profile. First, samples were treated with 3 and 7 layers and in some cases 4 and 8 layers of polyelectrolytes to enhance their internal polymer surface properties, and consequently to increase the adhesion of the BSA molecules to the charged polymer surface. Second, closed-cell modification was applied to PLA (biodegradable sample) to form a drug holding layer, allowing more control over the release rate.

The structures prepared using our method, have the advantage of not being limited to one type of polymer system. Using this method, high void volume and high internal surface

area are attainable. This method also allows a high level of control over the pore size (pore size ranging from microns to tenths of millimeters) and pore size distribution.

## RÉSUMÉ

La libération contrôlée de médicament est un vaste domaine de recherche qui vise à développer des systèmes permettant d'optimiser le taux de libération de médicament dans le corps. Les formulations conventionnelles de médicament ont été utilisées pendant plusieurs années. Traditionnellement, les méthodes utilisées favorisent la libération rapide de l'agent actif. Avec le développement de médicaments plus spécifiques, cependant, il est devenu évident que les systèmes thérapeutiques conventionnels souffrent de nombreux inconvénients, conduisant parfois à des effets nuisibles : la concentration du médicament fluctue fortement dans le plasma sanguin, l'efficacité du médicament est réduite, et la prise du médicament ne convient pas toujours au patient. La concentration, la durée, et la disponibilité biologique des agents pharmaceutiques ne peuvent pas être contrôlées. La technologie de libération contrôlée a été introduire pour éviter ces problèmes. L'objectif est maintenir une concentration thérapeutique d'un agent actif dans le plasma pendant une période soutenue en libérant l'agent d'une façon prévisible et contrôlable. Le terme « *libération contrôlée de médicament* » couvre une gamme très large de techniques utilisées pour contrôler le taux de libération de médicament, de maintenir la durée de l'activité thérapeutique, et/ou de libérer l'agent actif directement à un tissu spécifique.

Les polymères sont largement utilisés pour encapsuler des médicaments à l'intérieur de réservoir ou incorporés au polymère. L'agent actif peut être ainsi enfermé physiquement dans la matrice de polymère par un procédé d'émulsification, d'atomisation, ou par un procédé basé sur d'agitation, ou bien lié au polymère par des liaisons physiques ou chimiques. Typiquement la libération du médicament peut être contrôlée par la diffusion, l'érosion du polymère ou une combinaison des deux.

L'objectif de ce projet était de développer un nouveau polymère répondant aux critères d'une libération contrôlée. Nous proposons une nouvelle technique de fabrication de support poreux et d'encapsulation de médicament, qui pourrait être appliquée comme système de libération contrôlée. Nous avons également étudié deux types de modifications de la structure poreuse : une modification interne en tapissant la surface des pores de polyélectrolytes par la technique de couche par couche (LbL) et une modification externe qui consiste à fermer les pores à la surface de la structure poreuse. Dans cette étude, trois substrats ayant des tailles de pores de tailles différentes ont été utilisés pour examiner l'influence de la taille de pore sur le profil de libération d'une protéine.

Notre projet implique la préparation contrôlée de mélanges de polymères immiscibles co-continus, utilisant les technologies classiques de mise en oeuvre des polymères à l'état fondu, suivie d'une étape d'extraction en masse de l'une des phases. Cette approche est assez flexible, étant donné que la majorité des mélanges de polymères sont immiscibles et possèdent tous une région de co-continuité. Les structures poreuses pour les essais de diffusion de la protéine ont été obtenus à partir de trois mélanges: HDPE/SEB, HDPE/SEBS, PLA/PS.

Après extraction de la phase porogène (SEB, SEBS et PS), les structures poreuses ont été examinées par SEM, PARI, MIP et IA pour évaluer l'aire de surface interne, le diamètre moyen des pores et la microstructure. Nous avons obtenu une structure poreuse de HDPE poreux à partir du mélange HDPE/SEB, avec un diamètre moyen de pore de  $0.32\ \mu\text{m}$  et une surface interne de  $13.72\ \text{m}^2/\text{g}$ . Pour le HDPE poreux provenant du mélange HDPE/SEBS, le diamètre moyen était de  $0.63\ \mu\text{m}$  et la surface de  $8.2\ \text{m}^2/\text{g}$ . Le PLA poreux obtenu à partir du mélange de PLA/PS était caractérisé par un diamètre moyen de pore de  $1.56\ \mu\text{m}$  et une surface interne de  $2.15\ \text{m}^2/\text{g}$ . Une protéine modèle, l'albumine de sérum bovin (BSA) a été chargée dans ces substrats hydrophobes en appliquant alternativement pression et vide. Le pourcentage de chargement en eau était d'environ

80% pour les substrats de HDPE et de 96% pour celui de PLA. Des essais de libération de BSA ont été réalisés pour tous les échantillons. Pour améliorer le profil de libération de BSA, deux modifications ont été employées. D'abord, des échantillons ont été traités avec 3 et 7 couches et dans quelques cas avec 4 et 8 couches de polyélectrolytes afin d'augmenter les propriétés internes de surface du polymère et par conséquent, d'augmenter l'adhésion des molécules de BSA à la surface chargée. Ensuite, la création d'une peau fermant la porosité à la surface de la structure de PLA (échantillon biodégradable) a permis d'obtenir plus de contrôle sur la libération de la BSA.

Les structures préparées en utilisant notre méthode ont l'avantage de ne pas limiter à un type de système de polymère. En employant cette méthode, un volume élevé de porosité et une aire de surface interne élevée sont atteignables. De plus, cette méthode permet un bon contrôle de la taille des pores, s'étendant du micron au millimètre, et de la distribution de pore.



## CONDENSÉ EN FRANÇAIS

Pendant plusieurs décennies, les médicaments destinés au traitement d'une maladie aiguë ou d'une maladie chronique se sont limités à des composés chimiques simples à action rapide, et distribués oralement sous forme de capsule, de pilules, d'onguents, de liquides ou d'injections. Même aujourd'hui ces formulations médicales conventionnelles représentent les modes principaux d'administration des médicaments prescrits et excèdent les nouvelles formulations médicales. Les formulations médicales conventionnelles fournissent typiquement un dégagement rapide de médicaments. Pour les médicaments qui sont éliminés rapidement, atteindre et maintenir la concentration en médicament à la concentration thérapeutique utile exige une administration complexe, le plus souvent à répéter plusieurs fois par jour. Cette administration si inconfortable présente des inconvénients pour le patient et est à l'origine d'une fluctuation significative du niveau de médicament dans le plasma (2.1).

Récemment, plusieurs avancées techniques ont eu permis de développer de nouvelles technologies, capables de contrôler l'administration d'un médicament à un emplacement ciblé dans le corps avec un profil optimal de concentration dans le temps. On entend par système de libération contrôlée de médicaments une gamme très large de techniques employées pour libérer les agents thérapeutiques dans le corps humain. Ces techniques visent à contrôler le taux de la libération du médicament, de soutenir la durée de l'activité thérapeutique, et/ou de cibler la libération du médicament à un tissu donné.

Les formulations de médicaments à libération contrôlée offrent plusieurs avantages par rapport aux formes galéniques conventionnelles :

- 1- le médicament est libéré d'une façon contrôlée qui est la plus appropriée à l'application. Le contrôle peut viser le moment de libération (retardé au lieu d'être immédiat), sa durée de libération, et son profil de libération lui-même.
- 2- la fréquence des doses peut-être réduite, améliorant la condition du patient.
- 3- le médicament peut être libéré localement. Ceci est rendu possible en travaillant sur la formulation afin de libérer le médicament dans l'environnement spécifique de la région choisie ou en synchronisant sa libération.
- 4- sa libération à l'emplacement désiré permet également de réduire l'exposition systémique du médicament et ainsi de réduire les effets secondaires (particulièrement pour les médicaments toxiques).
- 5- le médicament peut-être protégé contre l'environnement physiologique plus longtemps, son efficacité peut ainsi être prolongée.

Les systèmes de livraison de médicaments ont été classés selon leur voie d'administration : parentérale, respiratoire, percutanée, etc. En outre, ils peuvent être groupés sur la base du mécanisme de libération du médicament. Les mécanismes les plus communs sont contrôlés par diffusion, contrôlés par dissolution, et contrôlés par dégradation/érosion des systèmes contrôlés. Deux types de systèmes commandés par la diffusion ont été employés comprenant des systèmes de réservoir (médicament enrobé par une membrane de polymère) et des systèmes de matrice (médicament dispersé dans une matrice de polymère). Dans les systèmes de réservoir, le médicament est encapsulé par une membrane polymère par laquelle le médicament est libéré par diffusion. Dans les systèmes monolithiques, le médicament est dissout ou dispersé uniformément dans toute la matrice insoluble dans l'eau du polymère qui peut être microporeuse ou non poreuse. Les systèmes monolithiques ne sont pas appropriés à la libération d'ordre zéro; cependant, ils peuvent être réalisés en ajustant la forme du dispositif ou par certaines modifications du système. Les systèmes par dissolution commandée peuvent également être classés comme des dispositifs de réservoir et de matrice. Pour les dispositifs de réservoir, les particules de médicaments sont enduites de membranes polymériques

hydrosolubles. La cinétique de solubilité d'une membrane dépend de son épaisseur et du type de polymère utilisé. Ainsi, la libération des médicaments peut être contrôlée en préparant des dispositifs avec des couches alternatives de médicaments et de polymères ou en préparant un mélange de particules enduites différemment. Les dispositifs de dissolution de matrice sont généralement préparés en comprimant le mélange de poudres de médicaments et d'un polymère hydrosoluble ou gonflant dans l'eau. L'utilisation de médicaments ayant une solubilité plus élevée mène à une légère accélération de leur libération en raison de la contribution de leur diffusion au processus de libération (provoqué par des canaux formés en raison de la solubilisation des médicaments). Dans les systèmes basés sur la dégradation par érosion, la dégradation du polymère élimine le besoin d'une chirurgie pour le récupérer après que le médicament ait été libéré. Elle réduit également les problèmes liés à l'innocuité à long terme du polymère. La dégradation peut être enzymatique (facilitée par des enzymes spécifiques dans le corps), hydrolytique, ou une combinaison des deux. Le médicament peut être physiquement encapsulé dans la matrice de polymère et être libéré par diffusion et/ou érosion de la matrice. Alternativement, le médicament peut être également lié chimiquement à la chaîne de polymère. Dans une telle situation, le médicament est libéré par la rupture hydrolytique enzymatique de la liaison chimique entre le polymère et le médicament.

Les polymères ont été employés couramment pour encapsuler des médicaments sous forme de réservoir ou de matrice afin de libérer ces derniers à proximité de l'emplacement désiré. Les questions de biocompatibilité, de toxicité, et d'élimination de ces polymères doivent être clairement abordées. L'agent actif peut être physiquement enfermé dans la matrice de polymère par une émulsification, par un processus d'agitation ou bien être lié à la chaîne de polymère par l'intermédiaire de liaisons physiques ou chimiques. On observe typiquement que la libération de médicaments est contrôlée par érosion du polymère, par diffusion, ou par une combinaison des deux. Par conséquent, les propriétés de libération des médicaments dépendent fortement des propriétés physiques et chimiques du polymère. Même une variation mineure de la structure du polymère, telle

qu'une modification de ses groupes situés aux extrémités de la chaîne, peut être suffisante pour modifier ses caractéristiques de dégradation et donc ses propriétés de libération de médicaments. En outre, différentes propriétés du polymère sont désirées selon les médicaments et les applications. Ceci a conduit à de nombreuses recherches dans le développement de nouveaux systèmes polymériques pour la libération contrôlée de médicaments.

L'objectif de ce projet est de mettre en œuvre de nouvelles techniques de préparation de structures poreuses polymères et d'encapsulation de médicaments qui pourraient potentiellement être appliquées aux systèmes contrôlés de livraison de médicaments. En outre, nous avons étudié ces substrats de polymères associés à la technique de déposition couche-par-couche (LbL) et en présence d'une peau de polymère à la surface externe de la structure poreuse. Trois substrats avec des tailles de pores différentes ont été utilisés pour nous fournir des données sur la façon dont la taille des pores peut affecter le profil de libération des médicaments.

L'encapsulation de l'agent thérapeutique dans une matrice de polymère peut être mise en œuvre par plusieurs méthodes. Ces méthodes dépendent de la fabrication désirée de la matrice de polymère. Certaines des techniques communes utilisées pour l'encapsulation de médicaments dans le polymère sont le séchage par atomisation, l'évaporation dissolvante, l'atomisation de jet de gel, la coacervation, l'enduit à lit fluidisé et la polymérisation dièdre. Dans cette étude, la structure poreuse est obtenue à partir de la structure co-continue dans les mélanges immiscibles de polymères. Les mélanges binaires ont été produits à l'état fondu en mélangeant HDPE/SEB, HDPE/SEBS, et PLA/PS à la composition 50/50 (% v/v). Ensuite, le SEB, SEBS, ou le PS ont été extraits par un solvant approprié. À 50/50 (% v/v) les phases des mélanges ci-dessus forment une structure co-continue : chaque phase est entièrement continue à travers le mélange. L'extraction de l'une de ces phases mène à une structure poreuse ouverte et continue à travers tout l'échantillon. Précédemment notre groupe de recherche a montré que la taille

des pores est aisément contrôlable de 0.2  $\mu\text{m}$  à plus de 300  $\mu\text{m}$ . Une petite taille de pore peut être atteinte en ajoutant des compatibilisants au mélange. Inversement, une grande taille de pore peut être obtenue par une étape de recuit. Dans cette étude nous avons travaillé avec une matrice de HDPE présentant une porosité de 0.32  $\mu\text{m}$  (extraction du SEB à partir du mélange HDPE/SEB,) une matrice de HDPE d'une porosité de 0.63  $\mu\text{m}$  (extraction du SEBS à partir du mélange HDPE/SEBS), et une matrice de PLA d'une porosité de 1.56  $\mu\text{m}$  (extraction du PS dans le mélange PLA/PS). Bien que les polymères biodégradables en tant que matrices résorbables peuvent être plus appropriés pour des applications médicales, nous avons utilisé le polyéthylène à haute densité (HDPE), un polymère non-dégradable, comme modèle pour obtenir de petites tailles de pore. La taille des pores de tous les mélanges préparés a été obtenue selon trois méthodes : l'analyse d'image, la technique d'adsorption d'azote BET, et la microscopie électronique à balayage (SEM) pour chaque échantillon après microtomie. Ici, nous nous référons aux résultats de la technique d'adsorption d'azote BET, puisqu'il semble plus précis dans notre cas. Pour effectuer la libération de médicaments, le médicament doit d'abord être encapsulé dans les polymères. Les méthodes habituelles incluent la plupart du temps une encapsulation *in situ* des médicaments, toutefois notre méthode diffère de ce qui a été exposé dans la littérature jusqu'à présent. Dans notre méthode, la capsule appropriée est tout d'abord préparée pour ensuite encapsuler une solution d'albumine de sérum bovin (BSA). L'avantage de cette technique par rapport aux autres est de ne pas impliquer le médicament dans l'étape de préparation et ainsi de préserver la structure du médicament des effets potentiels de la température, de la pression et de l'effet d'un dissolvant.

Pour l'encapsulation, nous avons forcé la solution de BSA à pénétrer dans la structure poreuse en suivant un cycle de vide-pression. Pour étudier l'effet de la pression sur l'efficacité du chargement pour trois tailles différentes de pore, nous avons entrepris des expériences de chargement à trois différentes pressions. Dans les expériences à pression constante, une plus grande taille de pore implique une efficacité plus élevée de chargement tandis qu'une plus petite taille de pore s'accompagne d'une efficacité

inférieure de chargement. Cet effet était dû aux pores d'entrée plus petits, à de plus petits canaux existants dans la structure et à la tortuosité accrue pour des échantillons ayant une plus petite taille de pore.

Pour l'étude *in vitro* de libération nous avons préparé des échantillons cylindriques semblables, d'un diamètre de 3 millimètres et d'une longueur de 5-7 millimètres. Les échantillons ont été incubés à 37° C dans de l'eau Milli-Q, et les mesures de concentration pendant la libération ont été réalisées par spectrophotométrie UV-Vis. Les essais initiaux de libération ont été effectués sur 3 types d'échantillons différant par la taille des pores. Nous avons observé que le profil de libération le plus rapide, la libération initiale la plus grande, était obtenu pour l'échantillon avec la plus grande taille de pore (PLA, diamètre = 1.56µm). Le PLA a montré une libération complète en 3.5 heures tandis que le HDPE libère la BSA en 24-28 heures d'une façon plus contrôlée. Ceci montre qu'une plus petite taille de pore, soit une plus grande superficie, a un effet sur la libération de BSA tandis que de plus petits canaux inter reliés limitent la diffusion des médicaments à plusieurs niveaux. Cette observation suggère fortement que le caractère hydrophobe du substrat de HDPE et du PLA et le caractère hydrophile de la BSA sont la cause principale pour la libération rapide de la BSA. Par conséquent l'utilisation de la modification extérieure pour améliorer l'attachement de la BSA sur la surface interne peut être une option intéressante pour améliorer le profil de dégagement.

Suite aux essais de libération, afin de compléter notre procédé de préparation, nous avons étudié l'effet de la température lors de l'étape de séchage dans la préparation des échantillons. Le protocole que nous avons suivi inclut une étape de séchage après celle du chargement d'une durée de 4 heures. Nous avons effectué le séchage à deux températures différentes (40°C et 60°C) pour observer l'effet de la température. Le taux de libération initial a diminué de 35.88 (% de libération/hr) à 7.97 (% libération/hr) en augmentant la température, et seulement 35% de la BSA chargée a été libérée au bout des 70 heures de l'expérience. Ce comportement dans le profil de libération (une libération plus lente) à

60°C est principalement dû aux changements structuraux de la BSA. La formation d'agrégation dans la matrice entraîne une libération lente et limitée.

Puisque les capsules non modifiées ont montré une libération rapide, nous avons préparé une série d'essais avec des surfaces traitées, afin d'augmenter l'adhésion de la BSA à la surface et diminuer le taux de libération. La modification extérieure par le dépôt d'un polyelectrolyte est reconnue comme une technique prometteuse. Pour améliorer le profil de libération de la BSA, nous avons étudié son association avec des polyelectrolytes. Nous avons entrepris des expériences de libération avec des échantillons de 3 couches et de 7 couches ou avec 4 et 8 couches de polyelectrolytes. La technique de LbL (couche par couche) a été employée pour deux diamètres de pores; HDPE de 0.63  $\mu\text{m}$ , et PLA de 1.56  $\mu\text{m}$ . Nous avons éliminé la plus petite taille de pore ( $d = 0.32\mu\text{m}$ ) de l'essai en raison de sa condition de chargement plus difficile. Chaque couche de polyelectrolyte a été chargée par le même procédé expliqué à l'annexe A. Après une étape de quatre heures de dépôt, une étape de lavage de quatre heures a été suivie. Pour le HDPE et le PLA, nous avons chargé des polyelectrolytes assemblés sous deux formes différentes; PSS/PDADMAC/PSS et PDADMAC/PSS/PDADMAC. Pour le substrat de HDPE la deuxième forme (PDADMAC/PSS/PDADMAC) n'a pas tout à fait réussi puisque des couches de polyelectrolytes ont commencé à se libérer avec de la BSA tout en modifiant l'absorbance. Toutefois, l'autre association (PSS/PDADMAC/PSS) a fonctionné parfaitement. Par conséquent, dans le cas du HDPE, nous avons employé le substrat traité de HDPE commençant par le PSS. Pour le PLA, le sandwich PDADMAC/PSS/PDADMAC était préférable pour la libération de la BSA que les couches PSS/PDADMAC/PSS. Ceci peut être expliqué par les charges en surface. En effet, à un pH proche de 7, la BSA porte une charge nette négative, tandis que le PDADMAC est chargé positivement. Ils peuvent alors être impliqués dans une adhésion forte et retarder ainsi le pic de libération. Par conséquent pour le substrat de PLA, le traitement extérieur commence avec une couche de PDADMAC.

Employer trois couches sur le HDPE a amélioré le profil de libération avec une diminution du pic initial de moitié et a pour eu pour résultat une libération plus soutenue. Pour des matrices de PLA en 3 couches de polyélectrolytes, le pic de libération initiale a diminué de 80%. Il s'accompagne d'une libération plus soutenue, et se rapproche davantage du profil de libération désiré théoriquement.

Pour étudier l'effet du nombre de couches de polyélectrolyte sur le profil de libération de la BSA, nous avons ensuite ajouté jusqu'à 7 et 8 couches de polyélectrolytes. Les résultats ont indiqué que l'augmentation du nombre de couches de 3 ou 4 à 7 ou 8 change complètement la surface et induit ainsi une interaction plus forte avec la BSA. La combinaison de ces effets peut mener à un taux de libération initiale plus lent et à une libération inachevée pour des substrats de HDPE et de PLA.

Pour étudier l'effet d'une peau fermant la porosité à la surface de la structure poreuses, cylindres de PLA chargés de BSA ont été plongés dans ldu chloroforme pendant 2 secondes. Avec cette méthode, nous pouvons contrôler l'épaisseur de cette couche externe en changeant la durée d'immersion dans le chloroforme. Ensuite, l'expérience de libération a été effectuée dans un milieu aqueux. Aucune diffusion du BSA n'a été enregistrée après 4-5 jours ce qui tend à confirmer que la surface extérieure de PLA était complètement fermée. La diffusion de la BSA ne pourra être observée que lorsque le PLA commencera à dégrader.

En conclusion, la combinaison de la technologie de peau en surface et de couche-par-couche (LbL) sur une matrice co-continue représente une nouvelle méthode de base offrant le potentiel de produire de nouvelles structures de polymères comme dispositif pour la libération contrôlée de médicaments. Notre recherche montre comment l'influence de la taille des pores de la matrice affecte le profil de libération dans des matrices de polymères non traitées et traitées, et comment la modification du polymère



par la méthode de couche-par-couche et la peau en surface améliorent le profil de libération de BSA.

Notre nouvelle méthode de libération contrôlée de médicaments exige des études plus approfondies. Nous avons compris que de nombreux facteurs peuvent affecter le profil de libération des médicaments pendant des études in vitro. Ces paramètres incluent l'effet de la concentration des médicaments et la masse moléculaire sur le profil de libération. Afin d'obtenir plus d'information sur la localisation des médicaments à l'intérieur de la structure poreuse après le chargement et pendant l'essai de libération, l'emploi de la fluorescence intrinsèque de la BSA est suggéré. Il est également de grand intérêt de développer l'idée de la structure fermée en employant des polymères se dégradant rapidement, ou de la gélatine.

## TABLE OF CONTENT

<b>ACKNOWLEDGMENTS.....</b>	<b>IV</b>
<b>ABSTRACT.....</b>	<b>VI</b>
<b>RÉSUMÉ.....</b>	<b>IX</b>
<b>CONDENSÉ EN FRANÇAIS .....</b>	<b>XII</b>
<b>TABLE OF CONTENT.....</b>	<b>XXI</b>
<b>LIST OF FIGURES.....</b>	<b>XXVI</b>
<b>LIST OF TABLES.....</b>	<b>XXXI</b>
<b>LIST OF APPENDICES .....</b>	<b>XXXII</b>
<b>LIST OF ABBREVIATIONS AND SYMBOLS .....</b>	<b>XXXIII</b>
<b>CHAPTER 1 INTRODUCTION.....</b>	<b>1</b>
1.1. CONTROLLED DRUG DELIVERY .....	1
1.2. POLYMER STRUCTURE AND DRUG DELIVERY .....	3
1.3. RESEARCH OBJECTIVES .....	6
<b>CHAPTER 2 LITERATURE REVIEW.....</b>	<b>8</b>
2.1 DRUG DELIVERY .....	8
2.1.1 <i>Controlled Drug Delivery</i> .....	8
2.1.2 <i>Advantages and Limitations of Controlled Release</i> .....	10
2.1.3 <i>Criteria of Active Agent and Routes of Administration</i> .....	11
2.1.4 <i>Release of Active Agent</i> .....	13
2.1.5 <i>Polymers in Control Release Formulations</i> .....	14
2.2 BOVINE SERUM ALBUMIN (BSA).....	17
2.2.1 <i>Introduction</i> .....	17
2.2.2 <i>Structure of BSA</i> .....	17

2.2.3 Effect of pH.....	20
2.2.4 Effect of Heat .....	21
2.2.5 Effect of Pressure.....	23
2.2.6 Functional Properties of BSA.....	24
2.2.6.1 Foaming.....	24
2.2.6.2 Gelation.....	25
2.2.6.3 Ligand –Binding.....	25
2.3 SPECTROPHOTOMETRY.....	27
2.3.1 Beer – Lambert Law.....	28
2.3.2 Protein Spectrophotometry.....	29
2.4 CO-CONTINUOUS STRUCTURE AND ITS CONTROLLING PARAMETERS .....	31
2.4.1 Introduction to Co-Continuity.....	31
2.4.2 Morphology Control in Co-Continuous Structures .....	33
2.4.2.1 Influence of Composition on the Morphology .....	34
2.4.2.2 Component Viscosity and Viscosity Ratio.....	34
2.4.2.3 Interfacial Tension and Compatibilisation of the Interface.....	35
2.4.2.4 Annealing .....	36
2.5 DRUG ENCAPSULATION TECHNIQUES .....	37
2.5.1 Coacervation.....	39
2.5.2 Solvent Evaporation Techniques.....	40
2.5.3 Spray Drying.....	43
2.5.4 Polymer–Polymer Incompatibility.....	44
2.5.5 Interfacial Polymerization.....	44
2.5.6 Fluidized–Bed Coating .....	45
2.6 DIFFUSION (DIFFUSION COEFFICIENT CALCULATION & DRUG RELEASE KINETICS).....	46
2.6.1 Steady –State Diffusion.....	46
2.6.2 Factors Affecting the Diffusion: Temperature and Molecular Size.....	50
2.6.3 Effect of Geometry and Dosage Form on Release Profile.....	51
2.7 DRUG DISSOLUTION.....	54
2.8 BURST RELEASE.....	55

2.8.1 Manufacturing Condition.....	57
2.8.2 Surface Characterization of the Matrix.....	58
2.8.3 Polymer–Drug Properties and Interactions .....	58
2.8.4 Methods to Prevent Burst Release and Induce Slower Diffusion Rates .....	59
2.8.4.1 Drug Surface Extraction.....	59
2.8.4.2 Drug-Loading Distribution.....	60
2.8.4.3 Double-Wall Formulation and Coated Surfaces .....	60
2.8.4.4 Surface Modification.....	61
2.9 INCOMPLETE RELEASE .....	62
2.10 ENCAPSULATION EFFICIENCY .....	63
2.11 CLOSED–CELL FORMULATION .....	65
2.12 POLYELECTROLYTES.....	67
2.12.1 Introduction to Polyelectrolytes.....	67
2.12.2 Polyelectrolyte Applications.....	69
2.12.3 Polyelectrolytes in Solution .....	70
2.12.3.1 Effect of Salt on Polyelectrolyte Conformation in Solution .....	70
2.12.4 Layer-by-Layer Deposition of Polyelectrolyte.....	73
2.12.4.1 Charge Distribution and Overcompensation - Multilayer Growth.....	75
<b>CHAPTER 3 EXPERIMENTAL METHODOLOGY .....</b>	<b>79</b>
3.1 MATERIALS.....	80
3.2. HDPE AND PLA POROUS DEVICE PREPARATION .....	80
3.3. MORPHOLOGY ANALYSIS WITH SCANNING ELECTRON MICROSCOPY (SEM) .....	82
3.4 CHARACTERIZATION OF HDPE AND PLA HIGHLY CO-CONTINUOUS STRUCTURES.....	83
3.4.1 Continuity of HDPE and PLA Templates .....	83
3.4.2 Internal Surface Area and Pore Diameters .....	83
3.4.2.1 Image Analysis (IA).....	83
3.4.2.2 BET Technique .....	84
3.4.2.3 Mercury Intrusion Porosimetry (MIP) .....	85
3.5 LOADING PROTOCOL AND LOADING EFFICACY CALCULATION .....	86

3.6 LAYER-BY-LAYER DEPOSITION OF POLYELECTROLYTES INSIDE THE HDPE AND PLA POROUS STRUCTURES.....	89
3.6.1 <i>Preparation of polyelectrolyte solution</i> .....	90
3.7 IN VITRO BSA RELEASE .....	91
3.7.1 <i>Preparation of Standard BSA Solutions</i> .....	93
3.7.2 <i>Calibration Curve</i> .....	94
<b>CHAPTER 4 POROUS DEVICES DERIVED FROM CO-CONTINUOUS POLYMER BLENDS AS A ROUTE FOR CONTROLLED DRUG RELEASE ...</b>	<b>96</b>
4.1 ARTICLE PRESENTATION .....	96
4.2 POROUS DEVICES DERIVED FROM CO-CONTINUOUS BLENDS AS A ROUTE FOR CONTROLLED DRUG RELEASE .....	98
4.2.1 <i>Abstract</i> .....	98
4.2.2 <i>Introduction</i> .....	99
4.2.3 <i>Experimental Procedure</i> .....	102
4.2.3.1 Materials.....	102
4.2.3.2 Blend Preparation.....	104
4.2.3.3 Solvent Extraction and extent of continuity .....	104
4.2.3.4 Microtomy and Scanning electron Microscopy .....	105
4.2.3.5 Image Analysis, BET, and Mercury Porosimetry on Extracted Samples.....	105
4.2.3.6 High- Pressure Loading Apparatus .....	106
4.2.3.7 In Vitro BSA Release studies.....	107
4.2.3.8 Surface Modification via L-b-L Deposition of Polyelectrolyte into the HDPE and PLA templates.....	107
4.2.4 <i>Results and Discussion</i> .....	108
4.2.4.1 Porous Device Morphology; Extent of Continuity and Pore Size Analysis.....	108
4.2.4.2 Drug Loading Protocol and Efficacy of Loading.....	112
4.2.4.3 In-Vital Release of BSA from the Porous Devices .....	113
4.2.4.4 Effect of Heating in the Preparation Process on Drug Release .....	115
4.2.4.5 Surface Modification of the Porous Medium .....	117
4.2.4.6 Effect of LbL Surface Modification on in-Vitro Drug Release .....	121

4.2.4.7 Effect of a Closed-Cell Template on Drug Release .....	127
4.2.5 Conclusion .....	130
4.2.6 Acknowledgment .....	131
<b>CHAPTER 5 GENERAL DISCUSSION AND CONCLUSIONS.....</b>	<b>132</b>
5.1. GENERAL DISCUSSION .....	132
5.1.1 Effect of Pore Size and Surface Area on BSA Loading and Release Rate.....	132
5.1.2 Effect of Modification on the BSA Release Profile .....	133
5.1.3 Future Work.....	134
5.2. CONCLUSIONS .....	136
<b>REFERENCES.....</b>	<b>138</b>
<b>APPENDICES.....</b>	<b>167</b>

## LIST OF FIGURES

FIGURE 2.1 DRUG LEVEL IN THE BLOOD A) WITH TRADITIONAL DRUG DOSING, B) WITH CONTROLLED-DELIVERY DOSING (EDLUND AND ALBERTSSON, 2002). ....	9
FIGURE 2.2 BENEFITS OF CONTROLLED RELEASE SYSTEMS (CHAUBAL, 2002). ....	12
FIGURE 2.3 DRUG DELIVERY FROM A <i>MATRIX</i> DRUG DELIVERY SYSTEM.....	15
FIGURE 2.4 DRUG DELIVERY FROM A <i>RESERVOIR</i> DRUG DELIVERY SYSTEM .....	16
FIGURE 2.5 CLASSICAL PERCEPTION OF THE STRUCTURE OF SERUM ALBUMIN .....	18
FIGURE 2.6 AMINO ACID SEQUENCE OF BSA .....	18
FIGURE 2.7 LOCATION OF DISULPHIDE BONDS.....	19
FIGURE 2.8 RELATIONSHIP OF ISOMERIC CONFORMATIONS OF BOVINE SERUM ALBUMIN....	20
FIGURE 2.9 DIAGRAM OF SERUM ALBUMIN IN ITS VARIOUS CONFORMATIONS; A) E FORM, B) N FORM, AND C) F FORM .....	21
FIGURE 2.10 PROTEIN P BINDING TO LIGAND A. THE DOUBLE ARROW STANDS FOR A REVERSIBLE BINDING. ....	26
FIGURE 2.11 SCHEMATIC VIEW OF A SPECTROPHOTOMETER .....	27
FIGURE 2.12 CO-CONTINUOUS STRUCTURE FOR A BINARY BLEND A/B A) PHASE A HAS BEEN EXTRACTED B) PHASE B HAS BEEN EXTRACTED (GREGEN ET AL., 1996) .....	31
FIGURE 2.13 SCHEMATIC REPRESENTATION OF THE PHASE CO-CONTINUITY-COMPOSITION DEPENDENCE .....	32
FIGURE 2.14 EFFECT OF ANNEALING TEMPERATURE ON DOMAIN SIZE AND SIZE DISTRIBUTION OF A BINARY BLEND .....	37
FIGURE 2.15 EFFECT OF ANNEALING TIME ON DOMAIN SIZE AND SIZE DISTRIBUTION, A) NON-ANNEALED, B) ANNEALED FOR 2 HOURS, C) ANNEALED FOR 4 HOURS.....	37
FIGURE 2.16 SCHEMATIC ILLUSTRATION OF MICROSPHERES PREPARED BY THE OIL-IN-WATER SOLVENT EVAPORATION TECHNIQUE.....	42
FIGURE 2.17 SCHEMATIC DIAGRAM OF THE INTERFACIAL POLYMERIZATION TECHNIQUE FOR DRUG ENCAPSULATION.....	45

FIGURE 2.18 SCHEMATIC ILLUSTRATION OF CONCENTRATION GRADIENT. ....	47
FIGURE 2.19 A) SCHEMATIC DIAGRAM OF THE CYLINDER CROSS SECTIONAL VIEW, B) CONCENTRATION PROFILE OF THE DRUG RELEASE FROM THE POLYMER MATRIX. ....	49
FIGURE 2.20 KINETICS OF THE DRUG RELEASE FOR DOSAGE FORMS OF SAME VOLUME AND DIFFERENT SHAPES CONTROLLED BY DIFFUSION.....	52
FIGURE 2.21 THE PERCENTAGE DRUG RELEASE VERSUS TIME FOR THE DIFFERENT GEOMETRIES (♦) COMPACT CYLINDRICAL SHAPE, (■) QUASI-SPHERICAL SHAPE (MARTINI ET AL., 2000).....	53
FIGURE 2.22 SCHEMATIC SHOWING THE BURST RELEASE EFFECT (HUANG AND BRAZEL, 2001).....	55
FIGURE 2.23 DRUG REDISTRIBUTION DUE TO CONVECTION DURING DRYING PROCESS (HUANG AND BRAZEL, 2001).....	57
FIGURE 2.24 EFFECT OF $Mg(OH)_2$ CONTENT ON BSA RELEASE KINETICS. MILLCYLINDERS WITH 15% BSA AND 0% (●), 0.5% (■), AND 3.0% (▼) $Mg-$ $(OH)_2$ .....	64
FIGURE 2.25 CROSS SECTION OF DOUBLE-WALLED MICROSPHERES UNDER FLUORESCENCE MICROSCOPE A) REPRESENTS MICROSPHERES (10 ×) MAGNIFICATION B) REPRESENTS MICROSPHERES (20 ×) MAGNIFICATION (RAHMAN ET MATHIOWITZ, 2004).....	67
FIGURE 2.26 POLYELECTROLYTE DISSOCIATION IN WATER .....	69
FIGURE 2.27 “RANDOM-WALK” MODEL FOR A POLYMER CHAIN (TANGLED MOLECULE IN RANDOM COIL).....	71
FIGURE 2.28 “WORM-LIKE” MODEL FOR POLYELECTROLYTE CHAIN.....	72
FIGURE 2.29 EFFECT OF ADDING SALT TO THE POLYELECTROLYTE SOLUTION .....	72
FIGURE 2.30 SCHEMATIC REPRESENTATION OF LAYER-BY-LAYER DEPOSITION.....	73
FIGURE 2.31 AFM TOPOGRAPHIC IMAGES OF THE MORPHOLOGY OF TEN BILAYER FILMS OF PDDA/PSS DEPOSITED FROM (A) 0.1M, (B) 0.3M, AND (C) 1.0M NaCl SOLUTIONS. IMAGES ARE $5\ \mu m \times 5\ \mu m$ , AND THE Z SCALES ARE AS SHOWN (MCALONEY ET AL., 2001).....	75



FIGURE 2.32 ZETA POTENTIAL AS A FUNCTION OF NUMBER OF LAYERS FOR COATED POLYSTYRENE SULFATE LATEX PARTICLES, DIAMETER 640NM: □ PSS/PDADMAC; ■ BSA/PDADMAC ○ PSS/PAH; △ DNA/PDADMAC (SUKHORUKOV ET AL., 1998).....	76
FIGURE 2.33 THICKNESS AS A FUNCTION OF THE NUMBER OF LAYERS FOR A PSS/PDADMA MULTILAYER DEPOSITED ON SILICON WAFER FROM POLYMER SOLUTIONS CONTAINING 1.0 M NaCl (SCHLENOFF ET AL., 2001) .....	77
FIGURE 2.34 (A) POSITIVE SURFACE AREAL CHARGE DENSITY FOR 15-LAYER PSS/PDADMA MULTILAYERS (PDADMA-CAPPED, ■) AND 14-LAYER MULTILAYERS (PSS-CAPPED, ♦) MADE FROM SOLUTIONS CONTAINING 1 mM POLYMER AND DIFFERENT NaCl CONCENTRATIONS (SCHLENOFF ET AL., 2001). (B) FILM THICKNESS VS SALT CONCENTRATION FOR MULTILAYERS WITH TEN LAYER PAIRS EACH (DUBAS ET SCHLENOFF, 1999).....	78
FIGURE 3.1 EXPERIMENTAL SUMMARY.....	79
FIGURE 3.2 POLYMER SAMPLE IN TEST TUBE, COMPLETELY KEPT INSIDE THE SOLUTION WITH A ROD .....	89
FIGURE 3.3 SPECTROPHOTOMETRY CELL WITH SEALED HEAD (TO PREVENT WATER EVAPORATION) AND ROD (TO KEEP THE SAMPLES INSIDE WATER).....	92
FIGURE 3.4 CALIBRATION CURVE OF BSA DIFFUSION IN WATER MEASURED AT 280 NM....	95
FIGURE 4.1 CONTINUITY OF THE POLYMERIC MATRIX (HDPE, PLA) AS A FUNCTION OF EXTRACTED PHASE (SEBS, SEB, PS) VOLUME PERCENT. ....	109
FIGURE 4.2 SEM MICROGRAPHS; A) AND B) HDPE/SEB (50/50), SEB EXTRACTED, C) AND D) HDPE/SEBS (50/50), SEBS EXTRACTED, E) AND F) PLA/PS (50/50), PS EXTRACTED.....	111
FIGURE 4.3 FRACTION OF PORES FILLED BY WATER AT DIFFERENT WORKING PRESSURES .....	112
FIGURE 4.4 EFFECT OF PORE SIZE ON THE DRUG RELEASE IN 3ML OF MILLI-Q WATER AT 37°C.....	115

FIGURE 4.5 EFFECT OF HEATING ON THE DRUG RELEASE PROFILE. POROUS HDPE FROM HDPE-SEBS, A) DRIED AT 40°C (▲); B) DRIED AT 60°C (●).....	116
FIGURE 4.6 DEPOSITED MASS AS A FUNCTION OF THE NUMBER OF LAYERS, HDPE POROUS DEVICE (PSS/PDADMAC/PSS...) WITH AVERAGE PORE SIZE 0.63 $\mu\text{m}$ ; PLA POROUS DEVICE ( PDADMAC/PSS/PDADMAC...) WITH AVERAGE PORE SIZE 1.56 $\mu\text{m}$ .....	119
FIGURE 4.7 CUMULATIVE DEPOSITED MASS OF PDADMAC AND PSS FOR HDPE AND PLA SUBSTRATES. POROUS PLA (PDADMAC ▲/ PSS ■/PDADMAC ▲/...) ,AND POROUS HDPE (PSS □ /PDADMAC ▲/PSS □/...).....	120
FIGURE 4.8 A) POROUS HDPE OF 0.63 $\mu\text{m}$ PORE SIZE, HDPE/BSA (♦); HDPE/ PSS/PDADMAC/PSS/BSA (□ ); B) POROUS PLA OF 1.56 $\mu\text{m}$ PORE SIZE, PLA/BSA (♦); LbL <sub>1</sub> = PLA/PSS/PDADMAC/PSS/BSA(Δ); LbL <sub>2</sub> = PLA/PDADMAC/PSS/PDADMAC/BSA (□).....	122
FIGURE 4.9 DRUG RELEASE PROFILE OF POROUS PLA OF 1.56 $\mu\text{m}$ (♦); PLA/PSS/PDADMAC/PSS (Δ); PLA/PDADMAC/PSS/PDADMAC/BSA (□); PLA/PDADMAC/PSS/...PDADMAC 7 <sub>LAYER</sub> /BSA (●).....	124
FIGURE 4.10 DRUG RELEASE PROFILE OF POROUS HDPE OF 0.63 $\mu\text{m}$ (♦); HDPE/PSS/PDADMAC/PSS/PDADMAC (Δ); HDPE/PSS/PDADMAC/ ...PDADMAC 8-LAYER (□).....	125
FIGURE 4.11 SEM MICROGRAPHS OF POROUS PLA WITH A CLOSED-CELL MORPHOLOGY, PREPARED FROM PLA/PS (50-50) (A) $\times$ 250 MAGNIFICATION, (B) $\times$ 2000 MAGNIFICATION (SARAZIN ET AL., 2006) .....	128
FIGURE 4.12 DRUG RELEASE PROFILE FOR CLOSED –CELL MORPHOLOGY. POROUS PLA FROM PLA/PS (50-50) .....	129
FIGURE A.1 INSTABILITY IN BSA RELEASE PROFILE .....	172
FIGURE A.2 DRUG RELEASE PROFILE A) POROUS HDPE OF 0.63 $\mu\text{m}$ , HDPE/PSS/PDADMAC/PSS/BSA(♦),HDPE/PSS/PDADMAC/..7 <sub>LAYER</sub> /BSA (□) .....	173

FIGURE A.3 RELEASE BEHAVIOR COMPARISON OF POROUS HDPE SAMPLES WITH 0.63 $\mu$ M A) RELEASE BEHAVIOR COMPARISON BETWEEN 3 LAYERS OF TREATMENT AND NEGATIVE OUTERMOST LAYER ( $\square$ ), AND 4 LAYERS OF POLYELECTROLYTE TREATMENT WITH POSITIVE OUTERMOST LAYER ( $\blacktriangle$ ). B) RELEASE COMPARISON BETWEEN 7 LAYERS OF TREATMENT WITH NEGATIVE OUTERMOST LAYER ( $\square$ ) AND 8 LAYERS OF POLYELECTROLYTE WITH POSITIVE OUTERMOST LAYER ( $\blacktriangle$ ). ..... 175

## LIST OF TABLES

TABLE 1.1 POLYMER ARCHITECTURE AND CONTROLLING FACTORS TO PREPARE CONTROLLED DRUG DELIVERY SYSTEM.....	4
TABLE 2.1 ROUTES FOR DRUG ADMINISTRATION .....	13
TABLE 2.2 PHYSICOCHEMICAL PROPERTIES OF BOVINE SERUM ALBUMIN .....	19
TABLE 2.3 RELATIVE NUCLEIC ACID AND PROTEIN CONTAMINATIONS.....	30
TABLE 2.4 CHARACTERISTIC OF POLYMERIC DOSAGE FORM.....	52
TABLE 2.5 POSITIVE AND NEGATIVE APPLICATIONS OF BURST RELEASE .....	56
TABLE 3.1 CHARACTERISTIC PROPERTIES OF MATERIALS .....	81
TABLE 3.2 DILUTION OF CONCENTRATED BSA.....	93
TABLE 3.3 SPECTROPHOTOMETER READINGS FOR PREPARED STANDARDS .....	94
TABLE 4.1 CHARACTERISTIC PROPERTIES OF THE MATERIALS .....	103
TABLE 4.2 PORE SIZE OF POROUS HDPE PREPARED FROM HDPE/SEB, HDPE/ SEBS AND PLA/PS BLENDS.....	110
TABLE 4.3 PERCENTAGE OF EACH INGREDIENT AND LOADING EFFICIENCY.....	114
TABLE A.1 ESTIMATION TABLE OF PROTEIN CONCENTRATED BY UV ABSORBANCE.....	171

## LIST OF APPENDICES

APPENDIX A. LOADING THE POROUS POLYMER WITH BSA.....	167
APPENDIX B. LOADING THE POROUS POLYMER WITH POLYELECTROLYTE.....	169
APPENDIX C. "F" FACTOR ESTIMATION TABLE.....	171
APPENDIX D. BSA INSTABILITY DURING THE RELEASE TESTS.....	172
APPENDIX E. EFFCET OF CHARGE ON BSA RELEASE.....	173

## LIST OF ABBREVIATIONS AND SYMBOLS

$A_{280}$ at	Light absorbance 280 nm	HDPE	High density polyethylene
AFM	Atomic force microscopy	IA	Image analysis
BSA	Bovine serum albumin	IR	Infra-Red
$C$	Concentration	$\sigma$	Interfacial tension
$C_s$	Solubility limit of the drug in matrix	$J_{lx}$	Molar flux
CDRS	Controlled drug release system	$j_{lx}$	Mass flux
CDRF	Controlled drug release formulation	$K$	Partition coefficient
$\varphi$	Composition	$\kappa$	Boltzmann Constant
$\theta$	Contact angle	LbL	Layer-by-layer
$D$	Diffusion coefficient, diffusivity	$M_t$	Fractional release at time t
$\delta$	Distance at which diffusion occurs	MDT %	Mean dissolution time
F	280:260 ratio Factor	$M_\infty$	Total amount of drug releasable at infinite time per unit area
$f, f_2$	Similarity factor	MIP	Mercury intrusion porosimetry
$f_1$	Difference factor	$\eta_m$	Matrix viscosity
$\rho$	Density	O/O	Oil-in-Oil
GI	Gastro intestine	O/W	Oil-in-water

P	Pressure	SEBS	(Styrene)- (ethylene- butylenes)- (styrene)
PBS	Phosphate buffer solution		
PDADMAC	Diallyldimethyl- ammonium chloride	SEM	Scanning electron microscopy
PDDS	Polymeric drug delivery system	$S(t)$	Radius of the unextracted core
PEM	Polyelectrolyte multilayer	$S(x,y,t)$	Source of drug molecules release
PEG	Poly (ethylene- glycolide)	t%	Time taken for x% drug release
PEO	Poly (ethylene- oxide)	THF	Tetrahydrofuran
pK	Dissociation constant	TPA	Tissue Plasminogen Activator
PLA	Poly lactide	UV	Ultra Violet
PS	Poly styrene	UV/VIS spectrophoto.	Ultraviolet- Visible spectrophotometer
PSS	Poly (sodium 4- styrenesulfonate)	$\eta$	Viscosity
$Q_d$	Energy	W/O/O	Water-in-Oil-Oil
QCM	Quartz crystal microbalance	W/O/W	Water-in-Oil-in- Water
$R(x,y,t)$	Metabolism and degradation rate	X, Y	Reactants
R	Pore diameter	$(X-Y)_n$	Polymerization product
SEB	(Styrene)- (ethylene- butylenes)		

# CHAPTER 1

## INTRODUCTION

### 1.1. Controlled drug delivery

Controlled drug delivery technology is one of the frontier areas of science, involving a multidisciplinary scientific approach and contributing to human health care. These delivery systems offer numerous advantages over conventional dosage forms, including improved efficacy, reduced toxicity, and improved patient compliance and convenience. Conventional drug administration does not generally allow for rate-controlled release or target specificity. In many cases of conventional drug delivery, the drug concentration increases sharply to potentially toxic levels and following a relatively short period at the therapeutic level, drops off until re-administration. The concentration, duration, and bioavailability of the pharmaceutical agents could not be controlled. Controlled release technology is designed to address these problems. Today, new methods of drug delivery and novel technologies are being developed. The desired drug release can be provided by rate-controlling membranes or by implanted biodegradable polymers containing dispersed medication.

Polymers are among the youngest members of the materials family, and recent progress in the area of applied polymer science is fascinating. Pharmaceutical uses of biodegradable polymers, such as resorbable sutures, hard and soft tissue implants, and drug delivery systems, are well established due to the low costs involved in their preparation process and unique properties such as processibility, reproducibility, resistance and mechanical properties. Over the past 25 years, much research has focused on degradable polymer microspheres for controlled drug release. Administration of medication via such systems is advantageous because microspheres can be ingested or



injected; they can be designed for their desired release profiles and, in some cases, can even provide organ-targeted release. Some reviews covering aspects of microspheres for drug delivery are available (Jalil et al., 1990, Edlund et al., 2002, Vasir et al., 2003). These reviews cover recent works and provide information regarding many factors affecting microsphere drug release and the manipulation of physical/chemical properties to achieve the desired results.

The idea of controlled release using polymers dates back to the 1960s with the employment of silicone rubber (Folkman et al., 1964) and polyethylene (Desai et al., 1965). Due to the lack of degradability in these systems, eventual surgical removal was required, which limited the applicability of these materials. In the 1970s, biodegradable polymers were suggested as appropriate drug delivery materials, eliminating the necessity of removal (Jalil et al. 1990). The idea of polymer microcapsules as delivery systems was reported as early as the 1960s, and degradation was incorporated by Mason et al. (1976) using a degradable polymer coating.

Recent literature suggests that degradable microspheres can be employed for sustained drug release at desired doses and by implantation without surgical procedures. Biocompatibility can be achieved using natural polymers, such as cellulose, chitin, and chitosan or polymers made from naturally occurring monomers, such as lactic and glycolic acids. Polymers derived from synthetic monomers also show excellent delivery properties; however, their toxicity effects may require evaluation.

The factors affecting drug release are controllable. They are mainly attributed to properties of polymers, such as molecular weight, microsphere size, distribution, and morphology. Controlled release is an attainable and desirable characteristic of drug delivery systems. The factors affecting the drug release rate revolve around the structure of the matrix where the drug is encapsulated and the chemical properties associated with both polymer and drug. For example, a drug encapsulated in a slowly degrading matrix

provides the opportunity for slower release effects. Polymer degradation is not the only mechanism for the release of a drug. Diffusion is also a controllable parameter as the drug can travel through the pores formed during capsule preparation.

In some cases, drugs containing nucleophilic groups can cause increased chain scission of the polymer matrix, which also increases the rate of drug expulsion. Polymer molecular weight, drug distribution, polymer blending, crystallinity, and other factors are important in manipulating release profiles. The best release profile would show a constant release with time. However, in many cases, release profiles are more complicated and often contain two main expulsion processes. The first is an initial burst of medication from the capsule surface, the second, usually a more constant stage with release rates dependent on diffusion and degradation. Researchers have been able to achieve a relatively constant release after the initial burst, close to zero-order kinetics without a significant burst effect (Narayani and Rao, 1996; Makino et al., 2000; Yang et al., 2000; Berkland et al., 2002; Kakish et al., 2002).

## **1.2. Polymer structure and drug delivery**

During the past two decades, a large number of drug delivery systems, mostly in the forms of microspheres, films, tablets, or implantation devices, have been designed to achieve sustained drug release by taking advantage of polymers. As various nano-systems have been developed, the importance of polymer architecture–property relationships has gradually been realized and emphasized. Any polymer used in drug delivery formulation can be classified according to various factors such as chemical nature, backbone stability (biodegradable, non-biodegradable), and water solubility (hydrophobic, hydrophilic). Table 1.1 summarizes the different polymer structures and their controlling factors that have been used in controlled drug systems.

Table 1.1. Polymer architecture and controlling factors to prepare controlled drug delivery systems (Qui et al., 2006).

Architecture	Drug carrier	Property	Controlling factor	
Water-soluble linear polymer	Drug conjugate	Solubility	Chain hydrophilicity Solubilizing moiety Drug content	
		Biodistribution and cytotoxicity	Molecular weight Electrical charge Targeting groups	
		Degradation	Backbone Spacer	
		Drug release	Spacer	
Block copolymer	Micelle	Shape, critical micelle concentration, size	Proportion of A block to B block Electrical charge	
		Drug encapsulation	Intrinsic affinity between drug and hydrophob block	
		Biodistribution	Molecular weight Electrical charge Targeting groups Proportion of A block to B block	
		Drug release	Interaction between drug and hydrophobic block Conjugation bond drug and copolymer	
		Injectable hydrogel	Sol-gel transition	Molecular weight
			Temperature and critical gel concentrartion	Proportion of A block to B block
	Polymer	Shape	Proportion of A block to B block	
		Hyperbranched polymer	Membrane thickness	Length hydrophob chain
	Micelle		Shape, critical micelle concentration, size	Proportion of hydrophilic to hydrophobic domain Electrical charge Complexed drug content
			Cytotoxicity and gene transfection efficiency	Molecular weight Electrical charge Surface hydrophilicity
Graft polymer	Injectable hydrogel (sol-gel transition)	Lower critical solution temperature	Graft ratio	
Star polymer	Micelle	Critical micelles conc.	Molecular weight	
	Unimolecular micelle	Drug encapsulation	Graft ratio	
	Injectable hydrogel	Lower critical	Dimen. of hydroph. core Graft ratio	
Dendrimer	(sol-gel transition)	Solution temperature	Arm number	
	Unimolecular micelle	Size, drug loading	Arm number	
		Capability and efficiency	Generation number Electrical charge	

During the last two decades, research has focused more on the preparation of a polymeric structure within which a drug can be loaded. Numerous methods have been developed in the fabrication of such polymeric structures, including coacervation, solvent evaporation techniques, coating, phase separation, and emulsion. All of these techniques are capable of fabricating polymeric structures with the desired properties and quality; however, in the field of drug delivery, they have some disadvantages. With the present study, we present a new approach in drug delivery and introduce a novel drug delivery system that has great flexibility with respect to technical modification.

Recently, a new method of polymer structure fabrication, based on blending immiscible polymers in the melt state, was described by Li et al. (2002), and Sarazin et al. (2003). The product of this approach is a fully co-continuous structure after blending two or three immiscible polymers. It was also shown that in the fabrication step, the co-continuous morphology (i.e. pore diameters of the porosity), is highly controllable. The morphology of these co-continuous structures is controlled via blend composition, static annealing and compatibilizers (Li et al., 2002, Sarazin et al, 2003, and Yuan al., 2004). Extraction of one phase in the blend results in a highly porous interconnected structure with a large internal surface area and pore diameters ranging from few microns to tens of millimeters. This method is very promising due to its potential in manufacturing complex substrates with well-controlled morphologies on a wide range of pore diameters. The void continuity is estimated to be 90%. The current study seeks to use these highly porous interconnected structures (~ 90% fully interconnected porosity) as carrier devices for drug delivery and to develop a technique to load a drug into these polymeric carriers. It also investigates the effect of pore size of the substrate on the drug release profile.

### 1.3. Research objectives

Although there has been much research into controlled drug delivery in the last 20 years, relatively few products are available on the market. Finding a polymeric structure that can fulfill all the requirements of application still remains an issue. Therefore, more investigation into perfecting drug carriers and new methods of drug delivery is needed.

General objectives of this study:

1. To develop a novel controlled release system by means of polymer melt blending two immiscible polymers.
2. To investigate the potential of this method in controlled release applications by analyzing the BSA release profile from a porous polymeric carrier.

Specific objectives of this research:

1. To study the effect of pore size of polymer substrate on the BSA release profile and evaluate the capability of pore size, surface and tortuosity of porous substrate as limiting factors in controlled drug release.
2. To investigate the effect of surface modification of the porous substrate using the LbL technique and closed-cell morphology on control of the BSA release rate.

This thesis is divided into four chapters. The first describes the important factors in controlled release. It reviews the properties of BSA and the effects of environmental conditions (such as pressure, temperature, and pH) on its structure, discussing various encapsulation methods and investigating the parameters that affect its release behavior. The second chapter describes the substrate fabrication method and the newly developed loading protocol as well as introduces the material, products and all the characterization methods used in this study. The third chapter presents the drug delivery tests, including

tests with both small and large pore size substrates with and without surface treatment. Finally, last chapter contains general conclusions and ideas for future research.

## CHAPTER 2

### LITERATURE REVIEW

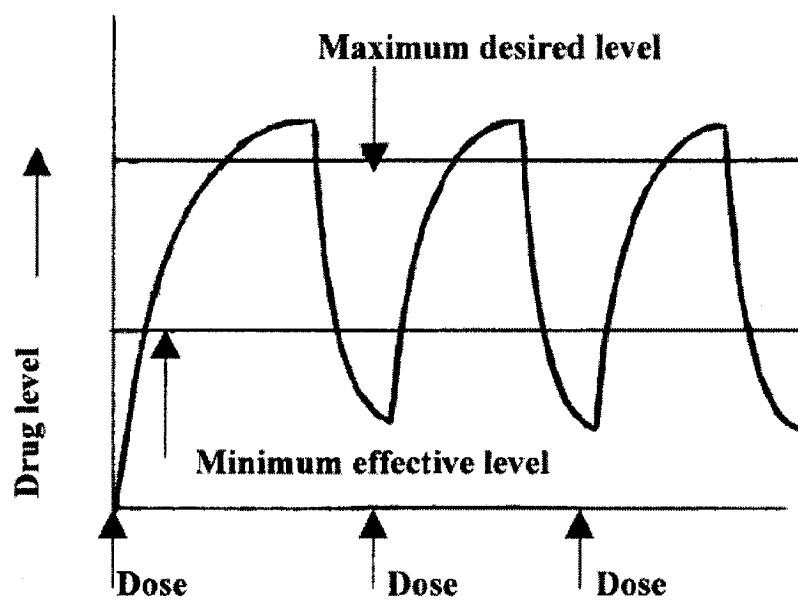
#### 2.1 Drug Delivery

The fate of a drug after administration is determined by a combination of several processes, depending on the intravascular or extravascular route of administration. In the last few decades, researchers have been dealing with improvement of delivery systems in ways that allow them to control the fate of drugs within the body. Using controlled release systems have assisted them in achieving this goal.

##### 2.1.1 Controlled Drug Delivery

Systems capable of carrying drugs at a pre-designed rate for a definite time period are known as “controlled drug delivery systems”. The release rate of the drug can be constant over a known period, can be cyclic or may be triggered by environmental conditions such as pH or other external events. Conventional drug delivery systems, such as tablets and intravenous injections administer the entire dose of a drug in one shot, which can lead to high or toxic drug concentrations in the blood. Repetitive administration results in strong fluctuation of the drug level in the body. Figure 2.1 a demonstrates the increase in drug level after each administration and its decrease before the next administration. The major advantage of controlled release systems over the traditional administrations is mainly the capability to preserve nearly constant drug concentration in the blood, over the long period, and within the efficient range (Figure 2.1 b). The efficient range is the level of the drug between a maximum drug level which represents a toxic level and a minimum level below which the drug is no longer effective (Edlund and Albertsson, 2002).

a)



b)

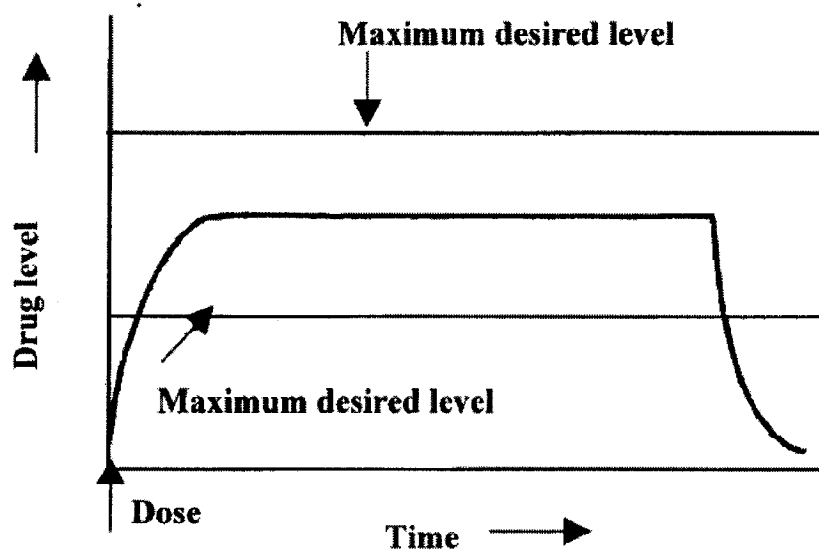


Figure 2.1 Drug level in the blood a) with traditional drug dosing, b) with controlled-delivery dosing (Edlund and Albertsson, 2002).



### 2.1.2 Advantages and Limitations of Controlled Release

Controlled release systems provide numerous benefits over the conventional mode of administration. Since controlled release systems keep the drug level in its therapeutic and effective range and eliminate the oscillation of the drug level in the blood, they are able to improve the efficiency of administration for any medical application. By increasing the drug release period, repetitive administration is no longer necessary, and a need for follow-up care will be reduced. This results in enhancement of the patient compliance.

Another advantage of using controlled drug delivery systems is targeting delivery of a drug to the target site in the body compartment at an appropriate time. This may be defined as drug targeting which reduces the systemic exposure and therefore the systemic side effects (Chaubal et al., 2002).

Moreover, controlled release systems may protect the active agent from various physiological environments inside the body and extend the effective life time of the drug. Since these physiological environments may destroy the activity of the drug, this is an important factor in cases of labile drugs typically biologically sensitive molecules such as peptides, proteins and enzymes. Providing control over drug release rates may also play an important role in cases where conventional administration is no more appropriate. These include situations, which require: the slow release of water-soluble drugs, the fast release of low-solubility drugs, or delivery of two or more agents with the same carrier (Brannon-Peppas, 1997). Figure 2.2 is a brief schematic summary of the benefits of controlled-release delivery.

However, there are some negative aspects which make the controlled release formulation unsuitable for all conditions. For drugs with a small therapeutic ratio or margin of safety, frequent administration is required to keep the drug level in plasma within that narrow range. Therefore, controlled drug release systems (CDRS) may not be feasible in these

cases. In addition, some drugs undergo high first-pass metabolism (first-pass clearance) and are removed in large amounts by the liver during their first passage in the portal blood through the systemic circulation. In controlled release formulations these drugs may suffer from bioavailability. Also there exists a certain risk of systemic drug accumulation for drugs with a long half-life. This accumulation causes slower elimination rate than absorption rate for the drug (Brikett, 1991). Moreover, in cases of oral controlled release administration, if the gastrointestinal tract (GI) interferes with the absorption of the drug, the effectiveness of CDRS will be limited. Some drugs are not suitable options for controlled release due to their mode of action, and their physical limitations. For instance drugs given at some special situations (such as TPA that is given during a heart attack to dissolve blood clotting), are usually not useful for controlled release, since any delay in medication may result in death. When someone is suffering from a headache and immediate relief is needed, using CDRSs may not be the best option. Another example would be drugs which are effective only at specific times during the day. Therefore they should be given at a specific interval, and in accurate dosage, otherwise it could result in unnecessary dose dumping (Kim, 2000).

Finally higher cost of the CDRS compare to conventional forms is known a negative point from economically point of view (Brannon-Peppas, 1997).

### **2.1.3 Criteria of Active Agent and Routes of Administration**

An active agent may be administrated to a patient in different ways. Before preparing a drug release system, it is necessary to select a route for drug delivery in which several factors including physical and chemical properties of the drug, dosage of the drug, desired therapeutic effect, physiologic release of the drug from the delivery system and bioavailability of the drug at the absorption site, should be considered (Robinson, 1997).

Drug properties can influence release characteristics from its delivery formulation.

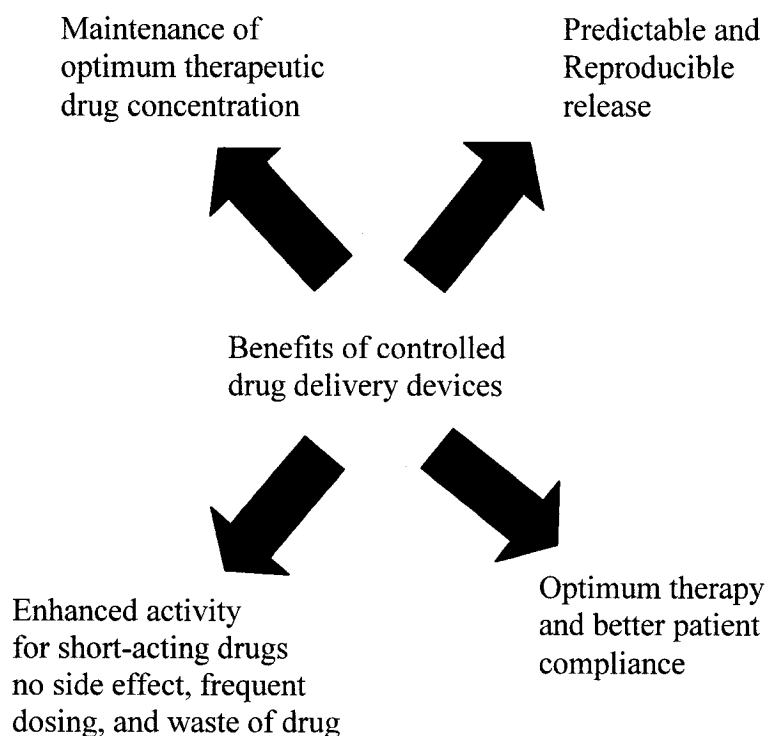


Figure 2.2 Benefits of controlled release systems (Chaubal, 2002).

Any local tissue environment differs from others in terms of pH and enzyme activity. Therefore the physiological properties of administration sites may have an effect on the performance of the drug and its carrier. According to the drug activity in the administrated site, drug half-life, drug solubility, and drug therapeutic index, selecting an appropriate route of administration for each drug seems to be critical (Edlund et Albertsson, 2002). Some common forms of administration are listed below in Table 2.1.

**Table 2.1** Routes of drug administration (Edlund et Albertsson, 2002).

<b>Sites of administration</b>	
Oral	by the mouth
Intraocular	in the eye
Intravenous	injection in a vein
Intra-arterial	injection in an artery
Intraspinal	injection in the spine
Intraosseous	in a bone
Transdermal	through the skin
Topical	on the skin surface
Nasal	to the nose
Instrarespiratory	to the lung
Vaginal	to the vagina

#### **2.1.4 Release of Active Agent**

Several factors are known to be responsible for the overall release of a therapeutic agent. These mechanisms can be listed as:

- 1- Diffusion of the drug molecules through the matrix
- 2- Degradation of the carrier in the case of an erodible polymeric matrix
- 3- Swelling of the carrier, followed by the drug diffusion
- 4- Dissolution of the drug in surrounding medium.

The importance of these mechanisms varies considerably from one system to another (Dimitriu, 2002). One or all of these mechanisms may occur in a given release system. In the first mechanism, the concentration gradient acts as a driving force for the drug diffusion and causes the drug molecules to diffuse out from the matrix (high concentration medium) to the surrounding environment (low concentration medium). For the second and third mechanism, drug particles which are encapsulated within a degradable carrier release as the matrix degrades or swells (Mahato, 2005). The last mechanism has a significant influence at the initial stage of incubation. Drug molecules which are located on the surface or somewhere close to the matrix-medium interface at a very early stage start to dissolve into the fluid medium (Narasimhan, 2001).

The kinetics of drug release depends on the size and shape of the carrier (Siepmann et al., 1999), and importantly, the physical properties of the drug such as molecular weight, and solubility. Diffusivity of a drug through a barrier is significantly influenced by the size of the active agent molecules, the location and distribution of the active agent within the matrix or capsule, the interactions between the drug molecules and matrix, and environmental conditions i.e. temperature and pH of the surrounding medium.

A number of mathematical models have been developed in the last few decades to explain the behavior of the drug during the release process. The objective in developing these models is to calculate *in vitro* drug behavior with modeling. This allows for capability of predicting the drug *in vivo* performance. The dissolution and diffusion models will be discussed extensively.

### **2.1.5 Polymers in Control Release Formulations**

Polymers have been widely used to encapsulate drugs in the form of a reservoir or matrix and to release them in the vicinity of the desired site. The diffusion can occur on a

macroscopic scale, as through pores in the polymer matrix, or on a molecular scale, by passing between polymer chains. Examples of diffusion-release systems are shown in Figures 2.3 and 2.4.

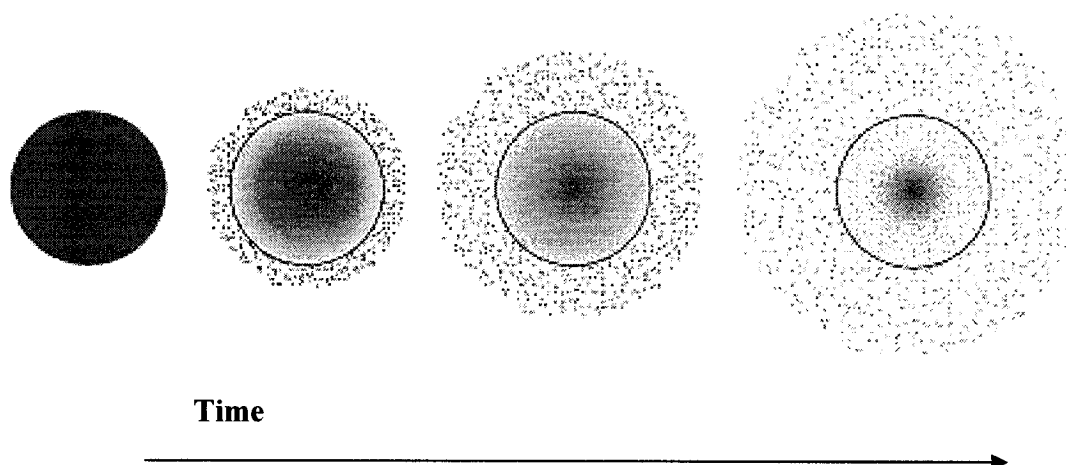


Figure 2.3 Drug delivery from a *Matrix* drug delivery system (Brannon-Peppas, 1997).

A *Matrix* delivery system is basically a polymer which has been mixed homogeneously with a drug. Diffusion occurs when the drug passes through the matrix barrier and reaches the external environment. The drug release rate normally decreases with the passing of time due to a decreasing concentration gradient and a progressively longer distance for the drug molecules to travel.

The *Reservoir* form of delivery system consists of a solid drug, dilute solution, or highly concentrated drug solution within a polymer matrix, which is surrounded by a rate-controlling film or membrane. The polymer layer surrounding the reservoir is the main effective limiting barrier for the release of the drug. Since this polymer layer has a

uniform and non-changing thickness, the active agent diffuses out at a fairly stable rate throughout the lifetime of the delivery system.

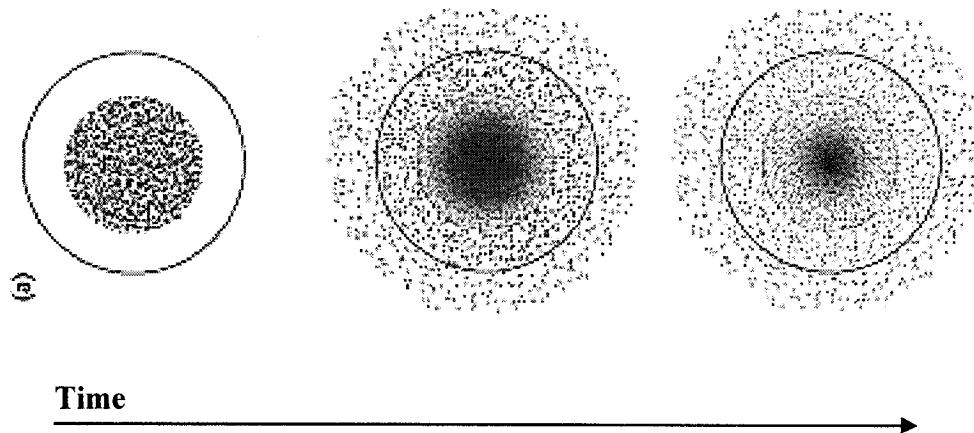


Figure 2.4 Drug delivery from a *Reservoir* drug delivery system (Brannon-Peppas, 1997).

Based on the polymer behavior in physiological environments, polymeric materials can be divided into two groups; biostable and biodegradable polymers. Biostable polymers are largely used in permanent applications where the polymer should keep its physical and mechanical properties for years, e.g. prostheses. Whereas biodegradable polymers are applied in temporary applications such as drug delivery and in scaffolds for tissue engineering (Dimitriu, 2002).

## **2.2 Bovine Serum Albumin (BSA)**

### **2.2.1 Introduction**

BSA is a protein that has been widely used in scientific research and physiological studies as a model active agent. The molecular weight of BSA has been cited differently; however it was revised finally to 66,430 Daltons. BSA is a single polypeptide chain consisting of about 538 amino acid residues and no carbohydrates. At pH 5-7 it contains 17 intrachain disulfide bonds and one sulfhydryl group. One of the major *in vivo* functions of BSA is to serve as a carrier protein (Budnick and Fitzgerald, 2003). Albumin is generally considered as serum albumin or plasma albumin (Bernal and Jellen, 1985). The word albumin is also used to describe a protein or a group of proteins defined by solubility in water. Albumin is the most abundant protein in blood plasma with a typical concentration of 50 g/l. It has been determined that serum albumin is mainly responsible for the maintenance of blood pH. It also plays an important role in regulating the colloid osmotic pressure of blood. Serum albumin functions as a transport protein for numerous endogenous and exogenous substances (Carter and Ho, 1994). Due to its ligand-binding properties, serum albumin has strong affinities for fatty acids, trace metals and ions, as well as for other endogenous and exogenous substances in blood plasma. Besides that very high affinity, a high rate of disassociation, under the right conditions can be observed. The affinity is typically hydrophobic-hydrophobic interaction, but may also be covalent or ionic in nature (Tai, 2004).

### **2.2.2 Structure of BSA**

Serum albumin was postulated to be an oblate ellipsoid with dimensions of  $140 \times 40 \text{ \AA}$  (Figure 2.5).



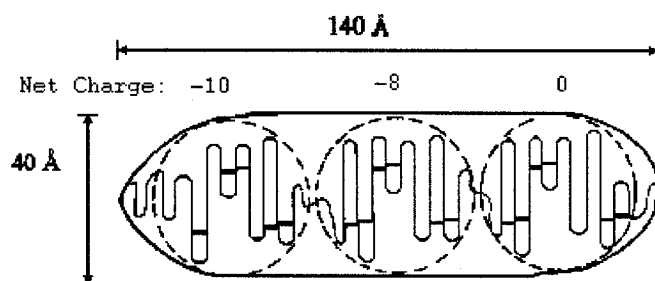


Figure 2.5 Classical perception of the structure of serum albumin (Peters, 1985).

The BSA molecule is made up of three homologous domains (I, II, III) which are divided into nine loops (L1-L9) by 17 disulphide bonds (Figure 2.6).

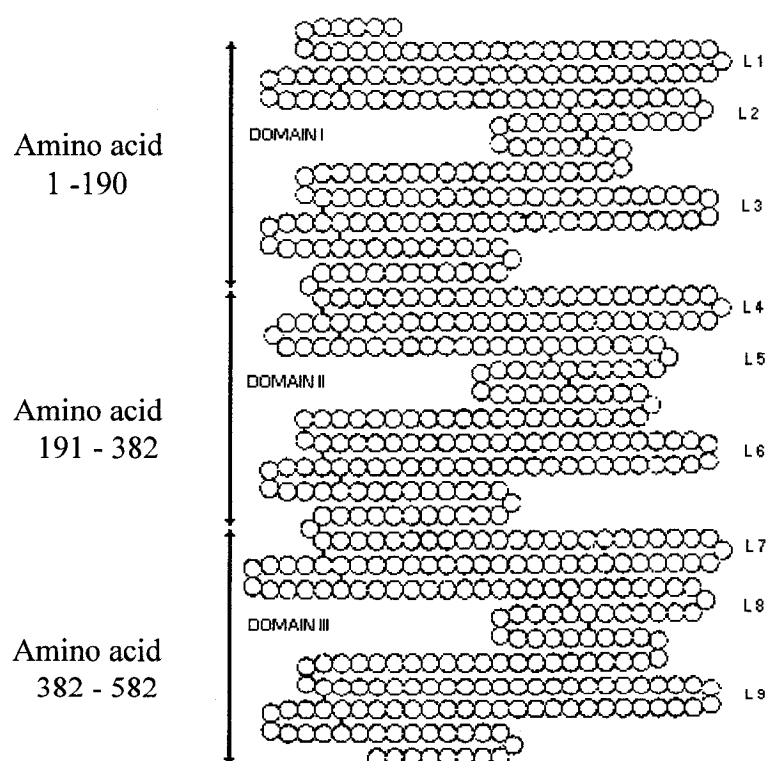


Figure 2.6 Amino acid sequence of BSA (Friedli, 2000)

In BSA the disulphide pairings are located in specific positions, exclusively between helical segments and in their conformation they have a torsion angle of  $\pm 80^\circ$  (Figure 2.7).

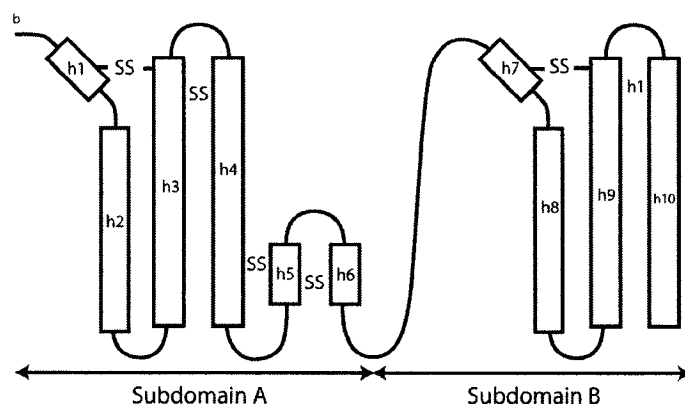


Figure 2.7 Location of disulphide bonds (He and Carter, 1992)

Apparently, in the BSA structure, the majority of disulphides are well protected and most of them are not easily accessible to the solvent. Some BSA properties are summarized in Table 2.2

**Table 2.2** Physicochemical properties of bovine serum albumin (Budnick and Fitzgerald, 2003; Sigma-Aldrich)

Property	BSA
Molecular weight	~ 66500 Daltons
Diffusion constant ( $D_{20}$ )	$5.9 \times 10^7$
Partial specific volume ( $V_{20}$ )	0.733
Sedimentation constant ( $S_{20}$ )	$4.5 \times 10^{13}$ (monomer), $6.7 \times 10^{13}$ (dimer)
Intrinsic viscosity	0.041
Overall dimension ( $A^\circ$ )	$41.6 \times 140.9$
Isoionic point	5.15
Isoelectric point	4.7
Hydrodynamics radius of gyration (nm)	2.65
Net charge per molecule	-17

### 2.2.3 Effect of pH

As a response to pH, reversible isomerization configurations may occur in serum albumin structure. Figure 2.8 summarizes these conformations and their relative pH.

Name of Transition:	Expanded	Fast	Normal	Basic	Aged
	E <-----> F <-----> N <-----> B <-----> A				
pH of Transition:	2.7 <-----> 4.3 <-----> 8 <-----> 10				

Figure 2.8 relationship of isomeric conformations of bovine serum albumin (Foster, 1977)

At pH values lower than 4, BSA turns into its full extension (Figure 2.9, A). This expanded form known as the “E form” has an increased intrinsic viscosity due to the cleavage of the disulphide bonds of BSA (Tu and Breesveld, 2005). F and N BSA conformations involve the unfolding of domain III. The F form as compared to N shows more significant loss in helical content which consequently results in a more extended conformation, higher viscosity and lower solubility. At pH 8-10 albumin is converted to the basic form, and aging the B form for 3-4 days, results in an “Aged Conformation” of BSA (Khan and Salahuddin, 1990).

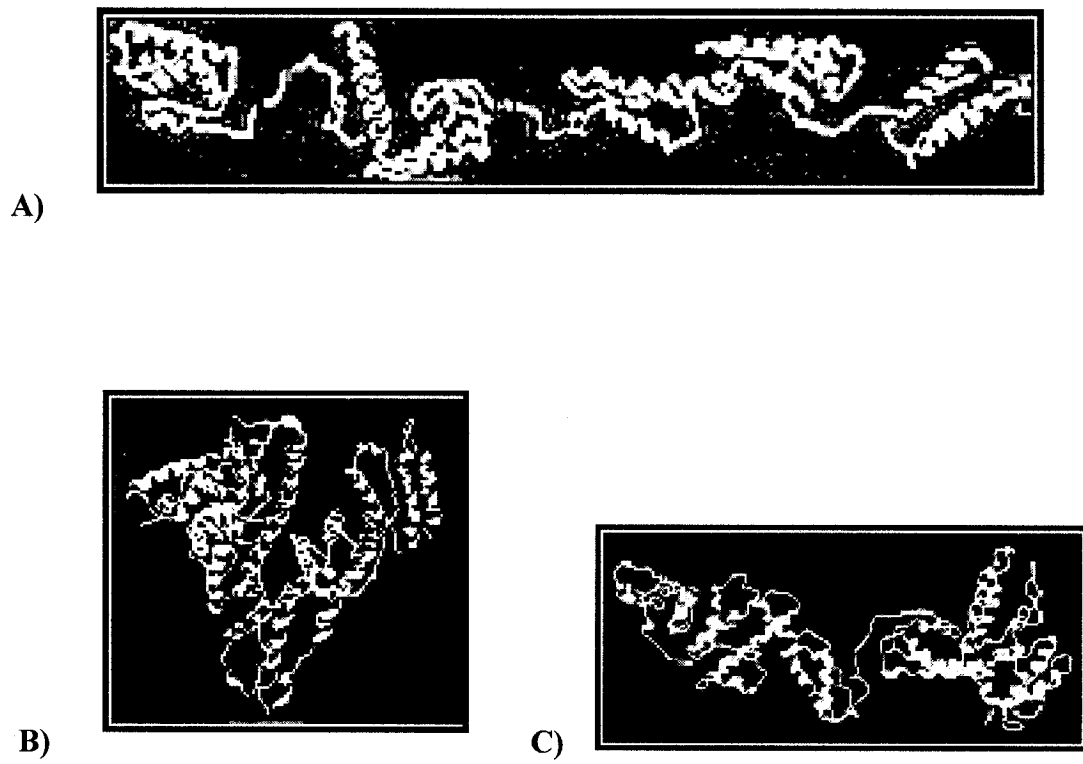


Figure 2.9 diagram of serum albumin in its various conformations; A) E form, B) N form, and C) F form (Carter and Ho, 1994).

#### 2.2.4 Effect of Heat

The three dimensional shape of a protein is critical to its function. A protein consists of one or more chains of amino acids held in place by chemical bonds. These bonds are strong covalent bonds. However most of the bonds that are responsible for the spatial three-dimensional shape of proteins are weak bonds (i.e. hydrogen bond) and can be broken readily by the effect of temperature or chemicals.

When heated, proteins vibrate violently; consequently the weak bonds break and the amino acid chains begin to unfold. The temperatures at which proteins begin to unravel vary enormously from one protein to another. Most proteins unfold at high temperatures, and some unfold even at very low temperatures. Many proteins unfold at temperatures only a few degrees higher than those at which they function. Others are stable to much higher temperatures such as the gluten proteins (Tilton et al., 1992). The driving force for denaturation is the increase in entropy that accompanies the transition from one conformation to another. With increasing temperature the contribution of this entropy increases and becomes more significant, and at some temperature it overcomes the energy effect (when the protein begins to heat denature). It is interesting to consider possible intermediate structures. Since the later stages of denaturation lead to larger increases in entropy, it may be assumed that the intermediate states are relatively unstable, and heat denaturation is often an all-or-none phenomenon. The unfolding of the protein exposes the buried non-polar amino acid residues. Their intermolecular clustering leads to aggregation of the denatured protein. Consequently, heat denaturation is essentially irreversible (Friedli, 1996).

Serum albumin, when heated undergoes several conformational rearrangements, and can be coagulated easily. The first stage of its structural rearrangements is reversible while the second stage is irreversible. This latter stage does not completely destroy the initial ordered structure. Several different results have been reported for the critical temperature at which this protein starts to aggregate. As reported by Wetzel et al., (1980) by heating up to 65°C, first stage of changes in structure occurs. Continued heating above 65°C, results in a second stage of rearrangements. Elsewhere, the critical temperature, found by DSC, is reported to be 58.1°C (Poole et al., 1987), and 62°C (Ruegg et al., 1977). Also, by CD and IR spectroscopy, the onset of denaturation temperature has been reported as 65°C (Wetzel et al., 1980) and 70°C (Clark et al., 1981b).

Thus, it may be concluded that, regardless of the method used for finding the critical temperature, when heated above 55°C, albumin starts to change its conformation. At lower temperatures and close to 55-60°C the conformation changes are reversible, but as heating continues to higher temperature, structural changes enter another stage that are no longer reversible and do not convert to the ordered monomers upon cooling.

### **2.2.5 Effect of Pressure**

Many researchers have studied the effect of pressure on the conformation, stability and functionality of proteins. As a basic concept, pressure effects are governed by Le Chatelier's principal, which indicates that an increase in pressure favors reduction of the volume of the system. The influence of pressure on protein structure and its function has recently been investigated. It had been reported that oligomeric assemblies separate with moderate pressure, however the changes in structure showed high degree of reversibility in most cases (Gross and Jaenicke A., 1994; Silva et al., 2001). Partial loss in the tertiary structure of proteins has been observed under high pressure (Silva et al., 1992). Fluorescence experiments demonstrated that moderate pressure (500-1000 bar) results in a change in structure, however these changes are reversible or can be considered negligible at lower pressure (Marabotti et al., 2006; Mozhaev et al., 1996). High pressure treatments lead to local and global changes in protein structure which finally result in protein denaturation. A pressure of 1 to 2 Kbar is enough to begin protein dissociation. These high pressures change the ensemble of conformers in the conformational space of the proteins therefore inducing change in the average conformation (Inoue et al., 1998). On the other hand, for some cases it was reported that, changes for the tertiary structure recovered after release from  $P > 100\text{MPa}$  to the ambient pressure (Ado et al., 2006). Elsewhere it was observed that the protein conformation under a pressure of 1 to 3 Kbar is stable (McCarthy and Grigera, 2006).

It has been generally accepted that high pressure treatment has a disruptive effect on the hydrophobic interactions of proteins. Formation of hydrophobic contacts proceeds with an increase in volume. Therefore a decrease in hydrophobic effects with a rise in pressure is expected (McCarthy and Grigera, 2006; Mozhaev et al., 1996). On the other hand, hydrogen bond formation is associated with small volume change. Thus, hydrogen bonds are not sensitive to pressure. This results from the smaller inter-atomic distances in the hydrogen-bonded atoms (Dickinson and Pawlowsky, 1996; and Mozhaev et al., 1996).

As a conclusion, one may say that hydrostatic pressures results in new protein dimensions and changes the functionality and properties to various levels. Depending on the pressure range and exposure time of protein to pressure, these changes can be either reversible or stable.

## **2.2.6 Functional Properties of BSA**

### **2.2.6.1 Foaming**

The formation and stabilization of gas bubbles in a liquid may be defined as foaming. In other words, a mass of air or gas bubbles in liquid films, or an accumulation of fine bubbles formed in or on the surface of a liquid as a result of agitation is known as a foaming phenomenon. Proteins at liquid interfaces have essential roles in many biological systems and industrial product formulations. Unlike some surfactants, proteins are able to form a continuous cohesive network at interfaces via complex intermolecular interactions (Friedli, 1996). Several studies have demonstrated that the foamability of proteins is basically related to their ability to create films at the air-water interface (Okumura et al., 1990). Disulfide bonds in the protein structure play important roles in function of proteins. Foaming is an important functional property of proteins which occurs under the

influence of disulfides. Foam stability is affected by the tertiary structure of proteins, which is stabilized by disulfide bonds (Yu and Damodaran, 1991).

#### **2.2.6.2 Gelation**

The Collins English Dictionary defines a gel as a semi-rigid jelly-like colloid in which liquid is dispersed in a solid. Gelation is known to be the conversion of a liquid to a gel state; the point at which a dramatic increase in viscosity occurs due to initial network formation. Various factors cause protein gelation, such as protein type, protein concentration, temperature, ionic strength, and pH. Probably the most important factor in gelation is the heating temperature. BSA forms soluble aggregates when heated above a certain temperature. Soluble aggregates are formed at the early stages of heating, but further heating results in a rigid gel network (Matsudomi et al., 1993). A two-step mechanism for gelation was suggested for proteins (Ferry, 1948); (1) unfolding or dissociation of the protein molecules, (2) an aggregation step in which association or aggregation reactions occur, resulting in gel formation.

#### **2.2.6.3 Ligand –Binding**

A ligand is simply a molecule which interacts with a protein, by specifically binding to the protein. The importance of protein ligand binding in biological systems should not be underestimated. Any organism must have a mechanism of interacting with its environment. Binding of a ligand to a protein is reversible. The ligand binds to the protein at a specific site. This site has the necessary physical characteristics to make ligand binding favorable (Figure 2.10).



BSA is the principal carrier of fatty acids that are otherwise insoluble in blood plasma. As a multifunctional transport protein, albumin has a high affinity for fatty acids, negatively charged aromatic compound, nitric acid and various metals such as Cu (II), Ni (II), Hg (II), Ag (II), and Au (I) (Stamler et al., 1992).

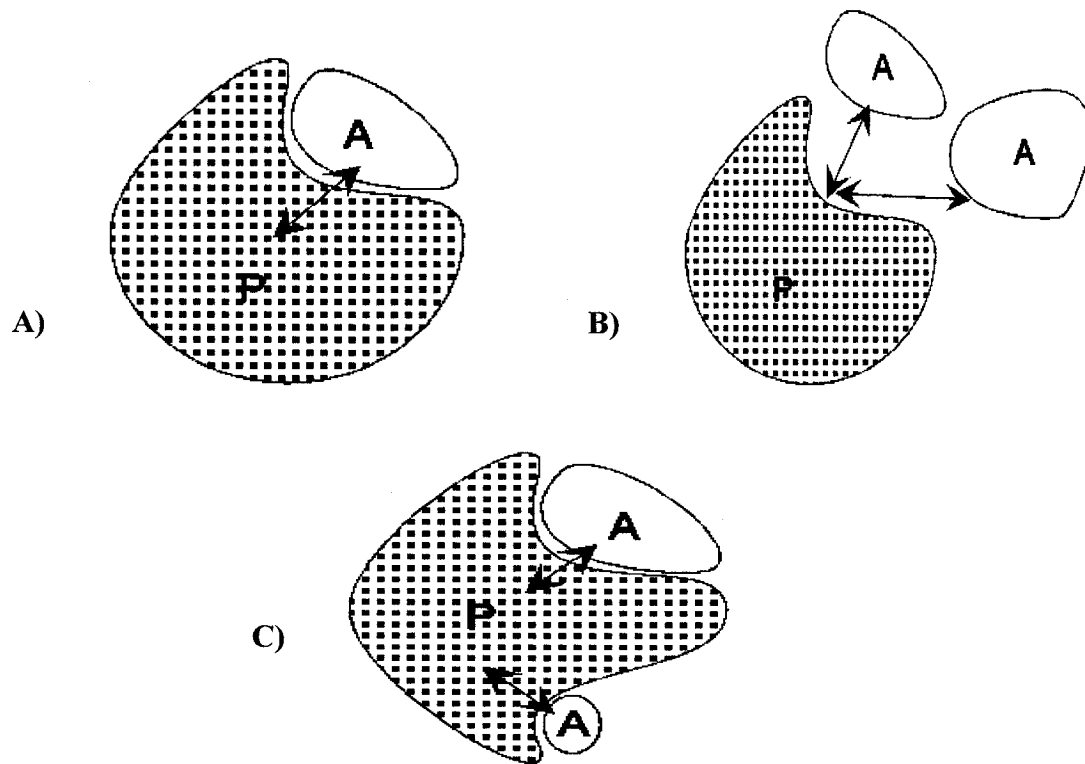


Figure 2.10 Protein P binding to ligand A. The double arrow stands for a reversible binding. A) Single binding, B) Two different ligands compete for the same binding site, C) Two ligands bind to different sites on the protein.

## 2.3 Spectrophotometry

Spectrophotometry is the quantitative study of electromagnetic spectra. It involves the use of a spectrophotometer that deals with visible light, near-ultraviolet, and near-infrared wavelengths. A spectrophotometer is a photometer (a device for measuring light intensity) that can measure intensity as a function of the color, or more specifically, the wavelength of light. Spectrophotometers can be classified by different parameters, for example: the wavelengths they work with, the measurement techniques they use, the way they acquire a spectrum, and the sources of intensity variation designed for measurements. The most common application of spectrophotometers is the measurement of light absorption. The most widely used spectrophotometers are used in the UV and visible regions of the spectrum. The spectrophotometer quantitatively measures the fraction of light that passes through a given solution. As shown in Figure 2.11, light, produced typically by a deuterium gas discharge lamp, is guided through a monochromator which picks light of one particular wavelength out of the continuous spectrum. Light passes through the sample that is being measured, and the intensity of the remaining light is measured with a photodiode or other light sensor. The transmittance for the collected wavelength is then calculated.

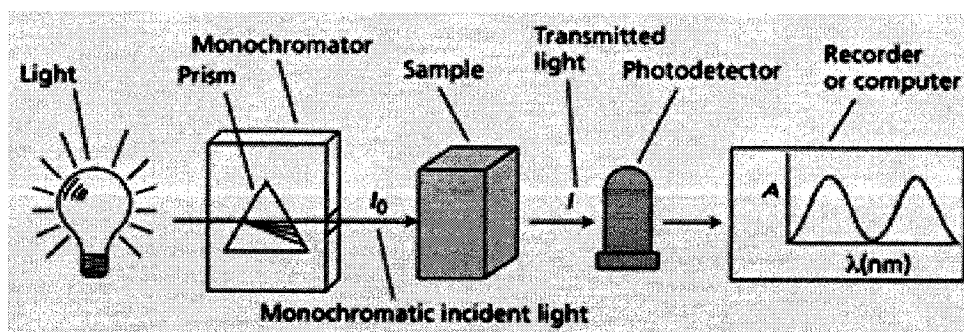


Figure 2.11 Schematic view of a spectrophotometer

### 2.3.1 Beer – Lambert Law

Ultraviolet-visible spectrophotometry (UV/ VIS) uses light in the visible and adjacent near ultraviolet (UV) and near infrared (IR) ranges. In this region of energy space, molecules undergo electronic transitions. UV/VIS spectroscopy is used to determine the concentration of a solution by following the Beer – Lambert law. The Beer-Lambert law states that the absorbance of a solution is directly proportional to the solution's concentration.

$$A = \alpha c \quad (2.1)$$

$$\frac{I_1}{I_0} = 10^{-A} = 10^{-\alpha c} \quad (2.2)$$

Where,

$$A = \log_{10} \left( \frac{I_0}{I_1} \right) \quad (2.3)$$

$$\alpha = \frac{4\pi k}{\lambda} \quad (2.4)$$

Here ,  $A$  is absorbance,  $I_0$  is the intensity of the incident light,  $I_1$  is the intensity after passing through the material,  $l$  is the distance that the light travels through the material,  $c$  is the concentration of absorbing species in solution,  $\alpha$  is the absorption coefficient or the molar absorptivity of the absorber,  $\lambda$  is the wavelength of the light, and  $k$  is the extinction coefficient.

Thus it is necessary to know how the absorbance changes with concentration. This can be taken from references (tables of molar extinction coefficients), or more accurately, can be determined from a calibration curve.

### 2.3.2 Protein Spectrophotometry

Using spectrophotometry, the quantitative analysis of nucleic acids and proteins is a routine method in many laboratories. It involves absorption measurements in the ultraviolet and in the visible range. Proteins in solution absorb ultraviolet light with maximum absorbance at 280 and 200 nm. Amino acids with aromatic rings (i.e., tryptophane, tyrosine, and phenylalanine) are the primary reason for the absorbance peak at 280 nm. Peptide bonds are primarily responsible for the peak at 200 nm. Since secondary, tertiary, and quaternary structures affect absorbance, factors such as pH and ionic strength can alter the absorbance spectrum.

The  $A_{280}$  method may be used within concentrations of up to approximately 4 mg/ml (3.0 A). This method is simple and rapid, but may be disturbed by the parallel absorption of non-proteins (e.g. DNA, RNA). DNA, RNA, oligonucleotides and even mononucleotides that can be measured directly in aqueous solutions in a diluted or undiluted form at 260 nm, while proteins are measured directly at 280 nm. The 260:280 nm absorbance ratio is commonly used to assess the purity of protein with respect to DNA contamination, since protein (in particular, the aromatic amino acids) tends to absorb at 280 nm (Table 2.3). The method was established in 1942, when Warburg and Christian showed that the ratio is a good indicator of nucleic acid contamination. Unfortunately, the reverse is not true since it takes a relatively large amount of protein contamination to significantly affect the 260:280 ratio. This difference occurs due to the much higher extinction coefficient of nucleic acids at 260 nm and 280 nm, compared to that of proteins. Thus, even relatively high concentrations of protein have little influences on the 260 and 280 absorbance.

Protein contamination can not reliably be assessed with a 260:280 ratio, and results in only small errors to DNA estimation (Glaser, 1995).

**Table 2.3** Relative nucleic acid contamination and protein contamination with various 260:280 ratios (Glaser, 1995)

% Protein	% Nucleic Acid	260:280 ratio
100	0	0.57
95	5	1.06
90	10	1.32
70	30	1.73
% Nucleic Acid	% Protein	260:280 ratio
100	0	2
95	5	1.99
90	10	1.98
70	30	1.94

The 260:280 nm absorbance ratio, relates the protein concentration to a factor of “F”. The tabulated F values, determine the nucleic acid percentage in the protein. Therefore the concentration of sample can be calculated by the following equation, where  $b$  is the distance that the light traveled through the material (Mount Allison University, 2003). A table in Appendix B presents the relation between the F factor and 280:260 ratios.

$$C_{protein} \left[ \frac{mg}{ml} \right] = F (A_{280}) \left( \frac{1}{b} \right) \quad (2.5)$$

## 2.4 Co-continuous structure and its controlling parameters

### 2.4.1 Introduction to Co-Continuity

Porous polymer materials are of great interest due to their extensive applications and challenges. Polymer blending has established a route to develop these high performance materials. Most polymer blends form an immiscible mixture. This immiscibility results from thermodynamics reasons, mainly an unfavorable enthalpy of mixing and negligible entropy. Two basic types of morphology can be characterized; dispersed droplet/matrix morphology and the co-continuous morphology. A droplet/matrix morphology occurs when the dispersed phase is at a low concentration in a binary polymer blend. Increasing the concentration of the dispersed phase results in a phase inversion, the minor dispersed phase becomes a major phase of the blend and the matrix becomes the dispersed phase. Near the phase inversion point, the co-continuous microstructure of the blend can be obtained. This particular structure can be described as a fully interpenetrating polymer networks with continuous pathways (Figure 2.12)

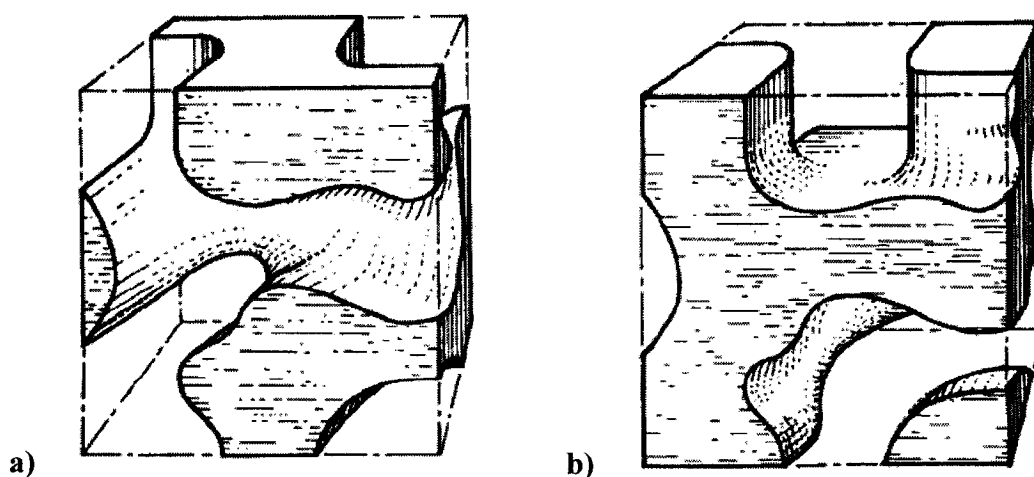


Figure 2.12 Co-continuous structure for a binary blend A/B a) phase A has been extracted  
b) phase B has been extracted (Gregen et al., 1996)

Co-continuous structures are usually formed within a composition region of the phase inversion. The width of this region mainly depends on the viscosity ratio of the components and interfacial tension (Figure 2.13).

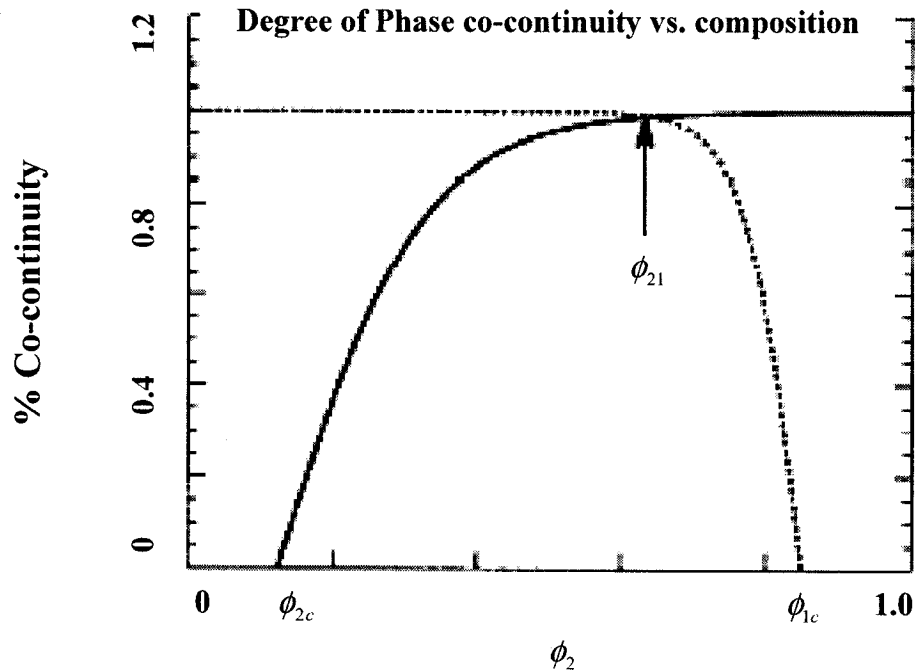


Figure 2.13 Schematic representation of the phase co-continuity-composition dependence (Utracki, 1991)

Many researchers have carried out a fundamental research on the co-continuous morphology and its application (Lyngaae-Jorgensen et al., 1991; 1999 Grgen et al.; 1996, Mekhilef et al., 1996; 1997). Polymer blends with a co-continuous morphology have gained much attention due to their potential for applications, such as: barrier properties, conductive polymers and impact resistance materials (Tchoudakov et al., 1996; Levon et al., 1993; Gubbels et al., 1994). PA6/PPE blends, PP/PU blends,

conductive modified PP/PE/EPR blends, and co-continuous blends based on PA6/ABS are a few examples of commercial co-continuous blends.

In this research project, a co-continuous porous structure was used as a polymeric device for drug delivery. Previously, our research group advanced a melt-blending technique to fabricate highly controlled polymeric structures. As number of fundamental studies have been carried out to control this interconnected porosity (Li et al., 2002; Sarazin and Favis, 2003; Yuan and Favis, 2004; Sarazin et al., 2004). It was shown that the melt-blending of two immiscible polymers and the consequent selective extraction of one of the phases, leads to a interconnected porous structure. It was also shown that a range of parameters is able to control the porosity, morphology and pore diameters. These parameters and their influence will be discussed in the following sections.

#### **2.4.2 Morphology Control in Co-Continuous Structures**

The control of polymer blend morphology, which is the control of shape, size and size distribution of the minor phase in an immiscible binary polymer blend, is affected by several basic parameters. These important factors in determining the size and shape of the minor phase are: composition, interfacial tension, time of mixing, shear rate, elasticity of the component and viscosity ratio (ratio of viscosity of the dispersed phase to that of the matrix). Processing parameters such as mixing time and shear rate have less influence in forming a co-continuous structure. Thus, they are not considered as controlling parameters in co-continuous morphologies. In the next sections, the influence of certain effective parameters in forming a co-continuous morphology will be discussed.



### 2.4.2.1 Influence of Composition on the Morphology

As mentioned before, the droplet/matrix and co-continuous morphology of a polymer blend highly depends on the composition of the component. It was shown for blends of polycarbonate/polyethylene, polypropylene/polycarbonate, and polyamide/polyolefin that the composition has a significant effect on their morphology (Favis and Chalifoux, 1988; Favis and Willis, 1990). However, within the co-continuous region, composition is not an effective parameter to control the size of the pores. Thus, it is important to investigate the parameters that affect the particle size within the co-continuous region at the given composition. These factors are the interfacial tension, viscosity ratio, and static annealing.

### 2.4.2.2 Component Viscosity and Viscosity Ratio

It is generally accepted that the viscosity of the components and their viscosity ratio affects the blend morphology and the critical composition of the phase inversion (Favis and Chalifoux, 1987; Jordhamo et al., 1986). Avgeropoulos et al. (1976) noted that for components with similar viscosity, smaller particle sizes are formed in blends whereas, pore size increases with an increase in viscosity ratio. A number of equations has been proposed to relate the viscosity to the composition at which phase inversion appears;

$$\frac{\phi_1}{\phi_2} = \frac{\eta_1(\gamma)}{\eta_2(\gamma)} \quad (\text{Miles et al., 1988}) \quad (2.6)$$

$$\frac{\phi_1}{\phi_2} = 1.22 \left( \frac{\eta_1(\gamma)}{\eta_2(\gamma)} \right)^{0.29} \quad (\text{Ho et al., 1990}) \quad (2.7)$$

$$\frac{\phi_1}{\phi_2} = \frac{\eta_1}{\eta_2} F\left(\frac{\eta_1}{\eta_2}\right) \quad (\text{Metelkin et al., 1984}) \quad (2.8)$$

where,  $\phi$  is the composition and  $\eta$  is the viscosity.

These equations were unable to systematically describe experimental results. These relations had neglected the influence of the classical parameters governing the formation of dispersions, such as shear rate, viscosity and interfacial tension. Finally, Willemse et al. (1998) reported an equation relating the critical composition of the minor phase at the co-continuous region to the matrix viscosity, interfacial tension, shear rate and phase dimension.

$$\frac{1}{\phi_{d,cc}} = 1.38 + 0.0213 \left( \frac{\eta_m \gamma}{\sigma} R_0 \right)^{4.2} \quad (\text{Willemse et al., 1998}) \quad (2.9)$$

#### 2.4.2.3 Interfacial Tension and Compatibilisation of the Interface

The interfacial tension between two liquid phases in a polymer blend has a major influence on the blend morphology. Lower interfacial tension favors the formation and the stability of the co-continuous structures. Coarsening depends on the interfacial tension and can be reduced by increasing the interfacial reaction by adding compatibilizer. As was stated previously by Verhoogt et al. (1994) and Willemse et al. (1999), binary polymer blends with low interfacial tension are known to have a large co-continuity region.

One way to improve the interfacial adhesion and reduce the interfacial tension is achieved by adding a suitable modifier to the blend. Blends are compatibilized to strengthen the interface and consequently, achieve a finer morphology (Matos and Favis, 1995; Willis and Favis, 1988). These compatibilizers are usually block or graft copolymers whose segments are often composed of the homopolymer phases having an affinity to each phase of the blend. Compatibilizers reduce the interfacial tension and prevent coalescence by steric stabilization of the structures (Elemans et al. 1990; Mekhilef et al., 1997). It was noted that efficiency of compatibilizers in decreasing the particle size in the blend is basically related to their capacity in limiting the coalescence.

Elemans et al. (1990) showed that the stability of a molten polymer thread increased by adding a diblock copolymer in blend. They reported a reduction in the interfacial tension by factor of 4. Adding a small quantity of a diblock copolymer to an incompatible polymer blend suppresses coalescence, achieved through stabilizing the interface resulting in a smaller particle size and a narrower particle size distribution (Sundaraj and Macosko, 1995; Bourry and Favis, 1998; Li et al., 2002).

#### **2.4.2.4 Annealing**

Static annealing is a processing factor which has a controlling role on the size of the domains in a given polymer blend. As reported by Yang and Han, (1996), the average domain size increases and its size distribution broadens with increasing annealing time. It is also reported that annealing at a higher temperature induced a much more rapid rate of domain growth. By increasing the annealing time or the annealing temperature, the probability of droplet motion and coalescence may increase and results in growth of the average domain size and its size distribution (Figures 2.14 and 2.15). Sometimes, the increase in phase size by static coalescence, changes the co-continuous structure into droplet/matrix morphology. These cases are the ones having a co-continuous structure at asymmetric compositions. The small co-continuous region associated with such blends, more rapidly disintegrates compared to the blends with symmetric composition which usually have a wider co-continuity region.

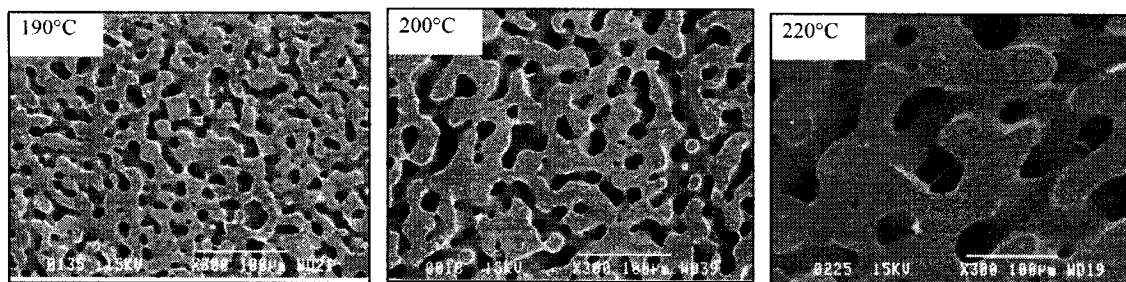


Figure 2.14 Effect of annealing temperature on domain size and size distribution of a binary blend (Sarazin et al., 2004)

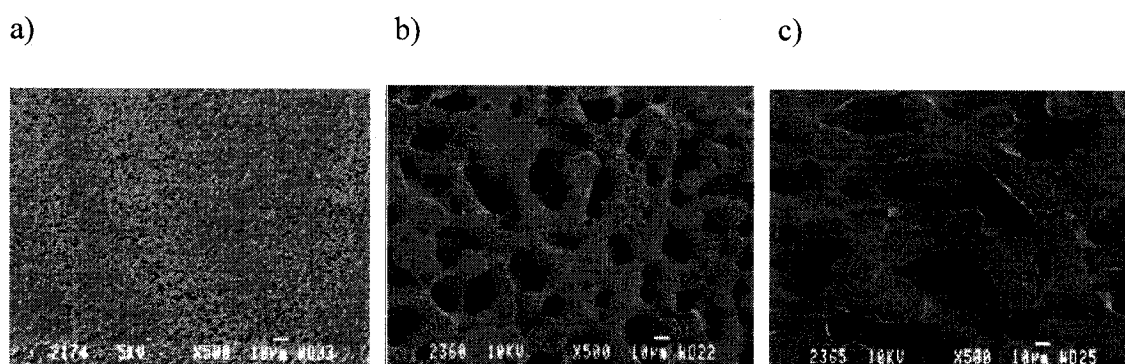


Figure 2.15 Effect of annealing time on domain size and size distribution, a) non-annealed, b) annealed for 2 hours, c) annealed for 4 hours (Sarazin et al., 2004)

## 2.5 Drug Encapsulation Techniques

Polymers are the most widely used materials for controlled release formulations due to their diversity in architecture and chemistry. As a specific advantage, polymers present opportunities to modulate the properties in drug delivery systems, and also meet important criteria of biodegradability and biocompatibility. During the last few decades, much polymer chemistry was dedicated to the synthesis, characterization, application, and evaluation, of new biocompatible and biodegradable polymers.

Polymeric drug delivery systems (PDDS) include: designed macromolecular vehicles for drug delivery (Langner and Ugorski, 2000; Sinha and Kumria, 2001), polymer–drug conjugates (Kolhe et al., 2004; Duncan et al., 2006), polymeric micelles containing covalently bound drugs (Kwon and Kataoka, 1995; Huh et al., 2005), and macro and nano spheres matrix. The clinical applications of a macro sphere matrix and its outcomes seem promising and recently are of great interest to researchers.

Encapsulation of therapeutic proteins in biodegradable, biocompatible polymeric capsules is considered a safe way for delivering enzymes and protein drugs. Unprotected therapeutic drugs and proteins show a short in-vivo half-life and antigenic properties when they are introduced into the body. For this reason, protection of the drug from the hostile immunological system of the body is necessary in order to efficiently deliver the drugs. Polymers of synthetic and biological origin have been used effectively in the delivery of various agents (especially proteins) to different sites in the human body (Jeong et al. 1998; Aboubakar et al. 1999). Entrapment of drugs such as proteins in nano and macro particle carrier systems is carried out through various approaches. A number of methods have been presented for drug encapsulation including coacervation, solvent evaporation, polymer-polymer incompatibility, *in situ* polymerization, interfacial polymerization at liquid-liquid and solid-liquid interface, spray drying, fluidized bed, centrifugal force process, and desolvation or extractive drying. From the above list, there are three common techniques used specifically in controlled release systems; 1- coacervation, 2- solvent-evaporation techniques, 3-spray-drying. A hot-melt method and microencapsulating processed by fluidized bed coating have also been reported (Nuwayser and Nusefora, 1986). However these latter techniques are not popular due to a number of limitations and level of difficulties. For example in the case of hot-melt techniques only a limited number of substances can be used. In the following sections these methods are introduced briefly.

### 2.5.1 Coacervation

Chemical microencapsulation is most frequently achieved by coacervation. Coacervation is the phase separation into two liquid phases in colloidal systems. The more concentrated phase in the colloid system is the coacervate, and the other phase is the equilibrium solution. In this technique the coating precipitates onto the drug droplet, much like the crystal formation in a supersaturated solution. Coacervation consists of three stages under constant agitation (Bakan, 1975).

*Step 1: Formation of three immiscible chemical phases:*

The solution must be formed with three immiscible chemical phases; (i) a liquid phase (solvent) (ii) a core material phase (active ingredient) and (iii) a coating material phase (polymer). In order to form the three phases, the core material is dispersed in a solution of the coating polymer, the solvent for the polymer is the liquid phase. The coating material phase, an immiscible polymer in a liquid state, is formed by using one of the methods of phase separation in the coacervation technique, which includes changing the temperature of the polymer solution, adding salt, adding a non-solvent, adding incompatible polymer to the polymer solution, and inducing a polymer-polymer interaction.

*Step 2: Depositing the liquid polymer coating on the core material:*

This is accomplished by controlled, physical mixing of the coating material (solution) and the active agent is in the solvent. Deposition of the liquid polymer coating around the active agent occurs if the polymer is adsorbed at the interface, formed between the active agent and the solvent, and this adsorption phenomenon is a prerequisite to the effective coating. Continuing the deposition of the coating material is promoted by a reduction in the total free interfacial energy of the system resulting from the decrease of the coating material surface area during the coalescence of the liquid polymer droplets.

*Step 3: Rigidizing the coating:*

This is usually done by thermal, cross linking or desolvation techniques, to form a self sustaining microcapsule. Particles produced by this method are capsular in structure. Thus, coacervation may be used for entrapment of liquids and oils. Capsule size typically ranges from 20 to 1000  $\mu\text{m}$ . Although core (drug) contents are often 80-90%, drug loading inside the capsules is much lower.

**2.5.2 Solvent Evaporation Techniques**

Several solvent evaporation techniques (Jalil and Nixon, 1990; Watts et al., 1990) have been used for drug encapsulation including O/W, W/O/W, O/O, and W/O/O. This encapsulation technology involves removing a volatile solvent from the above emulsions (Thies C., 1992; Mathiowitz et al., 1999). In most cases the shell material is dissolved in a volatile solvent. The active agent is dissolved, dispersed, or emulsified into this solution. To select the dispersed phase solvent, some factors must be considered; 1- ability to dissolve the polymer, 2- immiscibility with the continuous phase, 3- high volatility, and 4- low toxicity.

The processing temperature has a great impact on microspheres morphology. At high temperatures, the rate of precipitation is too fast, the solvent boils out of emulsion droplets and consequently results in highly porous spheres (Jalil and Nixon, 1990). The type and the concentration of emulsifier and also the viscosity of the phase affects the microspheres size, shape, porosity and encapsulation efficiency. The size of microcapsules produced by solvent evaporation processes ranges from below 1  $\mu\text{m}$  to over several hundred micrometers. This technique is used often to form drug-loaded microparticles from biodegradable materials (Okada, 1997, Thies, 1992).

The oil-in-water (O/W) solvent evaporation technique is among the most popular microencapsulation methods due to its easy processing. The therapeutic substance and the

polymer are dissolved in a volatile organic solvent. This oil phase is then added to the water containing a stabilizer under vigorous stirring. The immiscibility of two phases allows for the formation of a stable emulsion. The role of stabilizer (also referred to as emulsifier) is to prevent the droplets from coalescence. The polymer precipitates as the solvent is removed by evaporation. The hardened spheres are subsequently separated from the aqueous phase, washed and dried. A schematic illustration of this method is provided in Figure 2.16.

The double emulsion solvent evaporation technique, water-in-oil-in-water (W/O/W), was developed for the entrapment of water soluble drugs. In this method an aqueous solution of therapeutic substance is emulsified in an organic polymer solution. This water-in-oil emulsion is further emulsified into a continuous stabilized water phase. As the organic solvent is removed by evaporation, the polymer hardens and forms microspheres. This W/O/W encapsulation technique has been employed for encapsulation of bioactive macromolecules like proteins (Perez-Rodriguez et al., 2003; Pistel and Kissel, 1999) vaccines (Cleland et al., 1997; Hunter et al., 2001), and peptides (Couvreux et al., 1997; Hino et al., 2000).

The above techniques are not suitable for polymers which tend to hydrolyze such as polyanhydride. This is due to the induced degradation and consequent molecular weight loss caused by water-containing emulsions (Watts et al., 1990). Oil-in-oil (O/O) or water-in-oil-in-oil (W/O/O) solvent evaporation techniques may be more useful options (Mathiowitz et al., 1990). The advantage of O/O and W/O/O methods is using oil in the continuous phase. When oil is used as the continuous phase, it can prevent the partitioning effect of the drug during the preparation process.



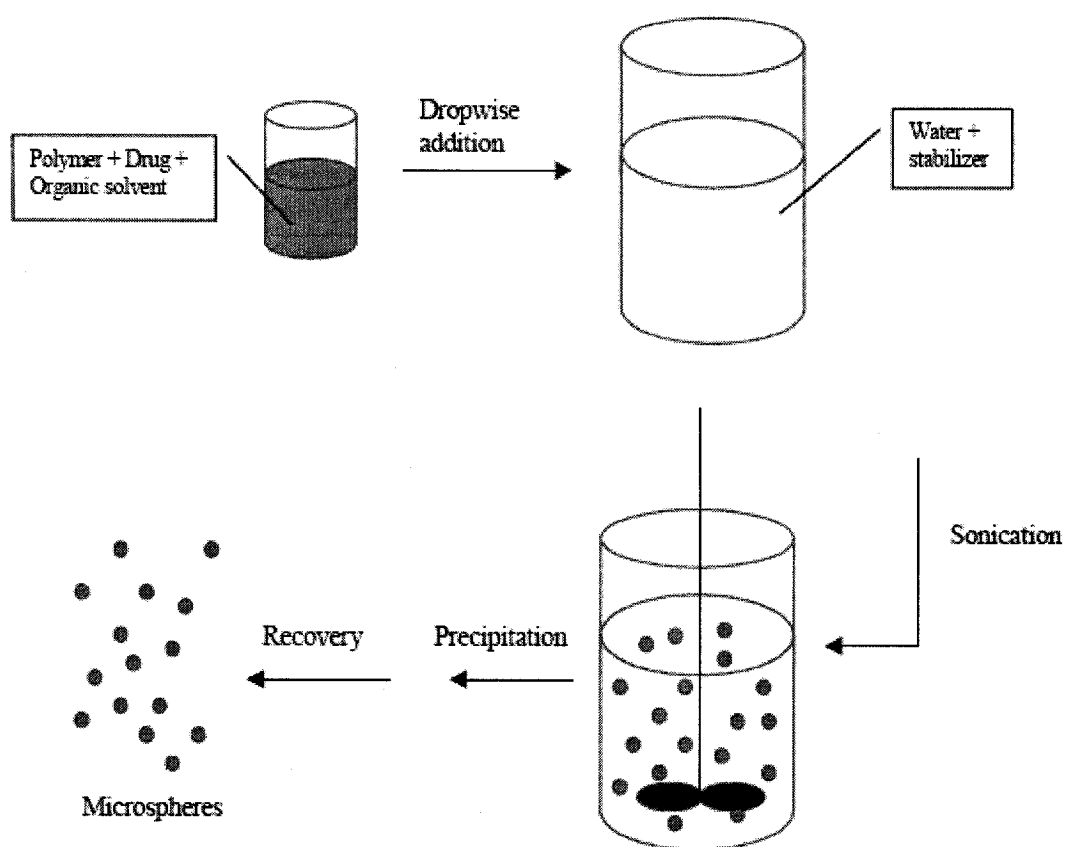


Figure 2.16 Schematic illustration of microspheres prepared by the oil-in-water solvent evaporation technique

The O/O technique is quite similar to the W/O technique. However in O/O both the polymer and the drug should be dissolved in an organic solvent (oil), and then this organic phase should be emulsified in a second stabilized organic phase. The W/O/O technique, also known as in-oil drying, involves an emulsification of aqueous solution of the drug in organic polymer solution and then this emulsion is added to the stabilized oil phase. Microparticles are formed when the organic solvent is extracted to the oil phase.

When solvent evaporation techniques are used to prepare the desired microencapsulation, various factors influence the final structure and morphology of the products (microspheres). The solvents, phase viscosity, the ratio of dispersed phase to the

continuous phase, mixing speed, processing temperature and processing time, all may affect the structure to some extent.

### **2.5.3 Spray Drying**

Spray drying is the preferred industrial technique of preparing the microspheres. The spray drying encapsulation process consists of spraying the mixture of the drug and the polymer (core and shell material) into a heated chamber. The chamber is heated by hot gas. Typically this hot gas is air; however, for sensitive pharmaceuticals and solvents like ethanol, oxygen-free drying is required. Therefore hot nitrogen gas is used instead. Due to the high temperature inside the chamber, rapid desolvation occurs and microcapsules are produced (Re, 1998; Wendel et Selik, 1997). The first step is to prepare a solution of the shell material or the polymer in a solvent that will be spray dried. In principle, any shell material can be used, but since water is the most common solvent for spray drying, water-soluble polymers such as starch and gelatin are often used. The second step is to disperse the drug into the polymer solution. Usually the drug is hydrophobic or water immiscible oil. An appropriate emulsifier should be used to facilitate the formation of the emulsion. Once the suitable emulsion is prepared, it is pumped through an atomizer device that produces fine droplets into the main hot chamber. The small droplets have high surface area and rapidly convert to a fine powder by desolvation in the chamber. Capsules produced by spray-drying mostly have a diameter of 10 to 40  $\mu\text{m}$ . The capsule geometry varies from an irregular to a spherical shape. Drug loading for commercial spray drying is normally between 20-30%; however, loadings up to 50% have been reported from experimental works.

Recently, biodegradable shell materials have received much attention. Spray drying is a convenient method of drying for heat-sensitive biological materials such as enzymes (Shahidi and Han, 1993; and Wang et al., 2004) and pharmaceutical proteins (Faldt and Bergenstahi, 1996; Carrasquillo et al., 2001) with minimal loss of activity.

#### 2.5.4 Polymer–Polymer Incompatibility

In this technique, two chemically different polymers are used. One of the polymers is designed to be the shell of microspheres. This polymer must be preferentially adsorbed by the active agent. These polymers should be incompatible when dissolved in the common solvent. When the insoluble active agent is dispersed into this mixture, it is spontaneously coated by a thin film that contains the shell polymer. Microcapsules are obtained by desolvating this coating polymer either by chemical cross-linking or addition of non-solvent (Mathiowitz et al., 1999; Bakan, 1994).

#### 2.5.5 Interfacial Polymerization

Figure 2.17 illustrates this type of encapsulation process, where X and Y are reactants and  $(X-Y)_n$  is the polymerization product. A key feature in this technique is that the reactant for the interfacial polymerization reaction is responsible for the shell formation. These two reagents are present in two mutually immiscible liquids. Reactant X is dissolved in the core material (active agent). This mixture is then emulsified in an aqueous phase that contains an emulsifier. Reactant Y is added to this aqueous phase. The two reactants must diffuse to the interface to react and initiate the interfacial polymerization and formation of the shell. Once the shell is formed, it becomes a barrier to diffusion and limits the rate of interfacial polymerization reaction.

Several studies have been made on this method of drug encapsulation. Aboubakar, et al. (1999) reported insulin encapsulation in capsules obtained by interfacial polymerization. They observed a high encapsulation efficiency and biological activity of encapsulated peptides. Another group prepared nanocapsules with an aqueous core containing bovine serum albumin (BSA) by interfacial polymerization. They stated that encapsulation efficiency and drug loading depended on the initial BSA concentration in an aqueous phase (Li et al., 2003).

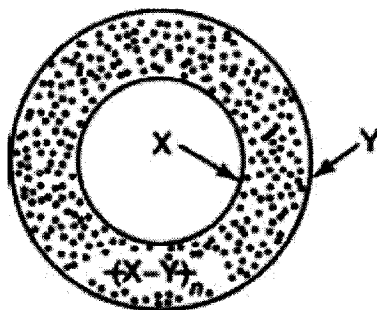


Figure 2.17 Schematic diagram of the interfacial polymerization technique for drug encapsulation

### 2.5.6 Fluidized-Bed Coating

Fluidized-bed encapsulation technology involves spraying shell material (polymer) in the form of a solution or a hot-melt onto the solid particles suspended in a stream of heated gas which usually is air (Arshady, 1999; Sparks et al., 1999). Among several types of fluidized-bed units, top and bottom spray units are the most popular candidates for microcapsule preparation. In top-spray units, hot melt shell materials are sprayed into the top part of the fluidized bed of the solid particles. The coated particles are then cooled and form capsules with solid shells. Since the sprayed shell material moves countercurrent to the gas stream, the top-spray units are not recommended for solutions due to high evaporation of solvent and poor coating quality. Therefore, bottom-spray units are mostly used for solutions, in which the solution is sprayed to the bottom of the column. The freshly coated particles are carried up in the coating chamber where the coatings solidify due to the solvent evaporation. This technology is especially used to encapsulate solid pharmaceuticals. Generally capsules larger than 100-150  $\mu\text{m}$  can be produced by this technique.

## 2.6 Diffusion (diffusion coefficient calculation & drug release kinetics)

Drug diffusion from a polymeric matrix into an external medium of finite volume is an important issue in the drug controlled release system. When the drug carrier is exposed to the liquid environment, the active agent located within the matrix, gradually dissolves into the liquid medium and diffuses out. Theoretically infinite time is required for complete drug diffusion from a polymeric matrix.

### 2.6.1 Steady –State Diffusion

Transportation of any substance in a liquid medium may be described by Fick's diffusion law. By this law, the diffusion rate of the substance is proportional to the concentration gradient of the substance between two certain positions (Figure 2.18). The differential form of the Fick's law is shown below for the diffusion in  $X$  direction:

$$J_{1x} = -D_{12} \frac{\partial C_1}{\partial X} \quad \longleftrightarrow \quad j_{1x} = -\rho D_{12} \frac{\partial W_1}{\partial X} \quad (2.10)$$

Where,  $J_{1x}$  (mol/ m<sup>2</sup>S) is the molar flux and  $j_{1x}$  (kg/m<sup>2</sup>S) is the mass flux of the active agent.  $D_{12}$  is the diffusion coefficient or the diffusivity. The negative sign reflects the natural tendency of a substance to diffuse from high concentration to low concentration.  $C_1$  is the concentration of active agent. Generally for liquids, the diffusion coefficient varies from  $0.5 \cdot 10^{-5}$  to  $5 \cdot 10^{-5}$  cm<sup>2</sup>/S at room temperature. Considering the hypotheses that the molar flux and the diffusion coefficient are constant, the first equation can be written in the following form:

$$J_1 = D_{12} K \frac{\Delta c}{\delta} \quad (2.11)$$

Where  $K$ , is the partition coefficient and  $\delta$  is the distance at which the diffusion occurs, or the solute travels. The partition coefficient is defined by:

$$K = \frac{\text{Concentration of active agent at interface}}{\text{Concentration of active agent in solution}} \quad (2.12)$$

Diffusion changes the distribution of molecules with time. Therefore to determine the evolution of diffusion, it is necessary to use Fick's second law.

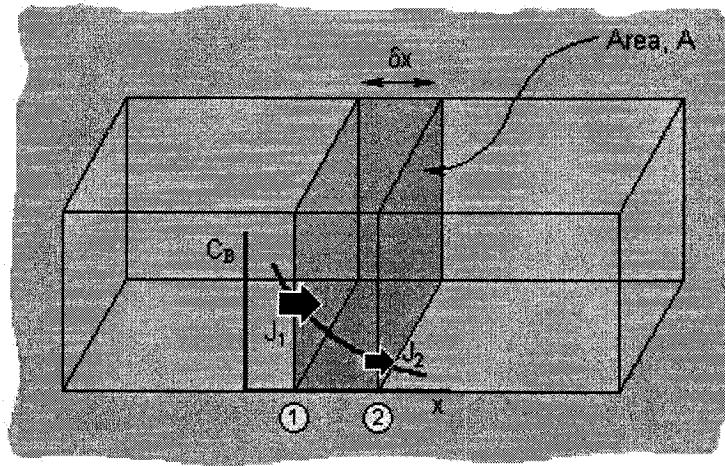


Figure 2.18 Schematic illustration of concentration gradient.

The following is the general equation for Fick's second law;

$$\frac{\partial C_1}{\partial t} = D_{12} \frac{\partial^2 C_1}{\partial X^2} \quad \longleftrightarrow \quad \frac{\partial W_1}{\partial t} = \rho D_{12} \frac{\partial^2 W_1}{\partial X^2} \quad (2.13)$$

This equation will vary according to the geometry of the capsule. Several theoretical solutions have been developed to analyze the release mechanism of a dispersed solute from a polymeric matrix (Colombo et al., 1995; Polishchuk and Zaikov, 1997; Hsu et al., 1996). Some of these present mathematical models which are useful in predicting the release kinetics (Liao et Lee, 1997; Ju et al., 1997). Siepmann, et al. (1999) used Fick's second law in a plane sheet to predict the release pattern. They used the following release kinetics equation for spherical microparticles.

$$\frac{M_t}{M_\infty} = 1 - \frac{6}{\pi^2} \sum_{n=1}^{\infty} \frac{1}{n^2} \cdot \text{Exp} \left( -\frac{D \cdot n^2 \cdot \pi^2 \cdot t}{R_s^2} \right) \quad (2.14)$$

Where  $M_t$  and  $M_\infty$  are the cumulative amounts of the drug released at time  $t$  and  $t = \infty$  respectively,  $D$  is the diffusion coefficient and  $R_s$  is the radius of the microparticle. Abdekhodaie, et al. (1997) used a moving boundary solution, based on a combination of variable methods for the release kinetics of a solute from planar and spherical matrices. For cylinder shape capsules, Tojo et al. (1999) worked with a model based on Fick's second law of diffusion for both membrane-controlled polymeric devices and rod-matrix systems (Tojo and Isowaka, 2001). In their study, they assumed that the drug molecules are released from the delivery system and distribute throughout the surrounding medium by diffusion. The concentration gradient is influenced by the rate of elimination of the drug by each surrounding tissue. Taken into account the above assumption, the concentration of drug in the body was modeled by:

$$\frac{\partial C}{\partial t} = \frac{1}{x} \frac{\partial}{\partial x} \left( xD \frac{\partial C}{\partial x} \right) + \frac{\partial}{\partial y} \left( D \frac{\partial C}{\partial y} \right) - R(x,y,t) + S(x,y,t) \quad (2.15)$$

Where  $D$  is the diffusion coefficient and  $R(x,y,t)$  is the metabolism and degradation rate of the drug and  $S(x,y,t)$  is the source of drug molecules released from the cylindrical delivery system.

Tan et al. (2001) used an analytical moving boundary solution for the diffusion release of drugs from a cylindrical polymeric matrix. The release kinetics were analyzed for non-erodible matrices. They made the following assumptions for their model: 1- the polymer is non-erodible, 2- the cylinder matrix is either long or thin or the ends are sealed so that the drug diffuses from the radius direction, 3- the diffusion coefficient is constant, 4- cylindrical matrices are in a perfect sink condition. A schematic diagram of the cylinder and its concentration profile are shown in Figure 2.19.

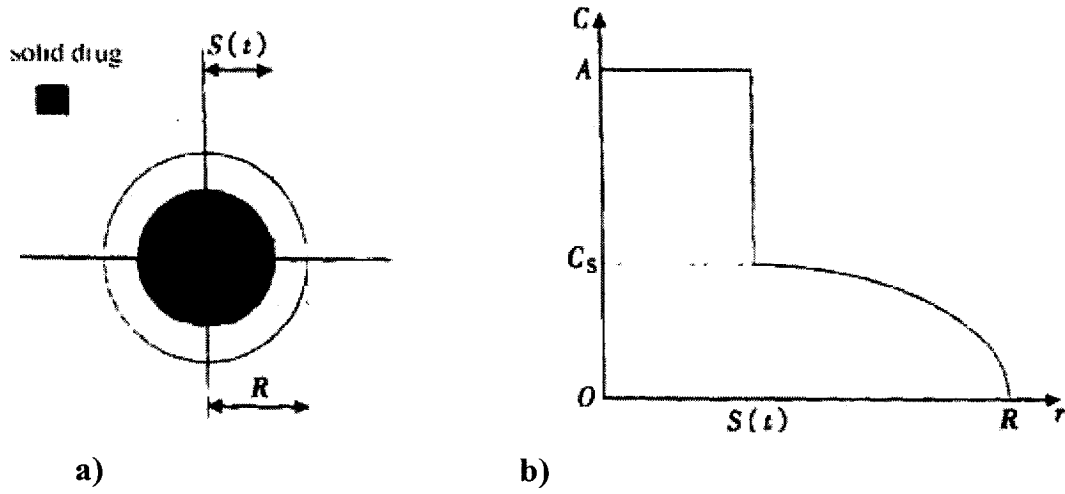


Figure 2.19 a) Schematic diagram of the cylinder cross sectional view, b) Concentration profile of the drug release from the polymer matrix.

Where  $R$  is the radius of the entire pellet,  $S(t)$  is the radius of the unextracted core (the moving diffusion boundary),  $A$  is the initial drug loading per unit volume, and  $C_s$  is the solubility limit of the drug in the matrix. The concentration in the partially extracted region ( $S(t) < r < R$ ) is determined by Fick's second law;

$$\frac{\partial C}{\partial t} = \frac{D}{r} \frac{\partial}{\partial r} \left( r \frac{\partial C}{\partial r} \right), \quad S(t) < r < R \quad (2.16)$$

$$C(R, t) = 0, \quad (2.17)$$

$$C(r, t) = C_s, \quad r = S(t), \quad (2.18)$$

$$D \frac{\partial C}{\partial r} = (A - C_s) \frac{dS}{dt}, \quad r = S(t), \quad (2.19)$$

$$S(t) = R, \quad t = 0, \quad (2.20)$$

By replacing dimensionless variables Tan et al., (2001) obtained the following equation;



$$\frac{M_t}{M_\infty} = (1 - \delta^2) - \frac{C_s}{2A \ln^2 \delta} (a_3 - a_3 \delta^2 - \ln \delta + a_3 \ln \delta + \delta^2 \ln \delta - 2 \delta^2 \ln^2 \delta) \quad (2.21)$$

Where,  $M_t$  is the fractional release at time  $t$  and  $M_\infty$  is a total amount of drug releasable at infinite time per unit area,  $\delta \equiv \delta(\tau) \equiv S(\tau)/R$  and  $\tau = D_t/R_2$ , and

$$a_3 = -\frac{A}{C_s} + \sqrt{\left(\frac{A}{C_s}\right)^2 - 1} \quad (2.22)$$

They calculated the moving boundaries and the fractional drug release at various loading levels by the above method and the mathematical results showed a good agreement with those of experiments. They were able to obtain a formula for estimating the available release time. This useful formula provides a theoretical tool to study the diffusion release of the drug and design the controlled release device.

## 2.6.2 Factors Affecting the Diffusion: Temperature and Molecular Size

It is well known that increasing the temperature results in an increase in the molecular diffusion rate, either in liquids or in solids (Laidler, 1965). There is a barrier to diffusion created by neighboring atoms. This barrier should be relocated in order to allow the diffusing atoms to pass. Temperature is a measure of molecular motion. Thus atomic vibrations created by temperature assist the diffusion. Lin et al. (2003) tested a drug delivery system involving the diffusion of the drugs and observed a significant increase in diffusion rate at 37°C compared to those obtained at 24°C. It was reported that the release rate increased by a factor of about 3, 2 and 5 for different drugs. The effect of temperature in diffusion is given by a Boltzmann relation:

$$D = D_0 \times \exp(-Q_d/kT) \quad (2.23)$$

Moreover, several groups investigated the effect of drug molecular size on the diffusion (Nara et al., 1992). They reported that smaller atoms diffuse more readily, and diffusion is faster in open lattices and in open directions. Sandor et al. (2001), conducted experiments on low and high molecular weight proteins to examine the effect of protein size on release from micron-size PLGA microspheres. At low loadings, release of larger proteins depended on diffusion through pores for the duration of the study. However, smaller proteins depended on the diffusion through pores initially and on degradation afterwards. It was observed that microspheres encapsulating large proteins maintained sustained release rates for 56 days, while those encapsulating low molecular weight proteins showed sustained release for 4 weeks.

### **2.6.3 Effect of Geometry and Dosage Form on Release Profile**

The revolution in drug delivery systems depends on the progress and development of two areas of knowledge: pharmacokinetics and effective drug delivery technology. Various studies have been done on therapeutic systems which are able to release the drug continuously in a pre-determined pattern for a fixed period of time. Many researchers have studied the controlling factors on the drug release pattern, but few of them have devoted their work to the effect of dosage geometry on the release profile. Aïnaoui and Vergnaud, (2000) conducted experiments to study this effect. In their research, the dimension of the dosage forms of various shapes was evaluated in such a way that they have the same volume. The dosage geometry includes sphere, cylinder, cube, and parallelepiped. The data are indicated in Table 2.4.

**Table 2.4** Characteristic of polymeric dosage form (Aïnaoui et Vergnaud, 2000)

Dosage form	Shape	Dimension (cm)	$t_r$ (h)	$V$ (cm/h)
1	Sphere	radius 0.182	24	0.00758
2	Cylinder	$2R = H = 0.318$	21	0.00758
3	Cube	$a = 0.293$	19.3	0.00758
4	Parallelepiped	$a = b = c/2 = 0.233$	18.4	0.00758

The kinetics of drug release from different dosage forms, are shown in Figure 2.20. They found that the kinetics of drug release of the dosage forms with control release depend on the shape of the dosage forms. It is faster for the parallelepiped because of the thinner dimension. They obtained similar results with dosages made from erodible polymers (Aïnaoui et Vergnaud, 2000).

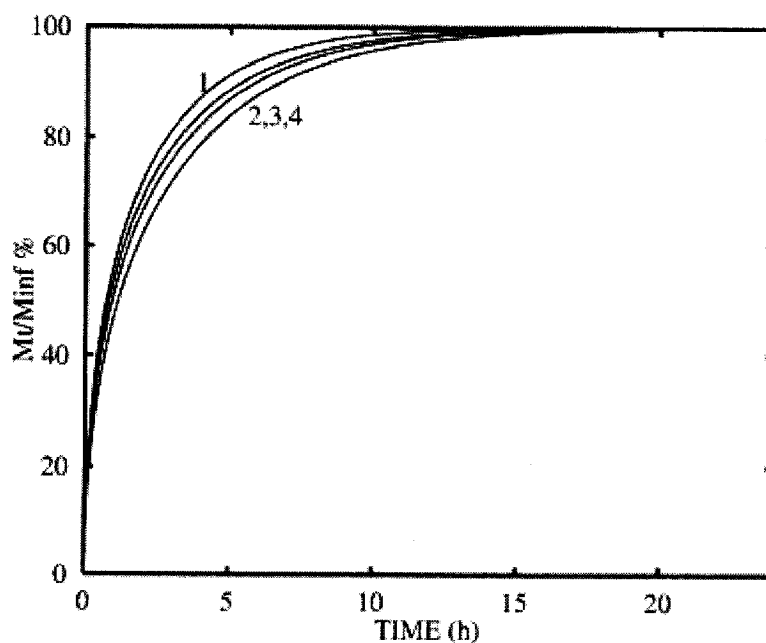


Figure 2.20 Kinetics of the drug release for dosage forms of same volume and different shapes controlled by diffusion. (1) Parallelepiped, (2) Cube, (3) Cylinder, and (4) Sphere (Aïnaoui et Vergnaud, 2000).

Also, Martini et al. (2000) conducted similar experiments with thin cylindrical compact and quasi-spherical shapes. Their investigation revealed the significant effect of geometry on the drug release rate. According to their results, the release rate from the compact dosage form was greater than that for the quasi-spherical shape by approximately 1.4 times. Their results are shown in Figure 2.21.

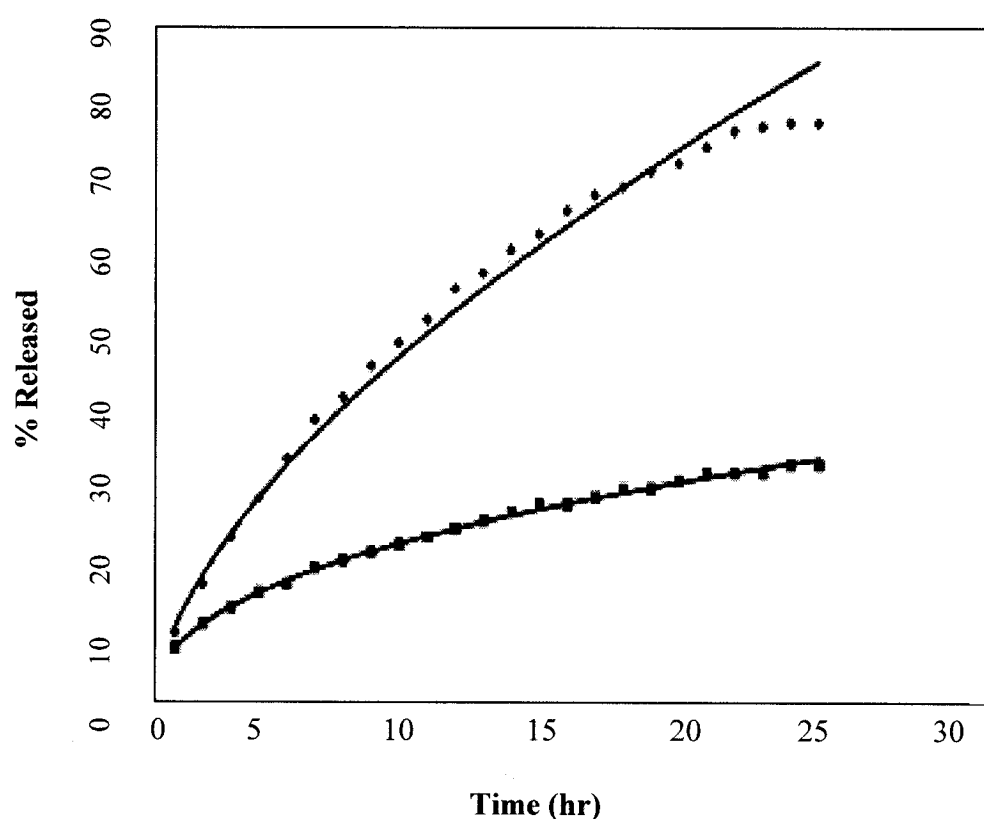


Figure 2.21 The percentage drug release versus time for the different geometries (♦) compact cylindrical shape, (■) quasi-spherical shape (Martini et al., 2000)

## 2.7 Drug Dissolution

Drug dissolution is a process by which a solid drug substance dissolves into the surrounding media or solvent. In the context of pharmaceutical drug delivery systems, dissolution is described as the phenomenon of drug availability from the dosage form after its administration. In pharmaceutical controlled release dosage forms, matrix-based systems are the most commonly used type. Materials that are frequently used as a matrix include: biodegradable polymers, hydrophobic non-erodible polymers, insoluble erodible polymers and hydrophilic polymers. Thus, depending on the type of the polymer and its structure, different drug dissolution mechanisms can be expected. Some initial mathematical models were developed through the 1960s as a route for analyzing drug dissolution in controlled release formulations. However, since the effect of swelling properties on dissolution were not taken into account, the models were not accurate enough (Higuchi, 1963; Roseman et al., 1970). Over the last few decades, some strategies for the development and validation of dissolution for conventional dosage forms were discussed (Bottom et al., 1997; Grundi et al., 1997). The technology rapidly shifted to the concept of controlled release delivery to improve clinical efficacy. As a result, dissolution strategies for conventional dosages had to be modified for controlled release formulations. Sood et Panchagnula (1999) prepared a complete list of mathematical models describing drug dissolution kinetics in controlled release drug delivery systems. In a recent investigation, Pillay et Fassihi (1998) used the time taken for x% drug release ( $t_x$ ) and mean dissolution time (MDT %) parameters, and the “similarity factor, f” as tools to explain dissolution behavior of different delivery systems under different hydrodynamic conditions. In order to determine the release profile similarity and dissimilarities, dissolution data were subjected to two categories of model-independent analyses: time-point and pairwise approaches. In the time points approach, the  $t_{50\%}$ ,  $t_{70\%}$  and  $t_{90\%}$  values and the mean dissolution times ( $MDT_{50\%}$ ,  $MDT_{70\%}$  and  $MDT_{90\%}$ ) were

calculated, whereas in the pairwise approach, the “difference factor,  $f_1$ ” and “similarity factor,  $f_2$ ” were estimated using the mean percentage released.

It can be concluded that dissolution studies for controlled release formulations are receiving more attention, while the dissolution experiment is a tool which requires more study for new applications.

## 2.8 Burst Release

In many controlled release systems, a large amount of the drug is released upon being placed in an aqueous medium, before the sustained release rate is achieved. This phenomenon, shown in Figure 2.22, is called “*burst release*”. As a result of burst release, higher initial drug delivery can decrease the carrier’s effective lifetime. However, since burst release occurs in a very short time as compared to the total release time, it has been mostly ignored in controlled delivery investigations.

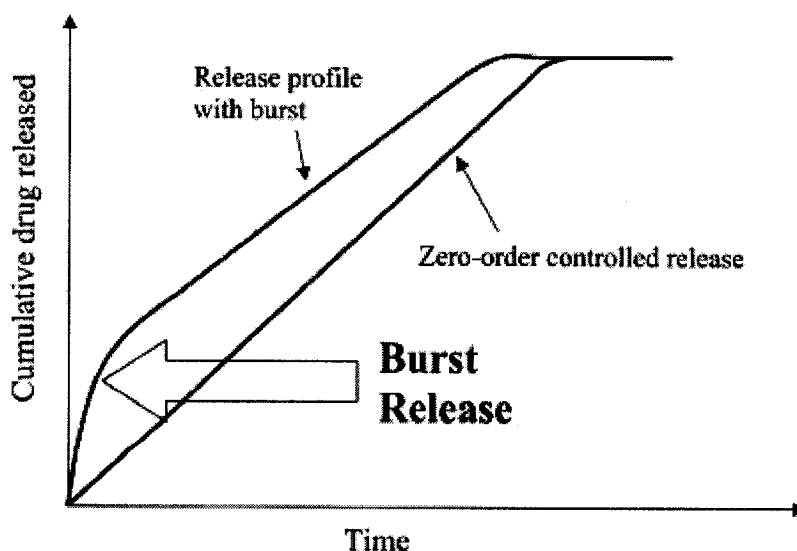


Figure 2.22 Schematic showing the burst release effect (Huang and Brazel, 2001).

Burst release effects have been observed by many research groups (Narasimham and Langer, 1997; Kishida et al., 1998; Brazel and Peppas, 1999; Jeong et al., 2000). Burst release can be examined from two different perspectives: positive and negative. The positive perspective focuses on situations in which rapid release of a high drug concentration is desirable, such as at the beginning of wound treatment. In these cases, an initial burst provides the patient with immediate relief followed by a prolonged release to improve gradual healing (Narasimham and Langer, 1997). The negative perspective looks at negative consequences in controlled delivery, such as a high level of toxicity and waste of an active agent. The negative and positive aspects of burst release are listed below in Table 2.5.

**Table 2.5** Positive and negative applications of burst release

Positive burst release situations	Negative burst release effects
Wound treatment (burst release followed by a diminishing need for drug)	Local or systemic toxicity (from high drug concentrations)
Encapsulated flavors	Short half-life of drugs in vivo (rapid loss in activity)
Targeted delivery (triggered burst release)	Economic and therapeutic waste of drug
Pulsatile release	Shortened release profile; requires more frequent dosing

Due to negative effects, researchers generally try to avoid burst release, because the initial high release rates may lead to drug concentrations near or above the toxic level. Any drug released during the burst stage may also be metabolized and excreted without being circulated in the body. Even if no harm is done during the burst release, this

amount of drug is essentially wasted, and the ineffective drug usage may have therapeutic and economic consequences. Some factors that may contribute to burst release are processing condition, surface characterization of the carrier, carrier geometry, morphology and porous structure of the polymer, and polymer-drug interactions (Brazel and Peppas, 1999).

### 2.8.1 Manufacturing Condition

One possible reason for the burst release in the matrix-reservoir formulation is drug entrapment on the surface of the polymer matrix during the synthesis process, especially in the case of high drug loading. Brazel and Peppas, (1999) showed that both the polymeric matrix and the solute size have important roles in determining the release profile and fraction of a drug in burst release. Also, migration of the drug while it is being dried and stored may result in a non-homogeneous distribution of the drug in the polymer matrix which finally leads to a burst effect (as shown in Figure 2.23).

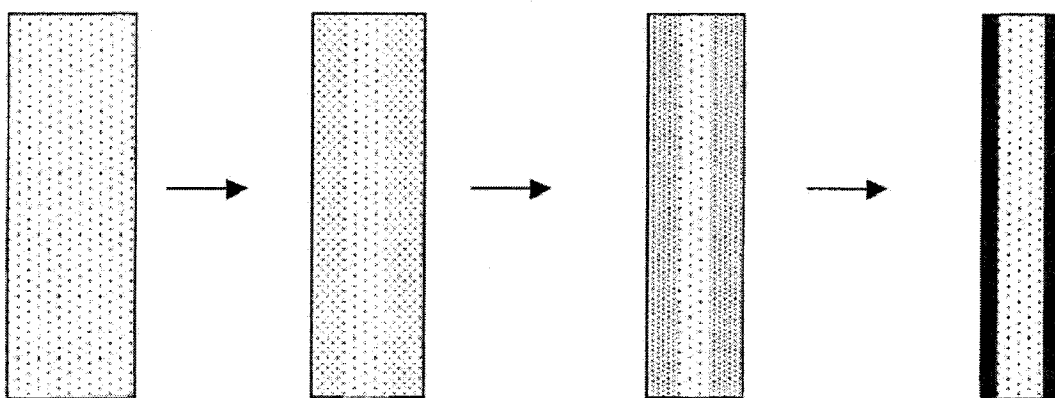


Figure 2.23 Drug redistribution due to convection during drying process (Huang and Brazel, 2001).



In solvent evaporation techniques, synthesis conditions (e. g. polymer: drug and polymer: solvent ratios) can be another factor potentially affecting the burst release. The polymer: suspending phase ratio is the determinant factor in controlling the density of the obtained matrix. The lower this ratio is, the less compact the polymer matrix is. A less compact matrix results in easier movement of the drug toward the polymer surface (Sah et al., 1994).

### **2.8.2 Surface Characterization of the Matrix**

Another explanation for burst release is the nature of the polymer. In most cases, burst release is related to the existence of micro and macro domains for drug release. Vasudev et al. (1997) suggested that the burst effect was due to the formation of pores and cracks during device fabrication. Others have shown that microspheres with denser formations and rough surfaces (high surface areas) result in higher initial burst than those with smooth surfaces (Chia et al., 2000). However, there is much evidence that the highly porous structure of the matrix is the main reason causing the burst release.

### **2.8.3 Polymer–Drug Properties and Interactions**

The chemical and physical structures of active agents and polymer matrices, as well as their interactions, can also have profound effects on the burst effect in controlled release systems. Results show that a sustained release with a lower burst effect can be obtained when a higher molecular weight solute is used, an effect attributed to the greater hindrance of pore diffusion by solute molecular size. Brazel and Peppas (1999) observed a decrease in burst release with an increase in protein molecular weight. Drugs with small molecular sizes are often highly soluble in aqueous systems and can pass easily through the porous structure of a matrix. Larger burst effects have been reported for polymers with small molecular weights. Burst effects have been observed to decrease with an

increase in polymer matrix molecular weight (Cohen et al., 1991) However, in most cases the burst release and the corresponding release behavior are attributed to the adhesion of the drug to the polymer surface. Thomasin et al. (1996) found that release kinetics was not affected by particle size, suggesting that the drug delivery is mainly controlled by drug–polymer interactions leading to slow diffusion. Experimental results have also shown that decreases in burst release may be caused by polymer–drug interactions which affect the drug distribution inside the matrix (Blanco-Prieto et al., 2004). The drug will be more evenly distributed throughout the matrix if it interacts more strongly with the polymer than with the solvent. Conversely, when the drug affinity for the solvent is high, the drug will locate preferentially at the periphery.

#### **2.8.4 Methods to Prevent Burst Release and Induce Slower Diffusion Rates**

Although burst release is favorable in some situations, under most circumstances it is considered a negative effect. An ideal controlled release system is one with a high drug loading and constant zero-order drug release with no burst release over a relatively long period of time. Due to the importance of preventing burst release, several studies have focused on developing methods to prevent or minimize burst release and increase the length of release in a wide range of polymer–drug systems. Technologies proposed to avoid burst release include surface extraction, non-uniform drug distribution, double-wall microspheres or coated surfaces, and surface modification.

##### **2.8.4.1 Drug Surface Extraction**

One of the simplest approaches that has been used to reduce the initial burst is drug surface extraction. This method involves extracting the drug formulations for a short period of time *in vitro* before using them in an *in vivo* application (Ficek et Peppas, 1993). This method is effective at reducing burst because excess drug on the outer

surface of the device is removed. However, the cost of extraction and the reduction in the effectiveness of the drugs must be taken into account. For systems working with higher drug concentrations, washing the surface of the sample as an extraction stage before carrying out the release experiment can be effective, but large fractions of the drug may be removed especially in the case of a microspheres formulation with a high amount of surface area. Therefore, this technique is better for larger release devices for which the surface area:volume ratio is relatively small.

#### **2.8.4.2 Drug-Loading Distribution**

Although non-uniform drug loading is difficult to achieve in real systems, it has been successful at reducing the burst effect. Research has shown that drug distribution has a controlling effect on sustained release behavior rather than on burst control release. Some researchers have examined (mathematically and experimentally) the effect of the initial drug distribution on the kinetics of drug release from polymer matrices. The experiments have shown that an initial drug distribution with the highest concentrations at the center results in near zero-order sustained release behavior. Recently, Lu et al. (1998) used multilaminate systems to produce matrix systems with non-uniform drug distributions. Their models proved the importance of drug distribution in matrices for controlling the release rate, but they could not address the impact of non-uniform drug distribution on the burst release. Kakish et al. (2002) claimed that a drug uniformly dispersed in a sphere matrix can increase an initial burst release. They were able to successfully modify the drug distribution so as to obtain a more constant drug release.

#### **2.8.4.3 Double-Wall Formulation and Coated Surfaces**

Another method to prevent burst release is surface modification by additional coating steps to provide an outer layer with no drug. In a study on the delivery of

biomacromolecules including proteins and dextran, triple coating with a polycation was used to prevent the initial burst release. Increasing the polycation concentration decreased the burst effect and caused the release to be more sustained (Wheatley et al., 1991). Double-wall formulation is another method that has attracted attention in recent years. These formulations, with small changes in preparation, are also referred to as core-shell formulations or closed-cell formulations. Core-shell formulations usually refer to spheres formed by making core units through a normal preparative method, followed by the addition of an outer layer by a dipping, mixing, or emulsion procedure (Ermis and Yuksel, 1999; Jones and Lyon, 2000; Lee et al., 2002; Sparnacci et al., 2002). The main reason to fabricate these formulations is to control the drug diffusion into the surrounding medium using a degradable drug-holding layer. This layer is capable of preventing the initial drug diffusion after administration, thereby decreasing the burst effect. Degradation of this layer provides some open channels to the surface of the matrix and drug diffusion occurs in a more controlled manner. A complete explanation of the closed-cell dosage formulation is given in Section 2.11.

#### **2.8.4.4 Surface Modification**

The surface modification of polymers has been extensively studied using conventional tools. Over the last two decades, different means of surface modification have been thoroughly explored. The absence of specific surface properties, such as hydrophilicity, roughness, selective permeability and adhesion to proteins or drug molecules, increases the need for tailoring the surface. Many methods have attempted to prevent burst release from porous polymer structures during processing, most of which are based on changing the surface characteristics of the devices. In one study, a PLA surface was treated with a poly (vinyl alcohol)–dioxane solution (Park et al., 1992). This treatment reduced burst to some extent. Another approach is to modify the polymer morphology by blending it with nonionic polymeric surfactants to form a matrix where the surfactants become entangled in the amorphous region of PLA. This produces an overall intact surface morphology

which results in a minimum initial burst release and longer release period (Park et al., 1992). Others have suggested methods to prevent burst release in PLGA by treating the wet microparticles with an organic/water mixture and adding organic solvents to the external aqueous phase during preparation, both of which result in a reduction in the pores present on the microsphere as well as the burst (Ahmed et al., 2000). In recent years, for protein controlled delivery, more attention has been focused on layer-by-layer (LbL) deposition of polyelectrolytes on the polymer surface. Surface modification via this technique has expanded to include sequential assembly of oppositely charged polymers (or biopolymers) to produce polyelectrolyte multilayer thin films for coating. Currently, a large number of components, such as DNA, proteins, and lipids have been used in the multilayer, yielding thin films with tailor-made properties. Most of the applications involve planar films. However, one application reported a polyelectrolyte capsule fabricated by LbL coating of colloidal templates (Donath et al., 1998). A complete explanation of surface treatment with polyelectrolyte layer-by-layer deposition is presented in Section 2.12.4.

## **2.9 Incomplete Release**

Very often, an incomplete release occurs in controlled release systems, especially when dealing with proteins. A high initial burst followed by a very slow release or no release has been observed. Varying degrees of incomplete protein release have been reported, even after the biodegradable polymer carrier was substantially degraded (Kim et Park, 2001). This is mainly because of inherent protein instability problems occurring within the polymer matrix. The reasons include protein denaturation (Kim, 2000), covalent/non-covalent aggregation (Crott et al., 1997), and non-specific adsorption on the degrading polymer surface (Zhu et al., 2000). Zhu et al. (2000) suggested that an acidic microenvironment progressively developing within gradually degrading polymer carriers was primarily responsible for such protein instability events. To overcome acid-induced

protein aggregation, basic salt particles were co-encapsulated within the capsule to neutralize acidic degradation products (Marinini et al., 2000; Zhu et Schwendeman, 2000). The effect of adding base salt on BSA release kinetics is shown in Figure 2.24. Zhu et Schwendeman (2000) explained the incomplete release of BSA differently. Acidity commonly develops inside a matrix because of the accumulation of acidic degradation products upon hydrolysis. At a highly acidic pH, the encapsulated BSA was rehydrated, causing the protein to unfold and undergo a conformational transition from the F to E form. This provides the driving force for noncovalent aggregation via hydrophobic interactions. Other groups have claimed that drug distribution in the surface or the core of the polymer capsule, influenced incomplete and complete release of BSA from PLA/PLGA capsules (Leo et al., 2006). Nevertheless, protein release profiles from polymer capsules have not yet been fully controlled and their release mechanisms, involving vastly different extents of diffusion, erosion, and protein aggregation /adsorption, have not been clarified.

In this work it was postulated that biodegradable microspheres with a micro-porous structure would better control a protein release profile. A built-in micro-porous internal structure within microspheres is expected to control the diffusion rate of entrapped protein molecules.

## **2.10 Encapsulation Efficiency**

Increasing or controlling the encapsulation efficiency is desirable in most cases of controlled drug delivery systems since it can prevent the loss of precious medication and extend the duration and dosage of treatment. The drug content of encapsulated microspheres can be described by two known methods. The most popular one is formulated below:

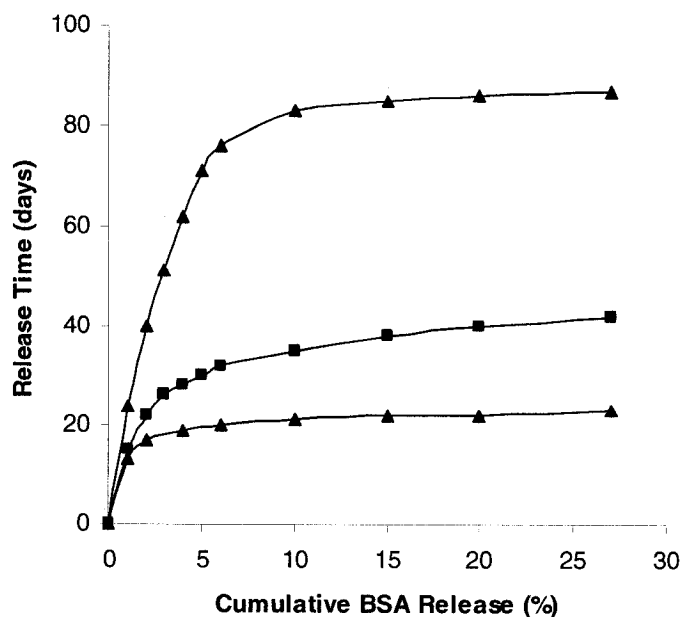


Figure 2.24 Effect of  $\text{Mg}(\text{OH})_2$  content on BSA release kinetics. Millicylinders with 15% BSA and 0% (●), 0.5% (■), and 3.0% (▼)  $\text{Mg}(\text{OH})_2$

$$\text{Encapsulation Efficiency} = M_{\text{experimental}} / M_{\text{theoretical}}$$

where  $M_{\text{experimental}}$  is the total amount of drug loaded during the experiment, and  $M_{\text{theoretical}}$  is the amount of drug which theoretically should be loaded.  $M_{\text{experimental}}$  is calculated by the weight difference of the capsule before and after loading, whereas  $M_{\text{theoretical}}$  can be estimated by knowing the void volume within the capsule (Gupta and Kumar, 2001). The loading capacity is defined as:

$$\text{Loading Capacity} = \text{LC} = M_{\text{experimental}} / M_{\text{capsule}}$$

where  $M_{\text{capsule}}$  is the weight of the drug carrier (Gupta and Kumar, 2001).

Different encapsulation techniques result in different encapsulation efficiencies. Capsules with both low and high drug efficiencies have been reported. Some researchers have worked to find a solution to prevent low encapsulation efficiency loadings. They found that different mechanisms governed the encapsulation process, depending on the method used. Yang et al. (2000) have provided a revealing study that correlated encapsulation efficiency with the capsule preparation temperature using a double emulsion method. They found that the highest encapsulation efficiencies occurred at the lowest and highest formation temperatures. At lower temperatures, increased immiscibility between the sphere and water resulted in a rapidly forming outer sphere wall, thus trapping the drug early in the evaporation process. At higher temperatures, an increased rate of solvent evaporation also resulted in a rapidly hardening sphere wall. In both cases, drug trapping was enhanced by a hardening of the sphere wall.

### **2.11 Closed–Cell Formulation**

The formation of core–shell carriers with the drug loaded in the inner core seems to be effective in gaining better control over release kinetics. The employment of a shell is usually meant to enhance controlled release and possibly reduce the effect of the initial burst. Huang et al. (1999) showed how dipping PLA–poly (ethylene glycol) (PEG) spheres into a gelatin solution can enhance controlled release. Spheres made from these polymers are highly porous and have a high burst effect. However, coating the spheres with gelatin resulted in a considerable decrease in the burst effect and a longer release duration. This method can be useful when the burst effect is too high.

There are several methods of making polymer carriers with a one or two layer structure. One method is to encapsulate a therapeutic agent in a polymer carrier using any microencapsulation technique and then to coat the device with a second polymer. This coating reduces the burst effect since no drug is encapsulated on the surface. However,



dip- or pan-coating processes result in matrices with uneven or incomplete polymer coatings, and each coating adds an additional step to the manufacturing process. Another method includes polymer-polymer phase separation of a binary blend of polymer solutions, which may lead to the formation of a drug carrier device with a two-layer structure (Pekarek et al., 1994a; 1994b). The modified solvent evaporation method to prepare double-walled microspheres is another recent method (Rahman and Mathiowitz, 2004). In this process, a modified solvent evaporation process is used to form double-walled microspheres and two polymer solutions are briefly mixed before being added to the aqueous non-solvent bath. As the solvent is slowly lost, the droplets of the polymer-polymer solution become more concentrated and the polymers begin to separate into one phase rich in one polymer, and a second phase rich in the other polymer. One polymer phase encapsulates the drug and the other polymer encapsulates the first polymer phase. Rahman et Mathiowitz (2004) used this method to fabricate a double-walled formulation with binary blends of various combinations of poly (L-lactide) and poly (D, L-lactide-co-glycolide). The obtained double-walled device is shown in Figure 2.25. Pekarek et al. (1994b) prepared microspheres containing an inner polyanhydride core and an outer layer of PLA. They found that the more hydrophilic anhydride inner core degrades into monomers after two months, which then start to escape their shell. This may be useful for the controlled release of a drug inside a core matrix since the release rate is controlled by diffusion through a shell of uniform thickness.

Yang et al. (2003) reported advanced degradation of the inner core (PEO) of PEO/PLGA microspheres. Some researchers have established targeted release by using pH-sensitive outer shells. The result is shell degradation at a specific pH value followed by rate-controlled drug release. Lorenzo-Lamosa et al. (1998) studied a chitosan microcore coated with poly (methacrylic acid-co-methylmethacrylate). Sustained drug release occurred only after the pH-sensitive coating was dissolved. Even though chitosan dissolves rapidly at pH 7.4, no drug was released from the microspheres until the pH of

shell degradation was attained. Such an outer shell has proven useful in pH-targeted release.

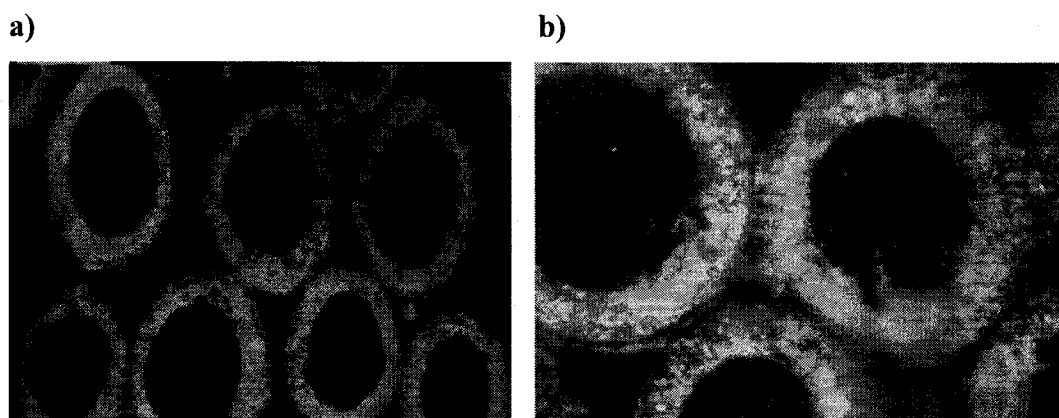


Figure 2.25 Cross section of double-walled microspheres under fluorescence microscope a) represents microspheres (10 ×) magnification b) represents microspheres (20 ×) magnification (Rahman et Mathiowitz, 2004).

## 2.12 Polyelectrolytes

### 2.12.1 Introduction to Polyelectrolytes

Polyelectrolytes are defined as polymers which, upon dissolution in a polar solvent (generally water), bear an electrolyte group on their repeating units. These groups will dissociate in aqueous solutions (water), charging the polymers. Polyelectrolyte properties are thus similar to both electrolytes (salts) and polymers (high molecular weight compounds) and are sometimes called polysalts. Like salts, their solutions are electrically

conductive. Like polymers, their solutions are often viscous. Many biological molecules are polyelectrolytes for example; polypeptides (thus all proteins) and DNA. Both natural and synthetic polyelectrolytes are used in a variety of industries.

Like acids and bases, polyelectrolytes can be divided into weak and strong types. A *strong polyelectrolyte* dissociates completely in solution at most pH values and reaches its maximum charge immediately after dissolution. A *weak polyelectrolyte*, has a dissociation constant ( $pK_a$  or  $pK_b$ ) in the range of  $\sim 2$  to  $\sim 10$ , meaning that it will be partially dissociated at intermediate pH. Thus, weak polyelectrolytes are not fully charged in solution, and their fractional charge can be modified by changing the solution pH, counter-ion concentration, or ionic strength.

Since polyelectrolytes are considered as macromolecules, their classification is performed in the same manner as neutral polymers. They can be classified as biopolymers, synthetic polymers, linear, branched or star-shaped polymers, and homo- or co-polymers. They can be classified according to their charge and ionic strength. Polyacids (polyanions) in solid form are neutral; when dissolved in a solvent, they dissociate to negative chains and protons ( $H^+$ ). On the contrary, polybases (polycations) in solution link to protons ( $H^+$ ) to create positively charged polymer chains (see Figure 2.26 as an example). Some polyelectrolytes can bear both cationic and anionic repeating groups. These are called polyampholytes. The competition between the acid–base equilibrium of these groups leads to additional complications in their physical behavior. These polymers usually only dissolve when there is sufficiently added salt, which screens the interactions between oppositely charged segments.

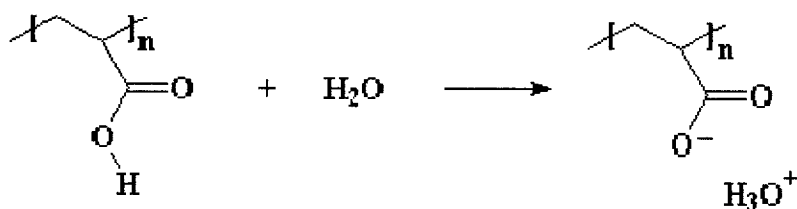


Figure 2.26 Polyelectrolyte dissociation in water

### 2.12.2 Polyelectrolyte Applications

Polyelectrolytes display a rich variety of properties not found in neutral polymers and are, therefore, of considerable interest from a basic scientific standpoint. While their importance as biological molecules (proteins and nucleic acids) has been known for a long time, their significance in industry has only been realized in the last two decades. Polyelectrolytes have many applications, mostly related to modifying the flow and stability properties of aqueous solutions and gels. For example, they can be used either stabilize colloidal suspensions or to initiate flocculation (precipitation). They can also be used to impart a surface charge to neutral particles, enabling them to be dispersed in an aqueous solution. They are thus often used as thickeners, emulsifiers, conditioners, flocculents, and even drag-reduction agents, as well as additives for many soaps, shampoos, and cosmetics. They are used in the manufacture of membranes, ion-exchange resins, gels, and modified plastics, in waste water treatment and for oil recovery. Finally, they are added to many foods. Because some of them are water-soluble, they are also investigated for biochemical, and medical applications. There is currently much research into using biocompatible polyelectrolytes for implant coatings in controlled drug release, as well as other applications.

### **2.12.3 Polyelectrolytes in Solution**

The conformation of any polymer solution is affected by a number of factors notably the polymer's architecture and the solvent affinity. For polyelectrolytes, charge also has an effect. The physical properties of polyelectrolyte solutions are usually strongly affected by their degree of charges. Since the polyelectrolyte dissociation releases counter-ions, this necessarily affects the solution's ionic strength, and therefore the Debye length. This, in turn, affects other properties, such as electrical conductivity. An uncharged linear polymer chain is usually found in a random conformation in solution (three-dimensional random walk conformation). The charges on a linear polyelectrolyte chain will repel each other (Coulomb repulsion), which causes the chain to adopt a more expanded, rigid-rod conformation. If the solution contains a great deal of added salt, the charges will be screened and consequently the polyelectrolyte chain will collapse to a more conventional conformation (essentially identical to a neutral chain in good solvent). When solutions of two oppositely charged polymers, are mixed, a bulk complex (precipitate) is usually formed. This occurs because the oppositely charged polymers attract one another and bind each other irreversibly. Polymer conformation affects many bulk properties (such as viscosity and turbidity). Although the statistical conformation of polyelectrolytes can be captured using variants of conventional polymer theory, it is quite computationally intensive to properly model polyelectrolyte chains owing to the long-range nature of the Coulomb interaction.

#### **2.12.3.1 Effect of Salt on Polyelectrolyte Conformation in Solution**

Normal uncharged polymer molecules in solution tend to be tangled. Successive chain units are able to rotate along the bonds of the backbone to acquire a jumbled conformation. This behavior is called a random coil (Figure 2.27). When dealing with polyelectrolytes, the polymer chain is no longer neutral. It has positive or negative charges along its chain. The polymer chain is covered with negative charges or positive

charges, which repel each other; therefore, the polymer can not form the random coil. Thus, the chain stretches out and acts as a stiff chain (Figure 2.28).

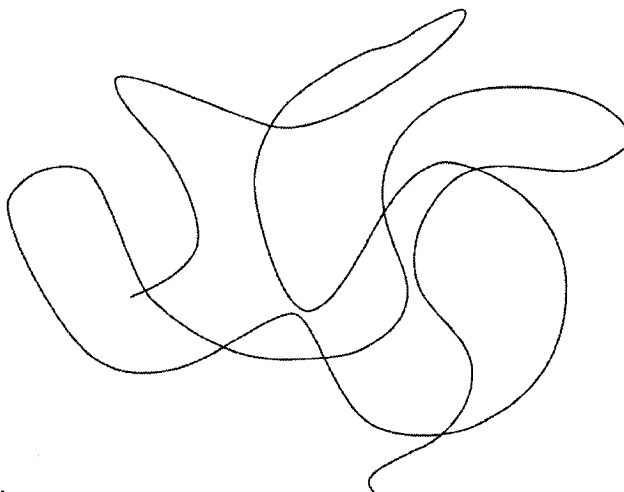


Figure 2.27 “Random-walk” model for a polymer chain (tangled molecule in random coil)

Unlike the random coil, a stiff chain cannot have rotation about the covalent bonds forming the chain backbone, and the polyelectrolytes will follow the “*worm-like*” model rather than “*random-walk*” model, which makes the polyelectrolyte solution more viscous. When the polyelectrolyte chain stretches out, it takes up more space, and thus is more effective at resisting the flow of the solvent molecules around it, resulting in it becoming thick and syrupy.

If enough salt is added to the polyelectrolyte solution, the stiff chain behavior of the polyelectrolyte in solution will change. The NaCl will separate into  $\text{Na}^+$  and  $\text{Cl}^-$  ions. In the case of a negatively charged polyelectrolyte, the positively charged  $\text{Na}^+$  ions will go between the negative charges and cancel them out in effect. Conversely, for a positively charged polyelectrolyte,  $\text{Cl}^-$  ions will locate between positive charges of the

polyelectrolyte chain. When this happens, the polymer chain collapses back into a random coil.

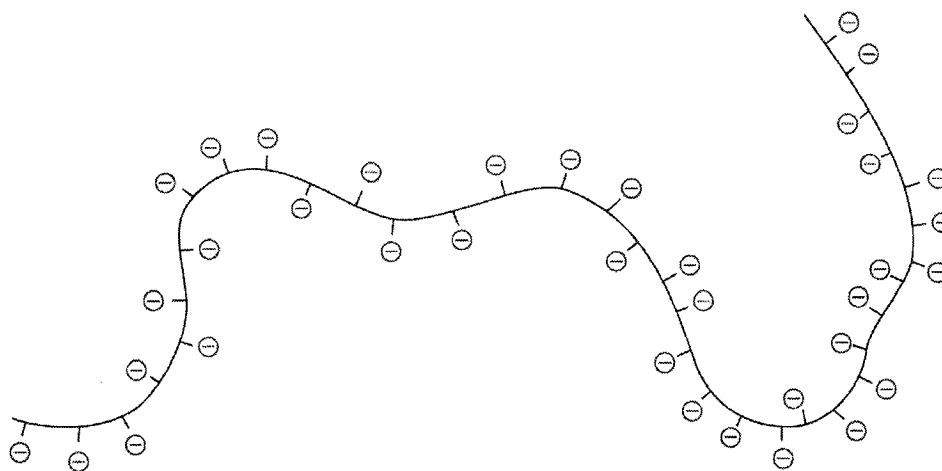


Figure 2.28 “Worm-like” model for polyelectrolyte chain.

The effect of adding salt to the polyelectrolyte chain in solution is shown in Figure 2.29. As can be observed, adding salt to the polyelectrolyte solution will cause the stiff chain to change into a random coil formation.

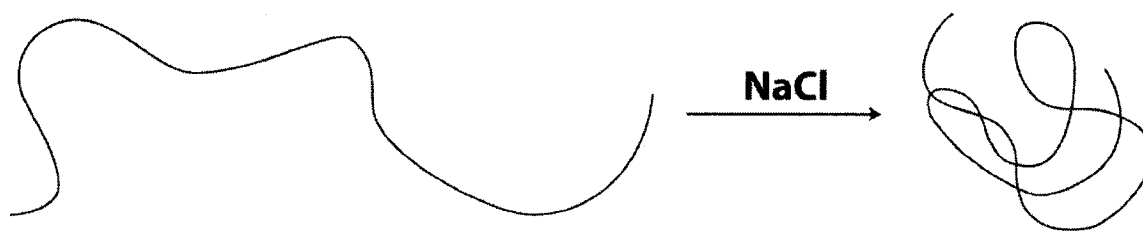


Figure 2.29 Effect of adding salt to the polyelectrolyte solution

### 2.12.4 Layer-by-Layer Deposition of Polyelectrolyte

In recent years, the field of drug delivery has focused on new techniques to develop suitable carriers for therapeutic molecules. The layer-by-layer (LbL) technique, originally introduced by Decher et al. (1992) has opened new avenues in drug delivery technology. The technique includes the sequential adsorption of oppositely charged polymers (i.e., polyelectrolytes) on a charged planar substrate. Adsorption of a polyelectrolyte layer leads to a reversal of the surface charge, promoting the adsorption of the next, oppositely charged, polyelectrolyte. Figure 2.30 is a schematic illustration of the LbL process.

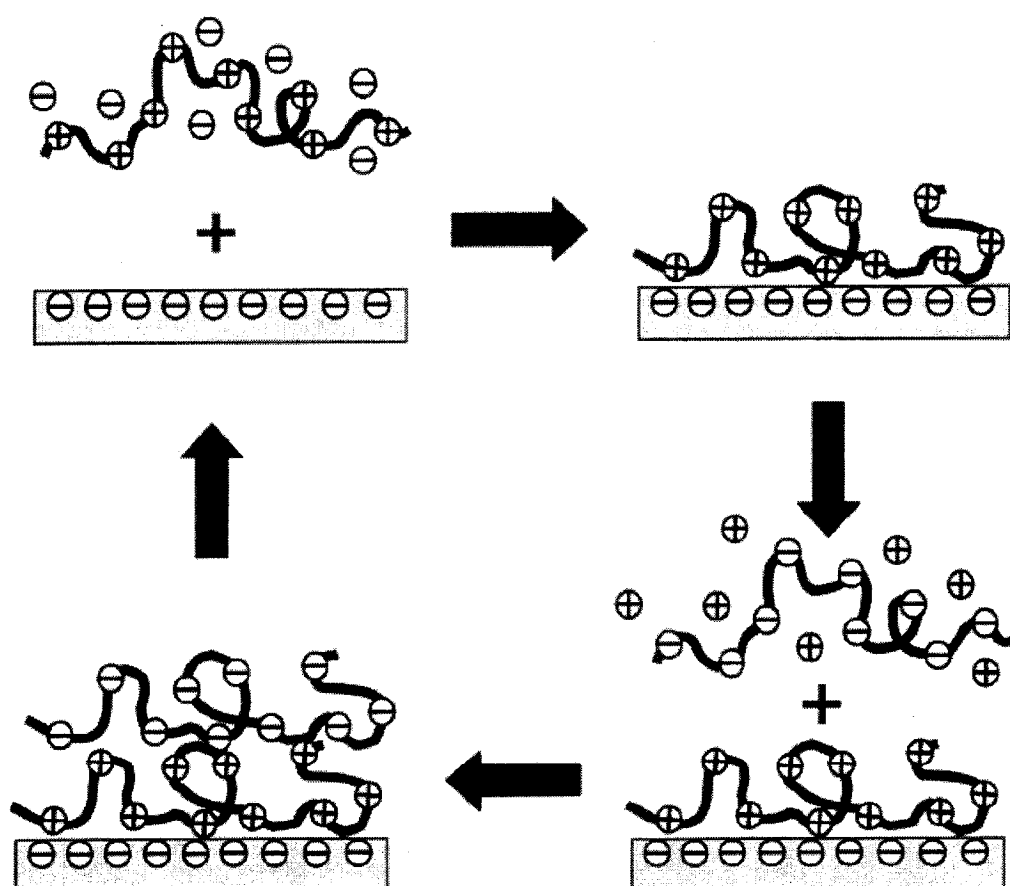


Figure 2.30 Schematic representation of layer-by-layer deposition (Bertrand et al., 2000)



The LbL technique was used to form new types of materials known as polyelectrolyte multilayers (PEMs). Upon adsorption of each layer, the surface charge is reversed, allowing the gradual and controlled build-up of electrostatically cross-linked films of polycation–polyanion layers. Scientists have demonstrated thickness control of such films down to the single-nanometer scale. The main benefits to PEM coatings are their ability to uniformly coat objects and the technique is not limited to coating flat objects. To characterize the multilayer build-up, several techniques have been used. Amongst them, UV-VIS adsorption, quartz crystal microbalance (QCM), and ellipsometry are the most effective at being able to determine both the mass and thickness increment upon adsorption of a single polyelectrolyte layer. Ferreira and Rubner, (1995) used UV-VIS absorbance measurements to reveal that in all cases the bilayer deposition process was linear and highly reproducible from layer to layer. The *in situ* QCM measurement has shown that the dye adsorption rate is similar to that of conventional polyion adsorption. The results obtained from QCM suggest that the formation of well-packed monomolecular dye layers is affected by the size, number of charges, and spatial orientation of dye molecules (Ariga et al., 1997). *In situ* ellipsometry allowed Harris and Bruening (2000) to investigate the permeability and stability of layered polyelectrolyte films while explaining the effect of pH on bilayer thickness.

The internal structure of the polyelectrolyte films (*ordered* or *fuzzy*) can be investigated by X-ray techniques while their surface morphology can be adequately analyzed by atomic force microscopy (AFM). Arys et al. (2001) studied the growth and structuring of polyelectrolytes using X-ray reflectometry. They showed highly ordered polyelectrolyte films may be obtained, consistent with the preferential orientation of chain fragments occurring in the films. Using *in situ* atomic force microscopy (AFM), Dubas and Schlendoff (2001) were able to show that polyelectrolyte multilayers swell on exposure to solutions containing salt. Mcaloney et al. (2001) employed AFM to observe the film morphology. They successfully examined the films produced after ten bilayers were

deposited in the presence of additional salt ranging from 0.1 to 1.0 M NaCl. Their results from AFM are summarized in Figure 2.31.

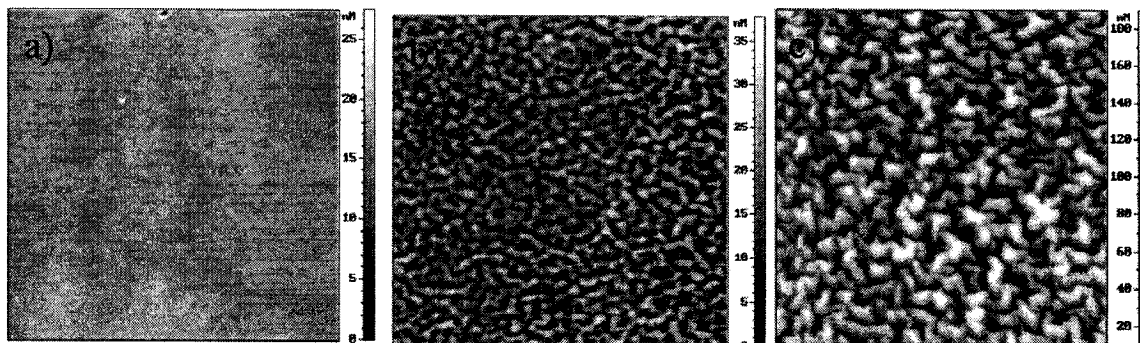


Figure 2.31 AFM topographic images of the morphology of ten bilayer films of PDDA/PSS deposited from (a) 0.1M, (b) 0.3M, and (c) 1.0M NaCl solutions. Images are  $5\ \mu\text{m} \times 5\ \mu\text{m}$ , and the z scales are as shown (Mcaloney et al., 2001).

At salt concentrations of 0.1M or less, the film is flat and featurless with only a slight granular texture. For concentrations more than 0.3M, a major change in morphology can be observed. A wormlike pattern emerges and makes the surface rough. At 1M NaCl concentration this pattern becomes more pronounced, ridges become deeper and the wormlike pattern gets wider.

#### 2.12.4.1 Charge Distribution and Overcompensation - Multilayer Growth

One necessary requirement for the formation of multilayers is that charge overcompensation must occur i.e., the surface charge must change sign upon adsorption of an oppositely charged polyelectrolyte so the next layer can be deposited (Figure 2.32). Because of the electrostatic nature of multilayer preparation via the LbL self-assembly, the charge density of the polyelectrolytes and the ionic strength of the deposition

solutions are predominant factors determining the growth and stability of the multilayer films (Decher, 1997). Several experimental observations have revealed the existence of a critical charge density, below which the successive LbL self-assembly cannot be carried out (Schoeler et al., 2002; Glinel et al., 2002).

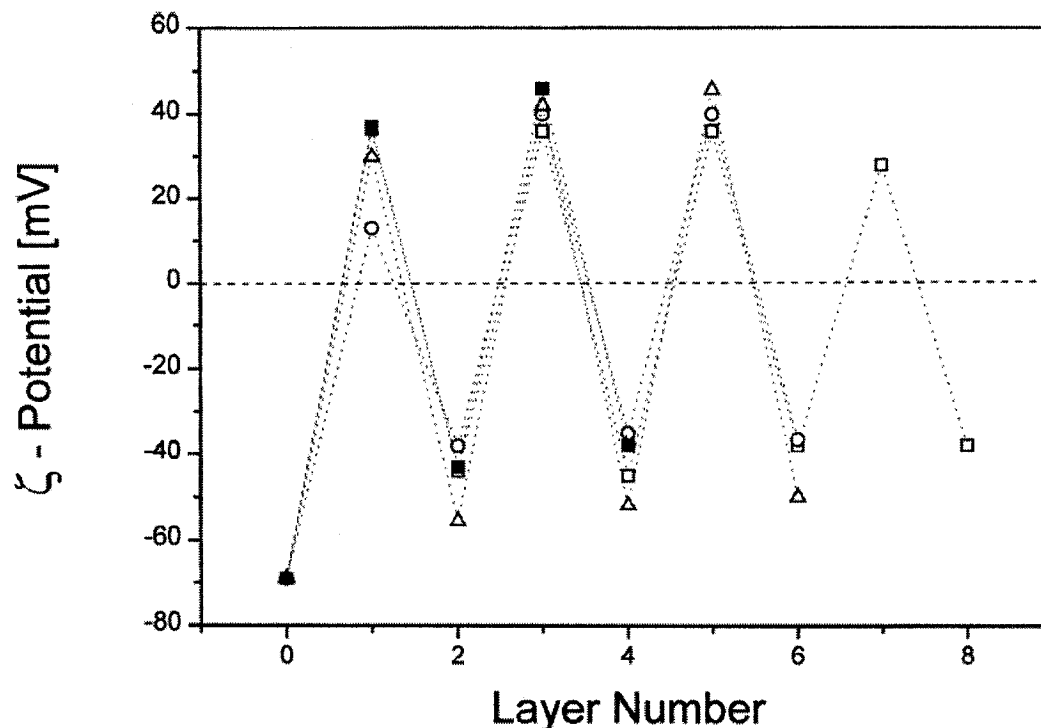


Figure 2.32 Zeta potential as a function of number of layers for coated polystyrene sulfate latex particles, diameter 640nm: □ PSS/PDADMAC; ■ BSA/PDADMAC ○ PSS/PAH; △ DNA/PDADMAC (Sukhorukov et al., 1998)

Some polymer pairs have been reported not to show the critical charge density, but they have special interactions contributing to the multilayer formation other than electrostatic attraction. The critical charge density is required for the charge overcompensation to reverse the surface charge and for the stabilization to withstand desorption of the following layer. Schlenoff et al. (1998) investigated the role of surface charge in

determining and limiting the increment of polymer added per deposition cycle. They reported that surface charge controls the amount of polymer deposited and represents, on average, one-half of the charge within a single molecular layer. With the strongly dissociated polyelectrolytes, PSS and PDADMA, a constant surface charge develops during multilayer buildup. Film thicknesses for PDADMA/PSS multilayers are plotted in Figures 2.33 as a function of layer number.

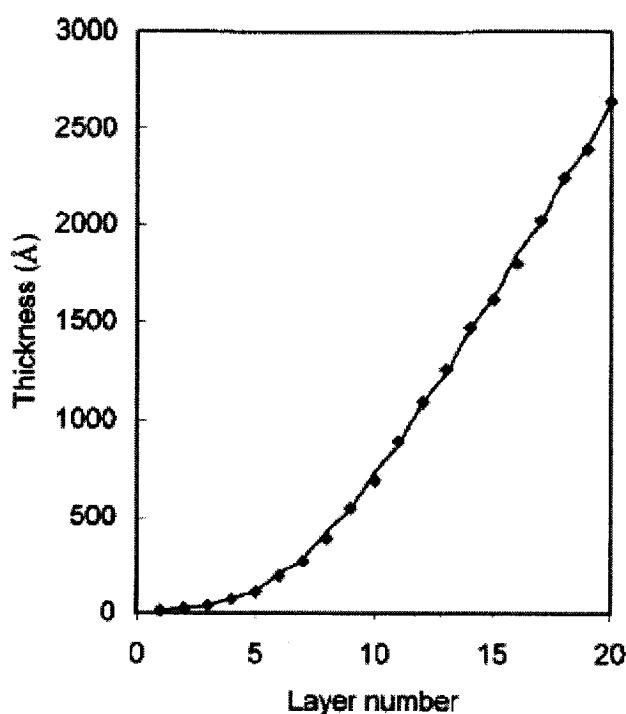


Figure 2.33 Thickness as a function of the number of layers for a PSS/PDADMA multilayer deposited on silicon wafer from polymer solutions containing 1.0 M NaCl (Schlenoff et al., 2001)

The surface charge, propagated and inverted by sequential adsorption steps, is overneutralized (overcompensated) at each step. A steady-state thickness increment vs layer number appears when the level of overcompensation is constant (Figure 2.33). In

this mechanism, the salt concentration determines the adsorbed amount (layer thickness) by controlling surface charge. Figure 2.34 (a) shows surface charge density as a function of salt concentration for PDADMA/PSS multilayers consisting of 14 (PSS-terminated) and 15 (PDADMA-terminated) layers, whereas Figure 2.34 (b) illustrates the thickness of polyelectrolyte multilayers. The thickness (which is assumed to be proportional to the amount deposited) of a 10-layer pair film shows an almost linear dependence on salt concentration between 10-2 M.

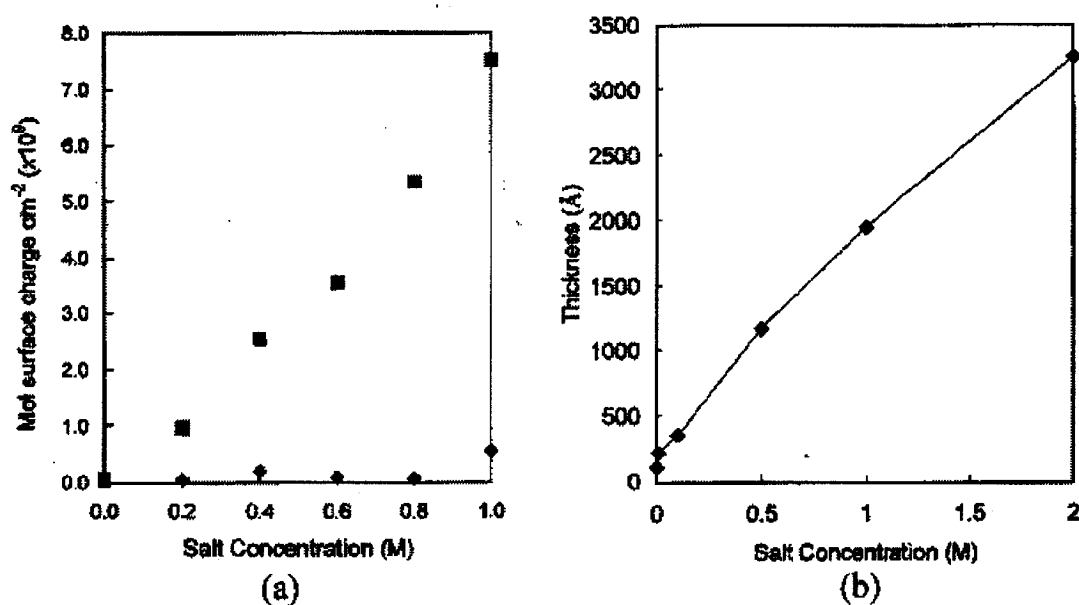


Figure 2.34 (a) Positive surface areal charge density for 15-layer PSS/PDADMA multilayers (PDADMA-capped, ■) and 14-layer multilayers (PSS-capped, ♦) made from solutions containing 1 mM polymer and different NaCl concentrations (Schlenoff et al., 2001). (b) Film thickness vs salt concentration for multilayers with ten layer pairs each (Dubas et Schlendoff, 1999).

## CHAPTER 3

### EXPERIMENTAL METHODOLOGY

Figure 3.1 summarizes the total experimental procedures.

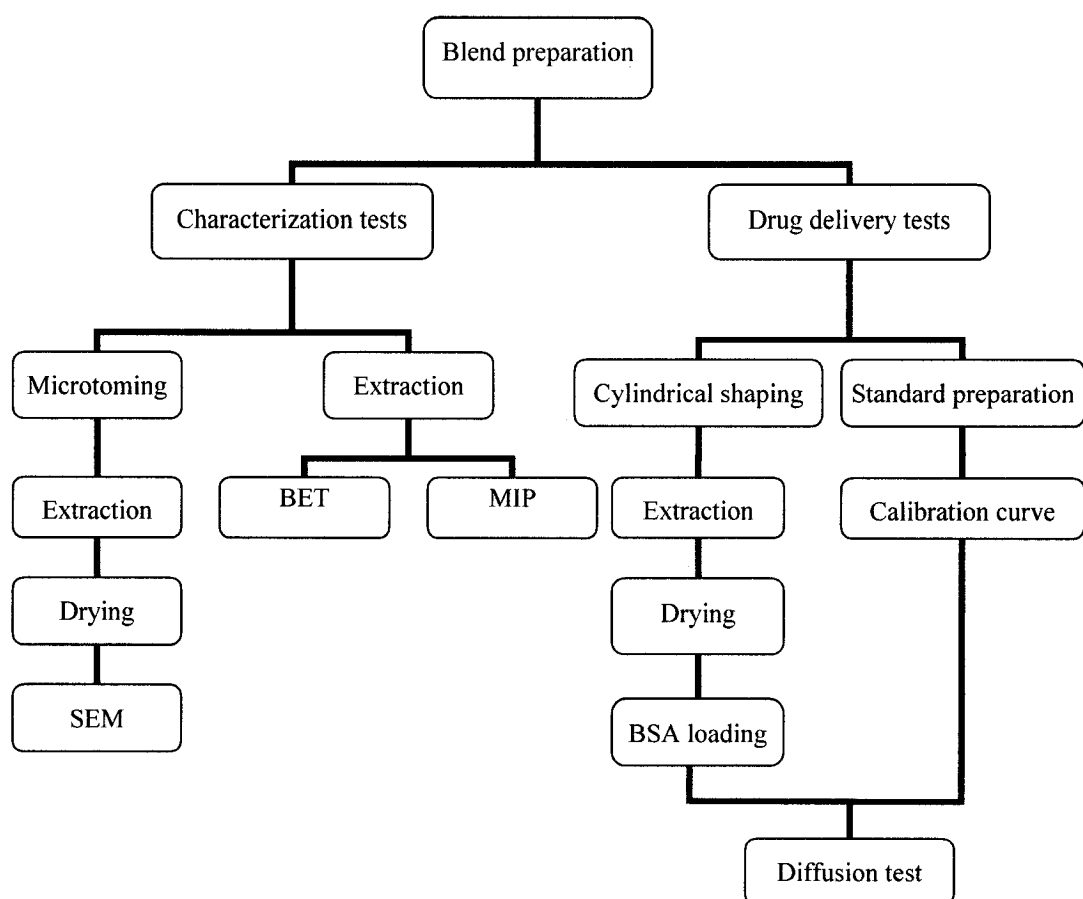


Figure 3.1 Experimental Summary

### 3.1 Materials

High-density polyethylene (HDPE) and Polystyrene (PS) used in this study with molecular weights of  $M_n=24000$  and  $M_n=100000$  respectively, were obtained from Dow Chemical of Canada. The copolymers were obtained from Shell USA. SEBS is a triblock copolymer of (styrene)-(ethylene-butylene)-(styrene) with a molecular weight of  $M_n=35000$  for the center block and  $M_n=7500$  for the PS blocks. The composition of PS in SEBS is 30%. SEB is a diblock copolymer of (styrene)-(ethylene-butylene) with a molecular weight of  $M_n=47000$  for (ethylene-butylene) block and  $M_n=20000$  for the styrene block. This copolymer has 30% PS. Polylactide (PLA), was purchased from Cargill (non-commercial grade: 5729B), in pellet form. The properties of the materials are listed in Table 3.1. The bovine serum albumin (BSA) as well as polycation poly (diallyldimethylammonium chloride) (PDADMAC),  $M_w=100000-200000$ , and polyanion poly (sodium 4-styrenesulfonate) (PSS)  $M_w=70000$  were purchased from Sigma-Aldrich. The viscosity of the BSA solution was measured by CVO 120, a stress control rheometer. Phosphate buffer solution (PBS) was purchased from Fisher Scientific. The tetrahydrofuran (THF), cyclohexane, chloroform, and sodium chloride were obtained from Laboratoire Mat, Beauport (Quebec). All polymers, polyelectrolytes, proteins, solvents and salts were used as received. Water used in all experiments was prepared by a three stage microfiltration system known as Milli-Q Millipore Biocel with a resistivity of at least  $18.2 \text{ M}\Omega \text{ cm}$ .

### 3.2. HDPE and PLA Porous Device Preparation

Preparation techniques of these HDPE porous structures were first developed by Li et al., (2002). Binary blends of HDPE/SEB and HDPE/SEBS, 40/60, 50/50, and 60/40 (v/v %) were prepared by melt mixing the polymers in a Brabender mixer at the chamber temperature of  $200^\circ\text{C}$  and blades rotating at 50 rpm. The blends were mixed for 5

minutes under a constant flow of nitrogen as an inert gas. After the mixing, the blends were dropped into liquid nitrogen to fix their morphology.

Table 3.1. Characteristic Properties of the Materials

Material	Mw	Mn	Density		Supplier
			At 20°C	At 200°C	
PS	215000	100000	1.04	0.974	Dow
HDPE	79000	24000	0.962	0.754	Dow
SEB	—	<i>S</i> = 20000 <i>EB</i> = 47000	0.910	0.820	Shell
SEBS	—	<i>S</i> = 7500 <i>EB</i> = 35000	0.910	0.820	Shell
PLA	—	—	1.24	1.09	Cargill

For the PLA/PS blends, PLA and PS were dried for 48 hours in a vacuum oven at 70°C and at room temperature respectively, prior to the blending. This technique was initially introduced by [Sarazin et al. \(2003\)](#) for the preparation of PLLA porous structures. In order to make a 50/50 (v/v %) blend, an accurate composition of each polymer was fed to the chamber. The temperature was set at 205°C and the blades rotating speed was set at 50 rpm. The polymer mixture was mixed for 7 minutes under a dry nitrogen flow which is essential in blending process to prevent a dramatic melt degradation of PLA during



mixing. Like the HDPE samples, the PLA blends were dropped into the liquid nitrogen for three minutes to freeze-in its morphology.

For the diffusion experiments, some samples were cut into cylinders with diameter of 3 mm to 4 mm and variable length of 6 mm to 10 mm, using a circular saw at high speed.

### **3.3. Morphology Analysis with Scanning Electron Microscopy (SEM)**

In order to achieve microscopic observation of our polymer structure, samples were microtomed by a Leica RM2165 equipped with glass knife in order to form a smooth surface. In order to eliminate the surface deformation during cutting, the samples were held at  $-150^{\circ}\text{C}$ . Then, solvent extraction of the blends was performed in a Soxhlet extraction apparatus. For the HDPE/SEB and HDPE/SEBS blends, tetrahydrofuran (THF) was used to extract SEB and SEBS, whereas for PLA/PS blends, cyclohexane was the appropriate solvent. The extraction was followed for 2 days for HDPE/SEB and HDPE/SEBS samples and for 7 days for PLA/PS samples. The temperature of the solvent during extraction was recorded as  $60\text{--}70^{\circ}\text{C}$ . After the extraction, samples were dried in a vacuum oven at  $60\text{--}70^{\circ}\text{C}$  until constant weight for each sample was achieved. The dried microtomed samples were coated with a gold-palladium alloy. Finally samples were observed under a Jeol JSM 840 Scanning electron microscope at a voltage of 10 or 15 kV.

### 3.4 Characterization of HDPE and PLA Highly Co-Continuous Structures

#### 3.4.1 Continuity of HDPE and PLA Templates

After blending, solvent extraction was performed for HDPE/SEB, HDPE/SEBS, and PLA/PS blends, where the copolymers and PS were extracted from the blends. Tetrahydrofuran and cyclohexane were used as extracting solvents for copolymers and the PS phase, respectively.

One way to analyze the continuity of the extracted substrates is a gravimetric method which includes measurement of weight loss. The expression of the continuity percentage is given by:

$$\% \text{Continuity} = \frac{(\text{weight of extracted phase})_{\text{initial}} - (\text{weight of extracted phase})_{\text{final}}}{(\text{weight of extracted phase})_{\text{initial}}} \quad (3.1)$$

#### 3.4.2 Internal Surface Area and Pore Diameters

##### 3.4.2.1 Image Analysis (IA)

A semiautomatic image analysis apparatus (IA) was used to measure the diameter of the dispersed phase. To obtain more accurate data, more than 250 diameters were used for each sample. To estimate the number average diameter  $d_n$ , and volume average diameter  $d_v$ , SEM images were analyzed for each sample. The IA results for samples are summarized in Table 4.2.

### 3.4.2.2 BET Technique

The domain size and surface area of co-continuous polymer blends are very important of morphological features. The conventional image analysis technique, which is based on the analysis of two dimensional photomicrographs, cannot be used to measure such an interpenetrating and intertwining three dimensional structure. The BET technique is an adequate approach to tackle the above problem. In this method surface area is measured by determining the quantity of gas that adsorbs as a single molecular layer (monolayer). This quantity can be calculated for a known volume of nitrogen, therefore the area covered by each molecule is known. The gas mixture, which is composed of nitrogen and helium, continuously passes through the sample cell. When the sample cell is immersed into and removed from the liquid nitrogen bath, the adsorption and desorption of nitrogen gas occurs. When nitrogen gas is adsorbed out of the gas mixture, the change in effluent gas composition during adsorption and desorption is analyzed by a thermal conductivity detector. The area of the sample is calculated from the number of adsorbed molecules derived from the gas quantity and area occupied by each nitrogen molecule.

To obtain the morphological parameters in the co-continuous region, it is assumed that (1) the geometric shape of the pore is an interconnected cylinder, (2) the total volume of the pore is equal to that of the extracted phase, (3) the total surface area is that of the pore wall.

The instrument that we used in our experiments is comprised of a Flowsorb 2300 II Micrometric, and a regulator of gas debit Cal Box de Sierra Instruments. Knowing the extent of continuity for each sample and assuming that the pores are interconnected cylinders, average pore diameter can be determined by equation 3.2:

$$d = \frac{4V}{S} \quad (3.2)$$

where  $d$  is the diameter,  $V$  is the total volume of the pores and  $S$  is the internal surface area. This method was applied previously by Li and Favis (2001), as a characterization method of highly continuous phases. The detailed explanations for the experimental and theoretical procedures are reported elsewhere (Li, 2001). The experimental error is  $\pm 4\%$ .

### 3.4.2.3 Mercury Intrusion Porosimetry (MIP)

Mercury Intrusion Porosimetry (MIP) is a technique used to measure pore size distribution, and has an advantage in that it is able to span the measurement of pore size ranging from a few nanometers to several hundred micrometers. MIP has become an important tool in the characterization of pore size distribution, pore diameter, and total volume of porosity.

Pore size and volume quantification are accomplished by submerging the sample under a confined quantity of mercury and then increasing the pressure of the mercury hydraulically. As the applied pressure is increased the radius of the pores which can be filled with mercury decreases and consequently the total amount of mercury intruded increases. The data obtained give the pore volume distribution directly and with the aid of a pore physical model, permit a simple calculation of the pore size. Determination of pore size by mercury penetration is based on the behavior of non-wetting liquids in capillaries. The pressure required to force the mercury into a small pore is a function of the pore size and the experimental data treatment follows the Washburn equation (Washburn, 1921):

$$Pr = - 2 \sigma \cos \theta \quad (3.3)$$

Where  $P$  is the applied mercury pressure,  $r$  is the radius of pore,  $\sigma$  is the surface tension of mercury ( $\sigma = 485 \text{ mN/m}$ ), and  $\theta$  is the contact angle between mercury and polymer ( $\theta = 160^\circ$ ). Lowell et Shields, (1991) provided a detailed procedure for this method. The

results of pore diameters for our different polymer substrates obtained by mercury porosimetry, are listed in Table 4.2.

### 3.5 Loading protocol and loading efficacy calculation

In order to force the solution to penetrate into the highly porous structure, we used a high pressure apparatus following a vacuum-pressure cycle as described previously by Roy et al. (2004, 2006). Prior to the loading procedure, test tubes are washed completely and filled with BSA solution. Dry porous samples are weighed before and after loading. Then each sample is immersed into the solution. The procedure follows a vacuum-pressure cycle including nine steps : V(30 min)+ P(15 min) +P(15 min) + V (45 min) + P(15 min) + P(15 min) + V( 60 min) + P(15 min) + V( 30 Min) ,where V is the vacuum and P is the pressure. The number in the parentheses shows the time for which vacuum and pressure are required to be applied. After each vacuum or pressure cycle, the system is released to ambient pressure for a few minutes and samples are stirred inside the BSA solution. After the last vacuum cycle, the loaded samples are brought out and their surfaces are washed with Milli-Q water. Samples are dried at 40-45°C until constant weight is achieved. The amount of loaded BSA can be obtained by calculating the difference between the initial and Final weight of the sample (detailed description of the procedure is shown in Appendix A).

After the loading, porous samples were washed with water and were dried under a vacuum oven at 45° C for 12 hours. Loading efficacy was calculated for each sample after BSA loading

$$\text{Loading efficiency} = \left( \frac{V_e}{V_i} \right) \times 100 \quad (3.4)$$

Where  $V_e$  is the volume of water penetrated into the porous sample calculating from measuring the weight of sample after loading, and  $V_t$  is the total porous volume of the sample.  $V_t$  was calculated by the following calculations for each HDPE and PLA samples.

### ***Calculation of HDPE and PLA void volume***

#### ***HDPE:***

$$\rho_{HDPE} \text{ at } 200^\circ\text{C} = 0.754 \text{ g/ml}$$

$$M_{HDPE \text{ extracted capsule}} = M_{initial HDPE} \quad (3.5)$$

$$M_{initial HDPE} \times \frac{ml}{0.754g} \times \frac{1g}{1000mg} = Volume_{matrix \text{ of HDPE substrate}} \quad (3.6)$$

*For blends of (50-50) % v/v*

$$Volume_{void} = Volume_{matrix}$$

#### ***PLA:***

$$\rho_{PLA} \text{ at } 200^\circ\text{C} = 1.09 \text{ g/ml}$$

$$M_{PLA \text{ extracted capsule}} = M_{initial PLA} \quad (3.7)$$

$$M_{initial PLA} \times \frac{ml}{1.09g} \times \frac{1g}{1000mg} = Volume_{matrix \text{ of PLA substrate}} \quad (3.8)$$

*For blends of (50-50) % v/v*

$$Volume_{void} = Volume_{matrix}$$

### ***Calculation of loading Efficacy***

#### ***HDPE:***

$$M_{\text{Loaded BSA}} = M_{\text{final HDPE after loading}} - M_{\text{initial HDPE before loading}} \quad (3.9)$$

$$V_{\text{Loaded BSA}} = M_{\text{Loaded BSA}} \times \frac{1}{\rho_{\text{BSA}}} \quad (3.10)$$

$$V_{\text{Loaded BSA}} / \text{Volume}_{\text{void}} \times 100 \quad (3.11)$$

#### ***PLA:***

$$M_{\text{Loaded BSA}} = M_{\text{final PLA after loading}} - M_{\text{initial PLA before loading}} \quad (3.12)$$

$$V_{\text{Loaded BSA}} = M_{\text{Loaded BSA}} \times \frac{1}{\rho_{\text{BSA}}} \quad (3.13)$$

$$V_{\text{Loaded BSA}} / \text{Volume}_{\text{void}} \times 100 \quad (3.14)$$

### 3.6 Layer-by-Layer Deposition of Polyelectrolytes inside the HDPE and PLA Porous Structures

Previously our group developed a method to prepare LbL deposition of polyelectrolytes onto a porous co-continuous template ([Roy et al., 2006](#)). This technique was a variation of an approach described by [Caruso et al., \(1999b\)](#). BSA, PDADMAC and PSS were used in the form of aqueous solutions containing respectively 150 mg/ml of protein, 10 mg/ml, and 10 mg/ml of polyelectrolyte in 1 M NaCl. The preparation of polyelectrolyte solution is explained in the following section. Three precursor polyelectrolyte films were initially adsorbed on a porous polymer surface in order to create a uniformly charged surface. In order to load each layer of polyelectrolyte, a vacuum-pressure cycle was followed similar to the one for BSA loadings (see appendix B). During the 4-hour loading process, polymer samples must stay completely inside the solution (BSA or polyelectrolyte). Note that while conducting the loading experiment one should not stopper the test tube (see Figure 3.2).

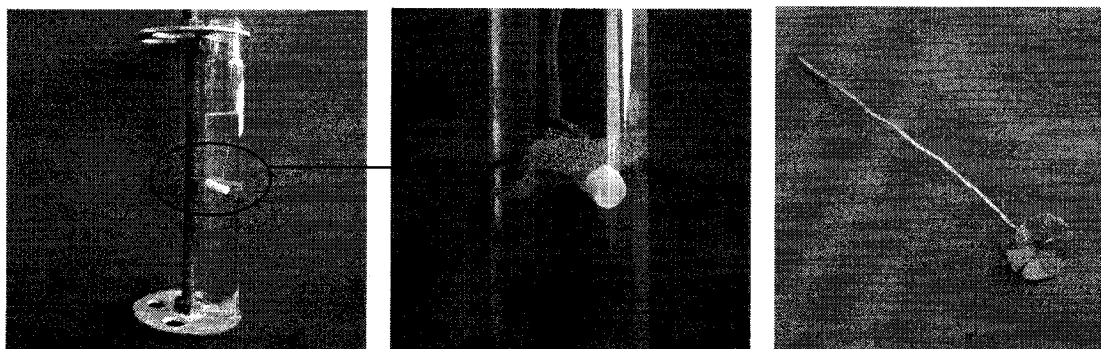


Figure 3.2 Polymer sample in test tube, completely kept inside the solution with a rod



After polyelectrolyte loading, porous samples were washed with water for 4 hours under constant shaking to remove the unattached macromolecules. Water was refreshed each hour. Following the washing step, the samples were dried under a vacuum oven at 45°C for 12 hours.

### 3.6.1 Preparation of polyelectrolyte solution

In order to prepare the standard solutions from a PSS solution of 30 wt %, we used the following equation to calculate PSS concentration.

$$30\% (w/w\%) = \frac{30(g)PSS}{100(g)Water} \times \frac{1g}{ml} \times \frac{1000mg}{1g} = \frac{300(mg)PSS}{ml} \quad (3.15)$$

In order to prepare 50 ml of PSS solution with concentration of 10 mg/ml, 1.67 ml of polyelectrolyte solution of 300 mg/ml should be added to 50ml of water. Since we prepared this solution in 1M NaCl solution instead of water, 1.67 ml of polyelectrolyte was added to 50ml of 1M NaCl solution.

$$\frac{10(mg)PSS}{(ml)water} = \frac{500(mg)PSS}{50(ml)water} \quad (3.16)$$

$$500(mg) PSS \div 300 \left( \frac{mg}{ml} \right) = 1.67 \text{ ml PSS} \quad (3.17)$$

The same calculations are applied for a PDADMAC solution of 20 wt %;

$$20\% (w/w\%) = \frac{20(g)PDADMAC}{100(g)Water} \times \frac{1g}{ml} \times \frac{1000mg}{1g} = \frac{200(mg)PDADMAC}{ml} \quad (3.18)$$

In order to prepare 50 ml of PSS solution with a concentration of 10 mg/ml, 2.5 ml of polyelectrolyte solution of 200 mg/ml should be added to 50ml of water. Since we prepared this solution in 1M NaCl solution instead of water, 2.5 ml of polyelectrolyte was added to 50ml of 1M NaCl solution.

$$\frac{10(\text{mg})\text{PDADMAC}}{(\text{ml})\text{water}} = \frac{500(\text{mg})\text{PDADMAC}}{50(\text{ml})\text{water}} \quad (3.19)$$

$$500(\text{mg}) \text{PDADMAC} \div 200 \left( \frac{\text{mg}}{\text{ml}} \right) = 2.5 \text{ ml PDADMAC} \quad (3.20)$$

### 3.7 In Vitro BSA Release

In order to study the BSA release profile from porous HDPE and PLA, the BSA-loaded porous carriers were immersed into 3 ml of Milli-Q water in spectrophotometry cell. They were incubated at 37°C under constant shaking. The water in the cell was replaced with fresh water every 24 hours and the supernatant was later used for the pH determination of the incubation medium. The concentration of the BSA from the polymeric matrix was monitored using a UV-Vis spectrophotometer (Cary 100, Varian) at pre-determined time intervals. Prior to the actual release test, a set of standard BSA solutions were prepared to obtain an accurate calibration curve. Due to the instability of peptide in the release medium reported by [Blanco-Prieto et al. \(1999\)](#), an indirect method for measuring the amount of released BSA was also used by measuring the amount of remaining drug in the polymer carrier (see appendix D for more explanation of BSA instability) . In this method dry polymer capsule is weighed after loading and before the release test. The dried porous polymers is weighed a second time after completing the release test. The difference between these measurements is the amount of released drug. This result is compared to the results from the spectrophotometry device.

While conducting the release experiment, to prevent the water evaporation from the cell, we used a plastic head to cover the cell. To gain more control over water evaporation, the head was sealed with Teflon tape. In order to obtain the accurate concentration of BSA at different time intervals, the whole system (cell + 3ml water + sample + head (sealed with Teflon tape)) is weighed at the beginning of the test. Once again the whole system weight is recorded after each spectrophotometer reading. The difference between these two weights is the evaporated water and therefore with a simple calculation we can obtain the accurate concentration of the BSA in 3 ml of water.

During the experiment the polymer capsule must be kept completely inside the release medium (Milli-Q water). For PLA samples, as water started to enter the pores, the samples sunk entirely into the water, however for HDPE capsules, at any time of the experiment, the samples floated on the water. Therefore to overcome this problem with HDPE, we used a head connected to a rod, to keep the samples inside the water at all times (Figure 3.3). Note that in the spectrophotometer light passes through the middle part of the cell; therefore the sample should keep inside the water, but above the middle part of the cell.

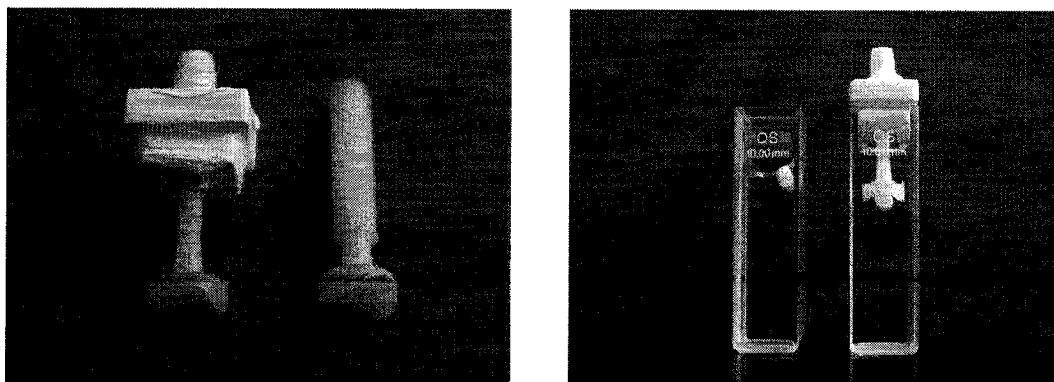


Figure 3.3 Spectrophotometry cell with sealed head (to prevent water evaporation) and rod (to keep the samples inside water)

### 3.7.1 Preparation of Standard BSA Solutions

In order to prepare the standard solutions from BSA solution of (30 wt %), we used the following equation calculate BSA concentration.

$$30\% \text{ (weight percentage)} = \frac{30(\text{g})\text{BSA}}{100(\text{g})\text{Water}} \times \frac{1\text{g}}{\text{ml}} \times \frac{1000\text{mg}}{1\text{g}} = \frac{300(\text{mg})\text{BSA}}{\text{ml}} \quad (3.21)$$

Using the following equation, we calculated the required volume which should be taken from original solution (30 %v/v) to prepare a solution with known concentration of  $C_2$ . The volumes and concentrations to prepare standard solutions are listed in Table 3.2.

$$C_1V_1 = C_2V_2 \quad (3.22)$$

$$V_{\text{added water}} = V_2 - V_1 \quad (3.23)$$

Table 3.2 Dilution of concentrated BSA

$C_1$	$V_1$	$C_2$	$V_2$	$V_{\text{added}}$
(mg/ml)	( $\mu\text{l}$ )	(mg/ml)	(ml)	(ml)
300	10	0.12	25	24.99
300	30	0.36	25	24.97
300	50	0.60	25	24.95
300	100	1.20	25	24.9
300	150	1.80	25	24.85
300	200	2.40	25	24.8
300	250	3.00	25	24.75

### 3.7.2 Calibration Curve

Using the standard solutions, the spectrophotometer provides a calibration diagram with a known equation. The rest of the measurements are based on this equation. In order to obtain a very accurate data, a new set of standard solution and new calibration curve should be obtained for each test. Below, one example of spectrophotometer readings and the resulted calibration curve is shown.

Table 3.3 Spectrophotometer readings for prepared standards

<i>Standard</i>	<i>Concentration (mg/ml)</i>	<i>Readings</i>
Std 1	0.12	0.1090
Std 2	0.36	0.2585
Std 3	0.60	0.4314
Std 4	1.20	0.8454
Std 5	1.80	1.2457
Std 6	2.40	1.6498
Std 7	3.00	2.0314

***Calibration Equation:***

$$Abs = 0.67218 \times Conc. + 0.02842 \quad (3.24)$$

$$R^2 = 0.99983$$

***Calibration Curve Diagram:***

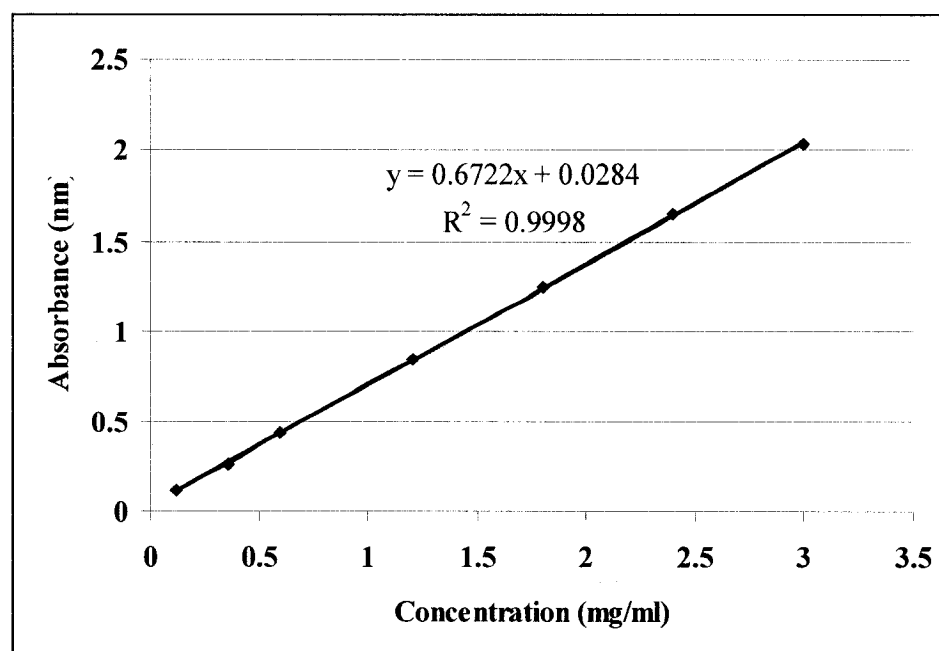


Figure 3.4 Calibration curve of BSA diffusion in water measured at 280 nm

## **CHAPTER 4**

### **POROUS DEVICES DERIVED FROM CO-CONTINUOUS POLYMER BLENDS AS A ROUTE FOR CONTROLLED DRUG RELEASE**

#### **4.1 Article Presentation**

Discoveries of new and promising pharmaceutical agents and development of appropriate therapies that compliment the advantage of these new agents continue to fuel inventions on appropriate drug delivery systems. Research in the area of controlled drug delivery has witnessed tremendous progress in recent years due to its great potential to improve human health. Meanwhile, the development of nanotechnology provides opportunities to characterize, manipulate and organize matter systematically at the nanometer scale. Biomaterials with nano-scale organizations have been used as controlled release reservoirs for drug delivery. Drug-delivery systems can be synthesized with controlled composition, shape, size and morphology. Biodegradable polymers enjoy the advantage of eliminating the problem related to the long-term fate of the implanted or injected drug carriers. Therefore, they have been extensively pursued in controlled drug delivery systems in the form of micro and nanospheres.

The objective of this article is to introduce a novel polymer substrate preparation and drug encapsulation technique which has the potential to be applied as a controlled drug delivery system. Also we aim to show other potential applications of this polymer substrate accompanied with a surface modification technique (LbL) and a closed – cell method which extend the possible application range of our porous substrate. In this study, three different substrates with pores of different size were utilized to provide data on how pore size may affect the drug release profile.

# Porous devices derived from co-continuous polymer blends as a route for controlled drug release

*Pouneh Salehi , Pierre Sarazin, and Basil D. Favis <sup>1</sup>*

CREPEC, Department of Chemical Engineering, École Polytechnique de Montréal, P.O.  
Box 6079 Station Centre-ville, Montréal, (QC) Canada H3C 3A7

---

<sup>1</sup> To whom correspondence should be addressed. Tel: +1-514-340-4711 ext. 4527; Fax:  
+1 -514-340-4159. *E-mail address:* basil.favis@polymtl.ca



## **4.2 Porous Devices Derived from Co-Continuous Blends as a Route for Controlled Drug Release**

### **4.2.1 Abstract**

In this study we examine the release profile of bovine serum albumin (BSA) from a porous polymer matrix derived from a co-continuous polymer blend. The porosity is generated through the selective extraction of one of the continuous phases. This is the first study to examine the approach of using morphologically tailored co-continuous polymer blends as a template for generating porous polymer materials for use in controlled release. A method for the preparation of polymeric capsules is introduced and the effect of matrix pore size and surface area on the BSA release profile is investigated. Furthermore, the effect of surface charge on release is examined by surface modification of the porous substrate using layer-by-layer deposition techniques. Synthetic, non-erodible polymer HDPE was used as a model substrate prepared by melt blending with two different styrene-ethylene-butylene copolymers. Blends with HDPE allow for the preparation of porous substrates with small pore sizes (300 and 600 nm). A blend of PLA and PS was used to prepare porous PLA with a larger pore size (1.5  $\mu\text{m}$ ). The extent of interconnectivity, surface area and pore dimension of the prepared porous substrates were examined via gravimetric solvent extraction, BET nitrogen adsorption, mercury porosimetry, and image analysis of SEM micrographs. Using a loading protocol into the porous HDPE and PLA involving the alternate application of pressure and vacuum, it is shown that virtually the entire porous network was accessible to BSA loading. Loading efficiencies of between 80% and 96% were obtained depending on the pore size of the carrier and the applied pressure. The release profile of BSA from the microporous structure was monitored by UV spectrophotometry. The influence of pore size, surface area, surface charge and number of deposited layers is demonstrated. It is shown that an

effective closed-cell structure in porous PLA can be prepared effectively eliminating all short-term BSA release.

#### 4.2.2 Introduction

Polymers are considered as important materials for use in controlled release due to their architectural and chemical diversity. As a specific advantage, they are able to present opportunities to modulate the properties in drug delivery systems, and, at the same time, meet important criteria of biodegradability and biocompatibility. Polymeric drug delivery systems (PDDS) include: designed macromolecular vehicles for drug delivery (Langner and Ugorskli, 2000; Sinha and Kumria, 2001), polymer-drug conjugates (Kolhe et al, 2004; Duncan et al, 2006), polymeric micelles containing covalently bound drug (Kwon and Kataoka, 1995; Huh et al, 2005; Torchilin, 2005), and macro and nano spheres matrix systems. However few of these formulations could be categorized as controlled release or targeted release applications. These conventional formulations are associated with an immediate, but highly localized drug release resulting in high peaks and low troughs of plasma drug level potentially leading to harmful side effects. To overcome these problems, several technical advances have recently led to the development of new delivery devices capable of controlling the administration of a drug at a targeted site in the body in an optimal concentration-versus-time profile (Langer, 1998; Vyas et al., 2000). Various devices have been studied and built in order to control the release of drugs, however special attention has been given to monolithic devices (devices, where the drug is dispersed in a polymer matrix) since their clinical applications and their outcomes seem to be promising in terms of controlled and targeted drug release.

The preparation techniques of these drug carrier devices mostly involve *in situ* drug encapsulation. Unprotected therapeutic drugs and proteins show a short *in vivo* half-life and antigenic properties when they are introduced into the body. For this reason, protection of the drug from the hostile immunological system of the body is necessary in

order to efficiently deliver the drugs. Polymers of synthetic and biological origin have been used effectively in the delivery of various agents (especially proteins) to sites in the human body (Lin et al., 1997; Jeong et al. 1998; Aboubakar et al. 1999). Entrapment of water soluble drugs, such as proteins, in nano and macro particle carrier systems has been carried out through various approaches. The first widely used technique is coacervation (Blanco-Preito et al. 2004; OwusuAbabio et al., 1996). Numerous studies have also been reported in the literature investigating solvent evaporation techniques (Kim, H. K. et al. 2004; Rahman, N.A., et al., 2004). This method is more advantageous over the others since it provides greater protection for the substance to be encapsulated but also has some disadvantages (low entrapment efficiency) (Atkins, T.W, 1997). Other encapsulation methods include spray drying, polymer-polymer incompatibility, interfacial polymerization, and fluidized bed coating; however these methods have not been reported to be used in controlled release formulations.

Recently, significant work has been carried out on co-continuous morphologies in immiscible polymer blends (Lee, J.K. et al., 1999; Willemse, R.C. et al., 1999; Steinmann, S. et al., 2001; Li, J. et al., 2001; Sarazin, P. et al. 2004; Galloway, J. A. et al., 2005; Yuan, Z. et al., 2006). This structure is distinguished by the mutual interpenetration of the polymer phases. When two immiscible polymers are melt blended at low concentration of one of the phases, the predominant morphology is the dispersed droplet/matrix type. Increasing the concentration of minor phase to intermediate concentrations results in a co-continuous morphology where the two immiscible phases commingle in such a way that each phase remains continuously connected throughout the bulk of the blend. Further extraction of one phase leads to a structure of fully interconnected porosity. This porosity can be highly controlled via compatibilization of the blends and annealing. It has been shown that controlled annealing can produce larger pore sizes compared to the initial pore size through coalescence effects while adding compatibilizer to the blends decreases the interfacial tension and allows for the preparation of very small pores (Sarazin, P. et al. 2003; Yuan, Z. et al, 2004). Thus, this

approach is very promising for the fabrication of porous structures of fully interpenetrated porosity with a high level of control over the pore size, pore distribution, morphology and porosity.

It is known that various factors determine the overall release kinetics, e.g., drug loading, tortuosity of the carrier, partition coefficient of the drug between polymer and water, and the drug particle size distribution. Many studies have been devoted to explain how these parameters affect the drug release profile and how to gain control over initial burst and drug diffusion. However, there has been little study on the relationships between the drug carrier pore size and its controlled drug release behavior. Since pore size, for the same void volume, exponentially affects the internal surface area of the device, this may also influence drug localization and the controlled release properties.

Surface properties of polymer carriers play an important role in drug adhesion within the carriers. However, most of the polymers used in biomedical applications lack the appropriate functionality. In order to circumvent this disadvantage, several surface modification approaches have been developed. Several research investigations showed that the surface modification of polymer surfaces is an important tool in modulating controlled release (Otsuka et al., 2000; Liu et al. 2000; Zhu et al., 2005; Zhang et al., 2006). Zhu et al., were able to successfully modify mesoporous silica spheres. They showed that with an increase of the number of functional groups via surface modification, the drug storage capacity decreases and so does the release rate. In their work, Zhang et al., demonstrated that in the absence of surface modification, diffusion equilibration of the drug occurred within 20 min, whereas with surface modification, the equilibration time was extended to 7 days. Among all the surface modification methods for drug delivery applications, one promising approach is “layer-by-layer self assembly of polyelectrolytes “. In this method, the sequential adsorption of anionic and cationic polyelectrolytes, , leads to the formation of ordered multilayer assemblies on the solid substrate surface (Lvov et al., 1993). Several studies have reported LbL modification in

drug delivery applications (Qui et al., 2001; Lvov et al., 2001; Ibarz et al., 2001; Ladam et al., 2002; Ai et al., 2003; Sheney et al., 2004). This approach preserves the microporous channel structure and can be used to strengthen the interaction force, between the device and the drug molecule. Therefore, this method could effectively control the drug release rate. In this study we investigate the effectiveness of LbL surface modification onto a porous co-continuous template in controlling the BSA release rate.

The objective of this study is to introduce a new preparation protocol for a controlled delivery device based on a generation of porous media from morphologically tailored co-continuous polymer blends. Using bovine serum albumin as a model drug, the influence of pore size and surface charge, by LbL deposition, on the BSA release profile will be examined.

### **4.2.3 Experimental Procedure**

#### **4.2.3.1 Materials**

High-density polyethylene (HDPE) with a molecular weight of  $M_n=24000$  and Polystyrene (PS) with a molecular weight of  $M_n=100000$  were obtained from Dow Chemical of Canada. The two copolymers were obtained from Shell USA. One is designated as SEBS, Kraton G1652 is a triblock copolymer of (styrene)-(ethylene-butylene)-(styrene) with a molecular weight of  $M_n=35000$  for the center block and  $M_n=7500$  for the PS blocks. The other SEB, is a diblock copolymer of (styrene)-(ethylene-butylene), Cap 4745 with a molecular weight of  $M_n=47000$  for (ethylene-butylenes) block and  $M_n=20000$  for the styrene block. The composition of PS in both copolymers is 30%. Polylactide (PLA) was purchased from Cargill (non-commercial grade 7592B), and was used in pellet form. The Bovine serum albumin (BSA) solution (30%wt) as well as polycation poly (diallyldimethylammonium chloride) (PDADMAC),  $M_w=100000-200000$ , and polyanion poly (sodium 4-styrenesulfonate) (PSS)  $M_w=70000$

were purchased from Sigma-Aldrich. Viscosity of BSA solution was measured by CVO 120, a stress control rheometer. The tetrahydrofuran (THF), cyclohexane, chloroform, and sodium chloride were obtained from Laboratoire Mat, Beauport (Quebec). All polymers, polyelectrolytes, proteins, solvents and salts were used as received. The water used in all experiments was prepared by a 3 stage microfiltration system known as Milli-Q Millipore Biocel and possessed a resistivity of at least 18.2 M $\Omega$  cm. The properties of the polymers are listed in Table 4.1.

Table 4.1. Characteristic Properties of the Materials

Material	$M_w$	$M_n$	Density(g/cm <sup>3</sup> )		Supplier
			At 20°C	At 200°C	
PS	215000	100000	1.04	0.974	Dow
HDPE	79000	24000	0.962	0.754	Dow
SEB		$S=20000$ $EB=47000$	0.910	0.820	Shell
SEBS		$S=7500$ $EB=35000$	0.910	0.820	Shell
PLA	—	—	1.24	1.09	Cargill

#### **4.2.3.2 Blend Preparation**

Binary blends of HDPE/SEB, HDPE/SEBS, and PLA/PS 50/50 (%volume) were prepared by melt mixing the polymers in a Brabender mixer with roller blades, under a constant flow of dry nitrogen. For HDPE/SEB, and HDPE/SEBS, the chamber temperature was set at 200°C with blades rotating at 50 rpm. Five minutes of mixing was carried out, considered after all the polymer mixture was fed into the chamber. For the PLA/PS blends, PLA and PS were dried for 48 hours in a vacuum oven at 70°C and at room temperature respectively, prior to the blending. Each polymer was then fed to the chamber with a set temperature of 205°C and rotating blades at 50 rpm. After feeding, the sample was mixed for seven minutes under dry nitrogen flow. This is essential in the blending process to prevent a dramatic melt degradation of PLA during mixing. All the blends were quenched for 3 minutes in a bath of liquid nitrogen to freeze-in the morphology. All the blends were prepared at a 50/50 volume percentage composition. Directly after the blending step, specimens were cut out into cylinders of 3 mm diameters and 6-7mm height, using a circular saw at high speed.

#### **4.2.3.3 Solvent Extraction and extent of continuity**

After blending, solvent extraction of all the blends was performed in a Soxhlet extraction apparatus. In order to extract SEB and SEBS from HDPE/SEB and HDPE/SEBS blends, tetrahydrofuran (THF) was used as the extracting solvent. For PLA/PS blends, cyclohexane was used as the selective solvent for the PS porogen phase. The temperature of both solvents during the extraction process was 55-65°C. For HDPE/SEB and HDPE/SEBS the extraction continued for 48 hours while for PLA/PS it took 7 days to complete the extraction. After extraction the specimens were dried in a vacuum oven at 60-70°C until constant weight was achieved.

A gravimetric method (weight loss measurement) was used to obtain the continuity percentage of the porogen phase. The expression of % continuity is given by;

$$\% \text{ Continuity} = \frac{(\text{weight of extracted phase})_{\text{initial}} - (\text{weight of extracted phase})_{\text{final}}}{(\text{weight of extracted phase})_{\text{initial}}} \quad (4.1)$$

#### 4.2.3.4 Microtomy and Scanning electron Microscopy

To form a smooth plane surface for microscopic observations, the non-extracted samples were then microtomed under liquid nitrogen with a Leica RM2165 microtome equipped with glass knife. The microtomed samples were later treated to a solvent extraction step and then coated with gold-palladium alloy. Finally samples were observed under a Jeol JSM 840 Scanning electron microscopy at a voltage of 10 or 15 kV.

#### 4.2.3.5 Image Analysis, BET, and Mercury Porosimetry on Extracted Samples

A semiautomatic image analysis apparatus (IA) was used to measure the diameter of the dispersed phase. The number average diameter,  $d_n$ , and volume average diameter,  $d_v$ , were analyzed for each sample. More than 250 diameters were analyzed for each sample. In highly continuous structures, obtaining correct  $d_n$  and  $d_v$  values with IA becomes more difficult. Therefore BET and MIP methods were performed. A Flowsorb 2300 BET instrument was used to determine the surface area of each sample by gas adsorption. Knowing the extent of continuity for each sample and assuming the pores as interconnected cylinders, the pore diameter can be determined by,

$$d = 4V / S \quad (4.2)$$



where  $d$  is the diameter,  $V$  is the total volume of the pores and  $S$  is the surface area. This method was applied previously as a characterization method of highly continuous phases and the detailed explanation for the experimental and theoretical procedure is reported elsewhere (Li and Favis, 2001). The experimental error is  $\pm 4\%$ .

The porosity of samples was also determined by mercury intrusion porosimetry (MIP) using a Micromeritics model porosizer 9320. This method provides  $d_n$ ,  $d_v$  and the pore size distribution. The experimental data treatment follows the Washburn equation (Washburn, 1921)

$$Pr = - 2 \sigma \cos \theta \quad (4.3)$$

where  $P$  is the applied mercury pressure,  $r$  is the radius of pore,  $\sigma$  is the surface tension of mercury ( $\sigma = 485 \text{ mN/m}$ ), and  $\theta$  is the contact angle between mercury and polymer ( $\theta = 160^\circ$ ). The detailed procedure for this method is explained by Lowell (Lowell et al., 1991). The error for the experiments was  $\pm 5\%$ .

#### 4.2.3.6 High- Pressure Loading Apparatus

In order to force the penetration of solutions into the highly porous structures and to achieve high accessibility of the porosity to the solutions, we assessed a high pressure apparatus following a vacuum-pressure cycle as described here; V(30 min)+ P(15 min) +P(15 min) + V (45 min) + P(15 min) + P(15 min) + V( 60 min) + P(15 min) + V( 30 Min) ; Where V is the vacuum and P is pressure. After each vacuum or pressure stage, the samples are kept at room condition for few minutes. Loaded porous samples were then washed with water for 4 hours under constant shaking to remove the unattached macromolecules. Water was refreshed each hour.

In order to clarify the optimum conditions for the highest possible loading percentage, initial experiments were performed by Sarazin et al., 2004 and they demonstrated that alternating vacuum and pressure cycles result in higher loading efficiencies. After loading, the porous cylinders were placed in a vacuum oven at 40°C for 12 hours. The effect of heating on the release profile was examined by carrying out some experiments with samples dried at 60°C.

#### **4.2.3.7 In Vitro BSA Release studies**

Cylindrical BSA carriers were immersed in 3 ml of Milli-Q water in a spectrophotometry cell. Incubation took place at 37°C with constant shaking. The water in the cell was replaced with fresh water every 24 hours. The supernatant was used to determine the pH value in the incubation medium. Due to the possibility of instability of peptides in the release medium reported by Blanco-Prieto, (1999), an indirect method for measuring the amount of released BSA was also used by measuring the amount of remaining drug in the carrier device. The release profile of BSA from the polymeric matrix was monitored using a UV-Vis spectrophotometer (Cary 100, Varian) at pre-determined time intervals.

#### **4.2.3.8 Surface Modification via L-b-L Deposition of Polyelectrolyte into the HDPE and PLA templates**

Previously our group advanced an approach to preparing LbL deposition of polyelectrolytes onto a porous co-continuous template (Roy et al, 2006). In order to generate surfaces of different surface charge, porous HDPE and PLA were used as large surface area substrates for LbL. PDADMAC positively charged polyelectrolyte and PSS (negative) polyelectrolytes were used in aqueous solution form containing 10 mg/ml of polyelectrolytes and 1 M NaCl. In order to create a uniformly charged, three precursor polyelectrolyte films are required. First, the PDADMAC layer adsorbed easily onto the

hydrophobic PLA surface and showed a strong stable attachment to the PLA surface during all the preparation steps and also during the in vitro drug release tests. However in the case of HDPE substrate using PDADMAC as a first layer was not as efficient as PLA substrate. Three precursor layers starting with PDADMAC in HDPE layers demonstrated a weak attachment of layers to the HDPE surface due to HDPE properties and some layers diffused out with BSA during the in vitro release experiments. However using PSS as the first layer of precursor for HDPE presented higher polyelectrolyte stabilities on the surface. Thus, for HDPE, all LbL protocols started with PSS as the first layer. PDADMAC was used as the first layer for porous PLA. A vacuum-pressure cycle was used to allow the solution to penetrate inside the hydrophobic porous device in a 4-hour process. The unattached polyelectrolyte was eliminated by washing the samples with water for 4 hours under constant agitation. The water was changed every hour. After depositing the appropriate number of layers of polyelectrolyte, the BSA was deposited from a solution of concentration 150 mg/ml. After each deposition, samples were then dried under the vacuum oven at 45°C for 12 hours and weighed.

#### **4.2.4 Results and Discussion**

##### **4.2.4.1 Porous Device Morphology; Extent of Continuity and Pore Size Analysis**

The evolution of the percent continuity of the porogen phase as a function of the blend composition for HDPE/SEB, HDPE/SEBS, and PLA/PS is presented in Figure 4.1. SEB, SEBS, and PS, extracted from their blends, are termed the porogen phases.

From Figure 4.1, it can be concluded that all three blends are highly continuous at compositions close to 50/50 volume fraction. Similar results were also reported

previously for other compatibilized and non-compatibilized binary blends (Sarazin and Favis, 2003; Yuan et favis 2004; Sarazin et al 2004; Li and Favis, 2002; Jaziri et al, 2005). In the present paper, all blend systems were prepared at a composition ratio of 50/50 volume fraction due to their >90% continuity.

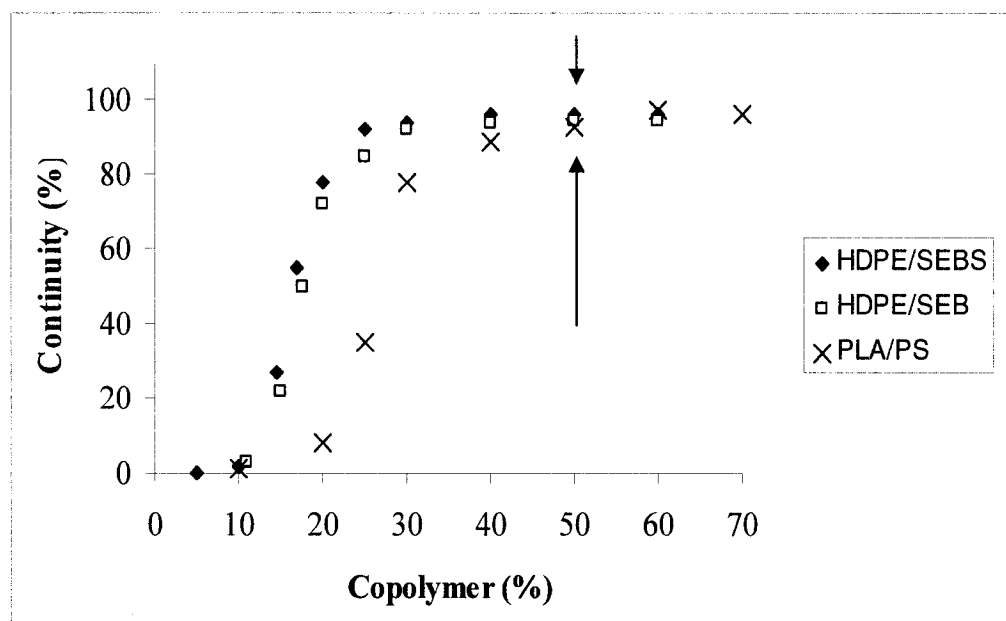


Figure 4.1 Continuity of the polymeric matrix (HDPE, PLA) as a function of extracted phase (SEBS, SEB, PS) volume percent.

Since one of the objectives of this study is to examine the influence of pore size and internal surface area on the drug release profile, quantifying the morphology of each blend is essential. Figure 4.2 shows the SEM micrographs for the three blends, HDPE/SEB, HDPE/SEBS, and PLA/PS. The fine co-continuous microstructure can be clearly observed for the extracted blends. Since co-continuous morphologies are complex three-dimensional structures, two-dimensional SEM micrographs and image analysis are limited in the information that they can provide. Thus, in these experiments, two other

methods, BET and mercury intrusion porosimetry, were also used to fully characterize the continuous porous morphology. Table 4.2 lists the pore diameters of extracted blends measured by these three different experimental methods.

Table 4.2 Pore size of porous HDPE prepared from HDPE/SEB, HDPE/SEBS and PLA/PS blends

Sample	Image Analysis		BET technique ( $\mu\text{m}$ )	Mercury Porosimetry		Surface Area ( $\text{m}^2/\text{g}$ )
	$d_v$ ( $\mu\text{m}$ )	$d_n$ ( $\mu\text{m}$ )		$d_v$ ( $\mu\text{m}$ )	$d_n$ ( $\mu\text{m}$ )	
HDPE/SEB (50/50)	0.46	0.27	0.32	0.35	0.25	13.72
HDPE/SEBS (50/50)	0.82	0.59	0.63	—	—	8.2
PLA/PS (50/50)	1.8	1.37	1.56	1.67	1.25	2.15

The data obtained by BET and mercury porosimetry show good agreement. However, for HDPE/SEBS blends, the MIP technique was unable to provide reliable results. In the case of porous HDPE, this is related to its low glass transition temperature which is far below room temperature. Tiny cracks in the material forms at high operating pressure (necessary for the examination of smaller pore sizes). For this reason, the nominal pore sizes referred to throughout this work are based on the BET data. Note that the BET reports a  $d_n$  value as discussed in previous work (Li and Favis, 2001).

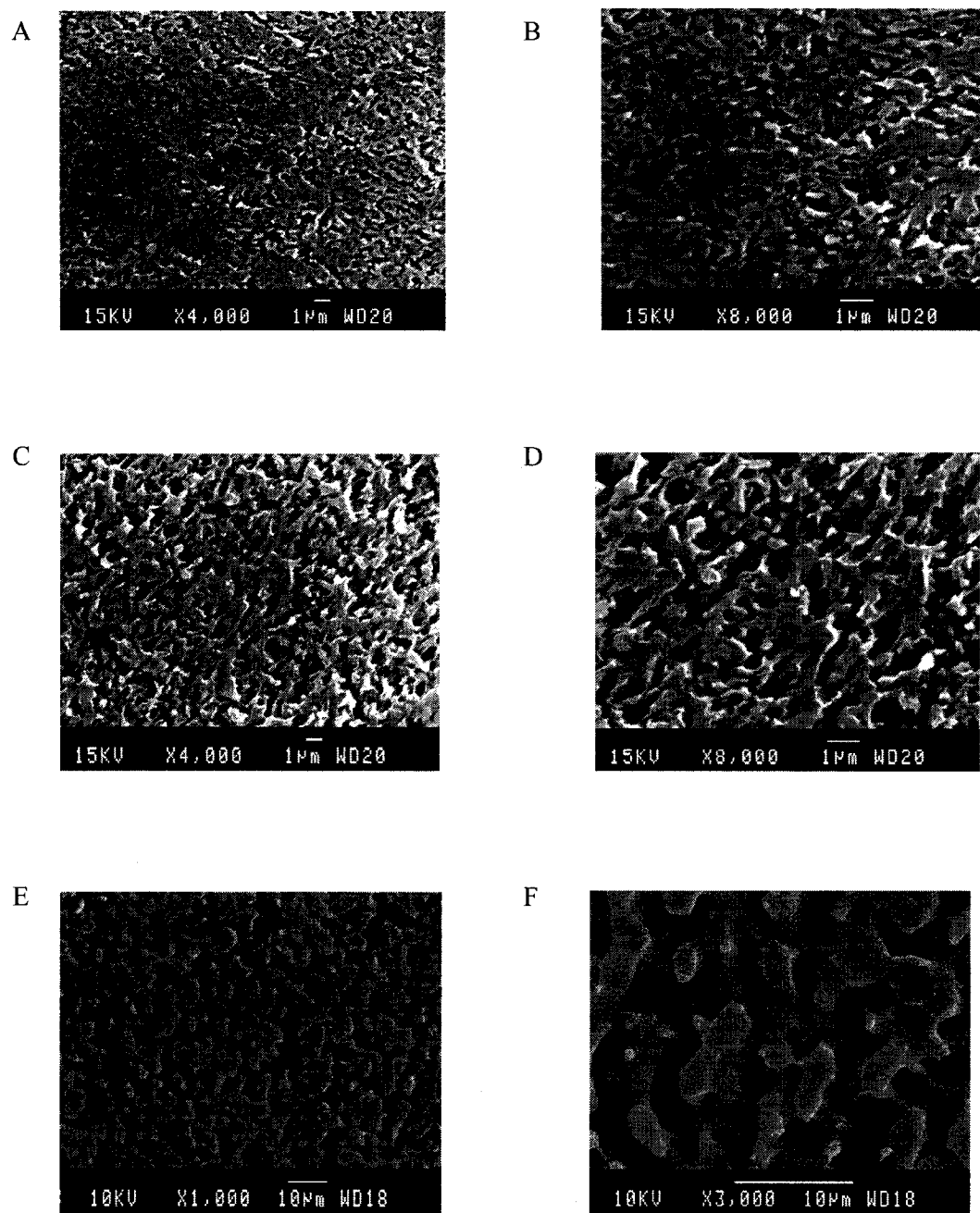


Figure 4.2 SEM micrographs; A) and B) HDPE/SEB (50/50), SEB extracted, C) and D) HDPE/SEBS (50/50), SEBS extracted, E) and F) PLA/PS (50/50), PS extracted.

#### 4.2.4.2 Drug Loading Protocol and Efficacy of Loading

The loading studies were carried out on 50% porous HDPE with an average pore size of 0.32  $\mu\text{m}$  (HDPE/SEB blends), 0.63  $\mu\text{m}$  (HDPE/SEBS blends), and porous PLA with an average pore size of 1.56  $\mu\text{m}$ . Since smaller pore size provides smaller and more tightly interconnected pathways within the porous polymer (Freiberg, S., et al, 2004), the loading efficacy at a given pressure varies for each sample. In order to study the effect of pore size and effect of pressure on the loading efficiency, we followed the vacuum-pressure protocol as outlined in the Experimental, section 4.3.6. The vacuum was held constant at 80 kPa and the effect of applied pressure on the loading efficacy of water was studied at three different values. Data are shown in Figure 4.3. The loading efficacy was calculated using the following equation:

$$\text{Loading efficacy} = \left( \frac{V_e}{V_t} \right) \times 100 \quad (4.4)$$

where  $V_e$  is the volume of water penetrated into the porous sample estimated by measuring the weight of the sample after loading, and  $V_t$  is the total porous volume of the sample.

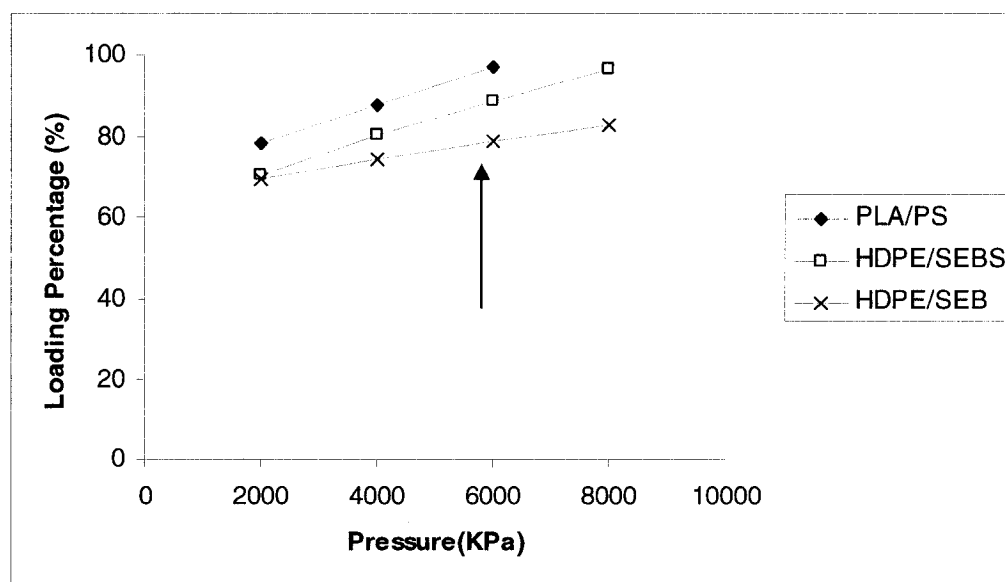


Figure 4.3 Fraction of pores filled by water at different working pressures

From the following loading results it can be concluded that for applied pressures of 6000 kPa and 8000 kPa, the porous volume is highly accessible to aqueous solution. It is interesting to note that the efficacy of loading is closely related to the pore size of the particular structure. Throughout this work  $P = 6000$  kPa was selected as the working pressure for all loading protocols.

#### **4.2.4.3 In-Vital Release of BSA from the Porous Devices**

BSA (bovine serum albumin) was used as a model active agent as it has been used extensively in other drug release studies (Wang et al., 2005; Moeda et al., 2003; Kedar et al., 1998; Tuovinen et al., 2004). Milli-Q water was used as the *in vitro* release medium since initial experiments revealed that in our case changing the medium from water to PBS (phosphate buffer solution, pH=7.4), (Jiang et al., 2002) did not have a significant effect on the release profile (data not shown). It is important to maintain a constant pH when dealing with pH sensitive carriers (Sutton et al., 2006; Lecomte et al., 2005), biodegradable polymers, and pH sensitive active agents. In this study, the pH was measured for each experiment by collecting the supernatant and was recorded to be 6.7-7.0 for all cases. It has been shown previously (Foster, 1977) that at a pH between 4.3 and 8, BSA maintains its so-called normal conformation. In order to examine the influence of pore size on the drug release, *in vitro* release studies were performed on 3 formulations which are listed in Table 4.3.



Table 4.3. Percentage of each ingredient, loading efficacy

Porous Polymers from 3 blends	BSA loading efficacy (%)	Burst release rate <sup>1</sup> (release%/ 2hr)	BSA release amount after 2 hours(%)	Final release Percentage <sup>2</sup>
1- HDPE/SEB	51	22.3	47	96.6
2- HDPE/SEBS	64	35.9	79	97
3- PLA/PS	79	69.0	88	97.5

<sup>1</sup> Best fit linear regression between zero time point and all data collected to 2 hours

<sup>2</sup> Total amount released by the end of the experiment

Figure 4.4 shows the cumulative release profile for the above 3 samples, with 0.32  $\mu\text{m}$ , 0.63  $\mu\text{m}$ , and 1.56  $\mu\text{m}$  pore diameters. Sample 1 with the finest pore size shows approximately a 22% release rate in the first 2 hours, while sample 3 with the largest pore size shows about a 69% release for the same period. For sample 3, 88% of BSA diffuses out in the first 2 hours. The release profile for sample 2 behaves in an intermediate fashion.

The driving force for the fast release of BSA from the porous polymer device is likely due to the hydrophobicity of HDPE and PLA, and the hydrophilicity of BSA. Surface modification can be used to improve the release profile ([Jaber et al, 2006](#)) and later in this paper, a surface modification strategy for those porous devices will be presented.

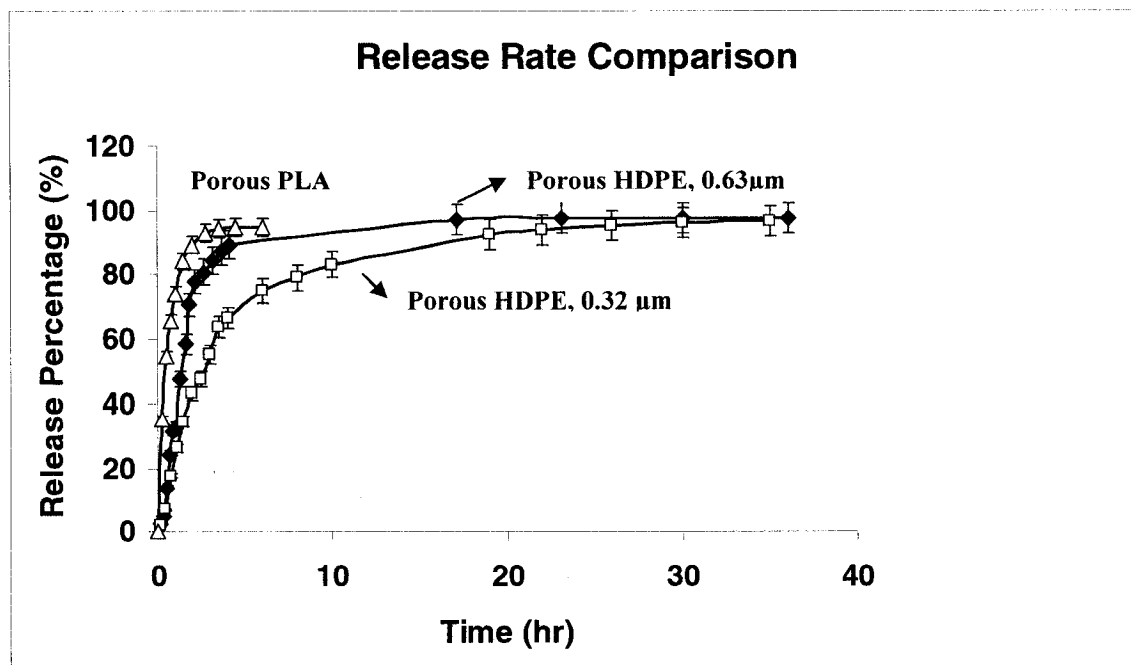


Figure 4.4 Effect of pore size on the drug release in 3ml of Milli-Q water at 37°C.

Sample 1, Porous HDPE from HDPE-SEB  $d = 0.32\mu\text{m}$  ( $\square$ ); Sample 2, porous HDPE from HDPE-SEBS  $d = 0.63\mu\text{m}$  ( $\diamond$ ); Sample 3, porous PLA from PLA-PS  $d = 1.56\mu\text{m}$  ( $\Delta$ )

#### 4.2.4.4 Effect of Heating in the Preparation Process on Drug Release

The effect of a heating stage in the preparation protocol on the release profile is estimated here. After loading the BSA (15 wt% solution), some samples were heated at 40°C and some at 60°C for 12 hours in a vacuum oven. In Figure 4.5, results are only reported for sample 2, (HDPE-SEBS,  $d = 0.63\mu\text{m}$ ). A similar behavior was noted for all other samples.

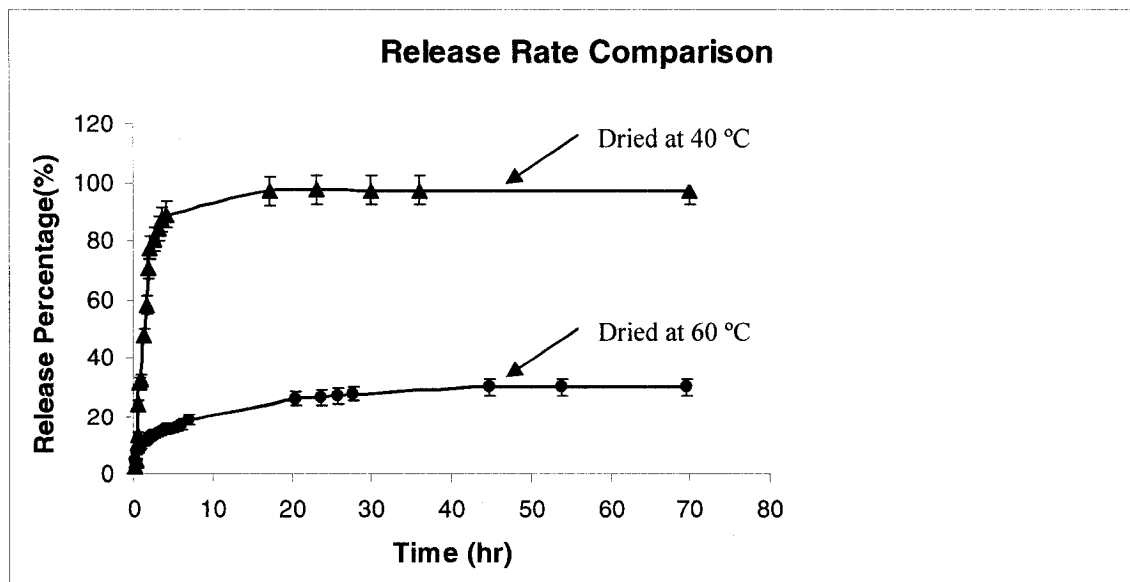


Figure 4.5 Effect of heating on the drug release profile. Porous HDPE from HDPE-SEBS, a) dried at 40°C (▲); b) dried at 60°C (●)

The initial release rate decreased to 7.97(release%/2hours) from 35.88(release%/2hours) by increasing the temperature in the preparation protocol from 40°C to 60°C. Moreover an incomplete release was observed for all the tested samples at 60°C. In order to further examine the effect of temperature, some experiments were also performed at 20°C. The release profile at 20°C showed a pattern similar to that at 40°C, but with a somewhat faster burst release.

The significant variation in release profile between preparation temperatures of 40°C or less and above 60°C is mainly due to the changes in BSA structure. When heated, proteins vibrate violently; consequently the weak bonds break and a string of amino acids begin to unfold leading to the BSA denaturation and conformational changes. An increase in temperature increases the contribution of entropy. Intermolecular clustering leads to irreversible aggregation of the denatured protein. Several papers have studied the temperature at which irreversible conformational changes occur and form BSA

aggregates (Wetzel R. et al, 1980; Poole S. et al, 1987; Ruegg M., et al, 1977; Clark A.H., 1981b). Most of these reports confirm that irreversible conformational changes for BSA start to occur rapidly when it is heated above 50°C. However at temperature lower than 50°C, if any structural changes occur, they are reversible. In light of the above, heating the BSA loaded polymer for 12 hours at 60°C induces the aggregation and coagulation of protein inside the pores. This forms large complexes of protein due to aggregation within the matrix and results in a slow and incomplete release of the BSA. In order to prevent high BSA aggregation (at 60°C) and also to avoid any migration of the drug to the surface during drying and storage steps (Huang et al., 2001) (at 20°C), the heating temperature during the preparation process was selected to be 40 °C.

#### **4.2.4.5 Surface Modification of the Porous Medium**

The effect of surface charge on BSA release is examined here by modifying the surfaces through the LbL deposition of polyelectrolytes. It is well known that the LbL approach requires the sequential adsorption of oppositely charged polyelectrolytes to form dense molecular layers (Lvov et al., 1993). By controlling the number of alternative layers, a positive or negative charge can be closely controlled. In this study we use PSS and PDADMAC as the polyelectrolytes. A layer of BSA is added in a final step, once the alternating polyelectrolyte layers have been laid down. Previously, this group proposed a novel approach for the LbL deposition of polyelectrolytes onto a porous co-continuous template (Roy et al., 2006).

In this study, the LbL surface modification approach was applied to porous HDPE of 0.63 µm and porous PLA of 1.56 µm. The smaller pore size ( $d = 0.32 \mu\text{m}$ ) was eliminated from LbL experiments since the smaller pore size resulted in more difficult loading conditions (see Figure 4.4) Since, in some cases, the pressure of loading created cracks within that polymer device.

After a 4-hour deposition step and a 4-hour washing step for each polyelectrolyte layer, the porous devices were dried and weighed. Figure 4.6 provides clear evidence for the alternating polyelectrolyte PDADMAC/PSS assembly of 7 layers obtained by gravimetric measurements. A constant mass of each polyelectrolyte is deposited on both HDPE and PLA substrates. The BSA is adsorbed in a higher amount compared to polyelectrolytes, due to its greater concentration. Also the formation of thick dense layers of BSA, results from its globular conformation ([Caruso, 1999](#)). Experimental results shown in Figure 4.6 are in good agreement with data reported by [Roy et al., 2006](#).

Differences in the slopes of the curves in Figure 4.6 for HDPE and PLA are due to differences in surface area and material density. From the results obtained by BET, the HDPE device of 0.63  $\mu\text{m}$  pore size has a specific surface area of 8.2  $\text{m}^2/\text{g}$  surface area while PLA with pores of 1.56  $\mu\text{m}$  have 2.2  $\text{m}^2/\text{g}$ . Clearly, the larger surface area allows for greater adsorption. Although the HDPE surface area is four times larger than that of PLA, BSA loadings of HDPE do not show a four times increase in the amount adsorbed. Compared to PLA this can be explained since not all the pores and surface area are fully accessible to the BSA solution due to the BSA viscosity. The loading experiment with water revealed a high level of interconnectivity within the polymer device and accessibility of water to most of the available surface area. However this is not the case for BSA solution with a viscosity of 0.0189 Pas.S at 25°C (water viscosity at 25 °C is reported as  $8.9 \times 10^{-4}$  Pas.S). The BSA loading efficacy, reported in Table 4.3, also confirms this fact.

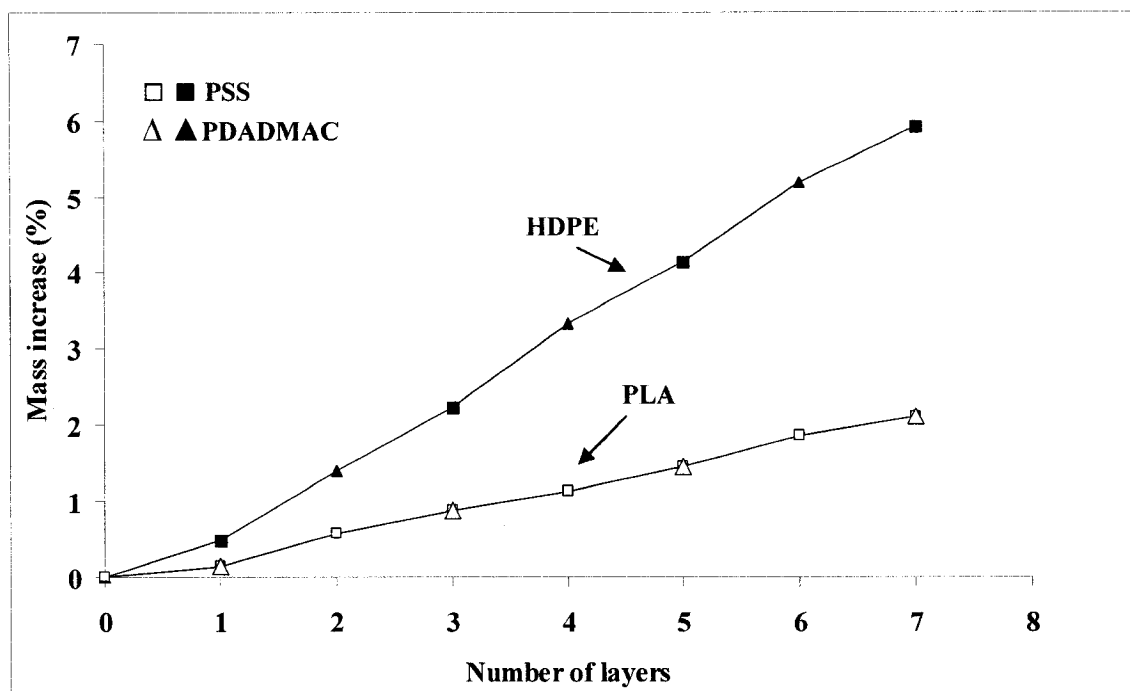


Figure 4.6 Deposited mass as a function of the number of layers, HDPE porous device (PSS/PDADMAC/PSS...) with average pore size  $0.63 \mu\text{m}$ ; PLA porous device (PDADMAC/PSS/PDADMAC...) with average pore size  $1.56 \mu\text{m}$ .

In Figure 4.7 the cumulative mass per layer specific to each polyelectrolyte is shown and can be clearly seen that, in all cases, the amount deposited in a particular step is highly uniform.

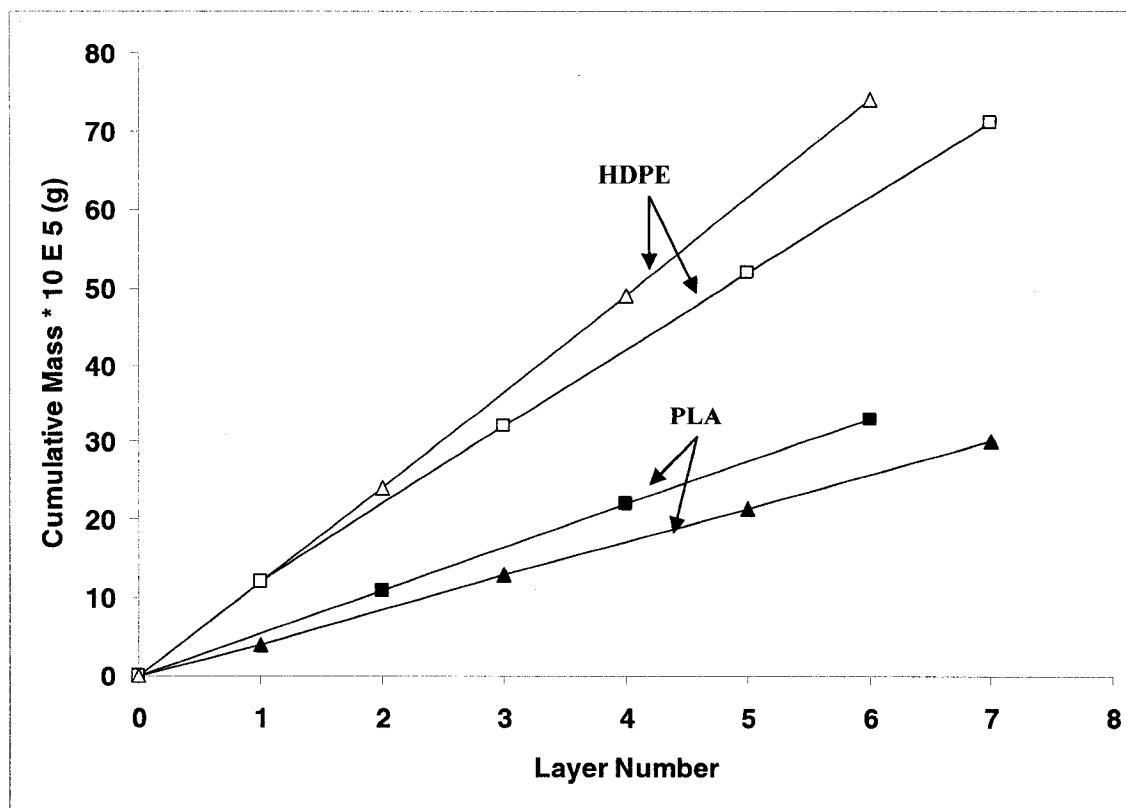
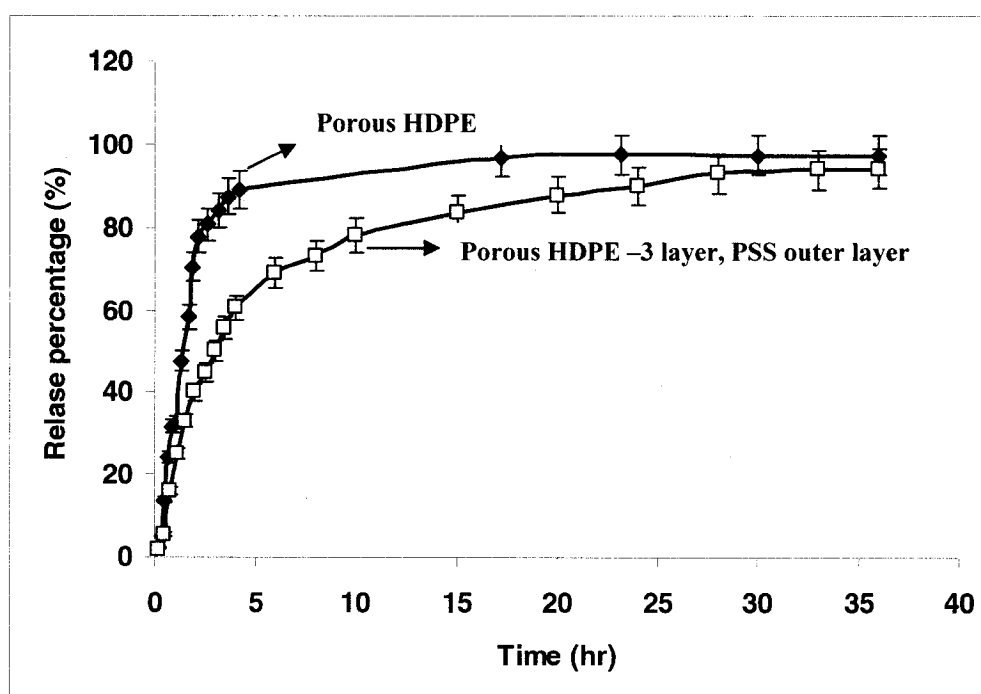


Figure 4.7 Cumulative deposited mass of PDADMAC and PSS for HDPE and PLA substrates. Porous PLA (PDADMAC  $\blacktriangle$ / PSS  $\blacksquare$ /PDADMAC  $\blacktriangle$ /...), and porous HDPE (PSS  $\square$ /PDADMAC  $\blacktriangle$ /PSS  $\square$ /...).

#### 4.2.4.6 Effect of LbL Surface Modification on in-Vitro Drug Release

The BSA release profile and kinetics from porous HDPE and PLA with 3 layers of polyelectrolyte are compared to those without polyelectrolytes in Figure 4.8. Both the effects of a negative outer layer (PSS) or positive outer layer (PDADMAC) are examined. LbL surface modification with a PSS outer layer on porous HDPE (0.63  $\mu\text{m}$  pore size) improves the release profile and decreases the initial burst to half resulting in a more sustained release. The release profile for HDPE/LbL/BSA (0.63  $\mu\text{m}$  pore size), is very similar to the HDPE/BSA (0.32  $\mu\text{m}$ ) without surface modification.

a )





b)

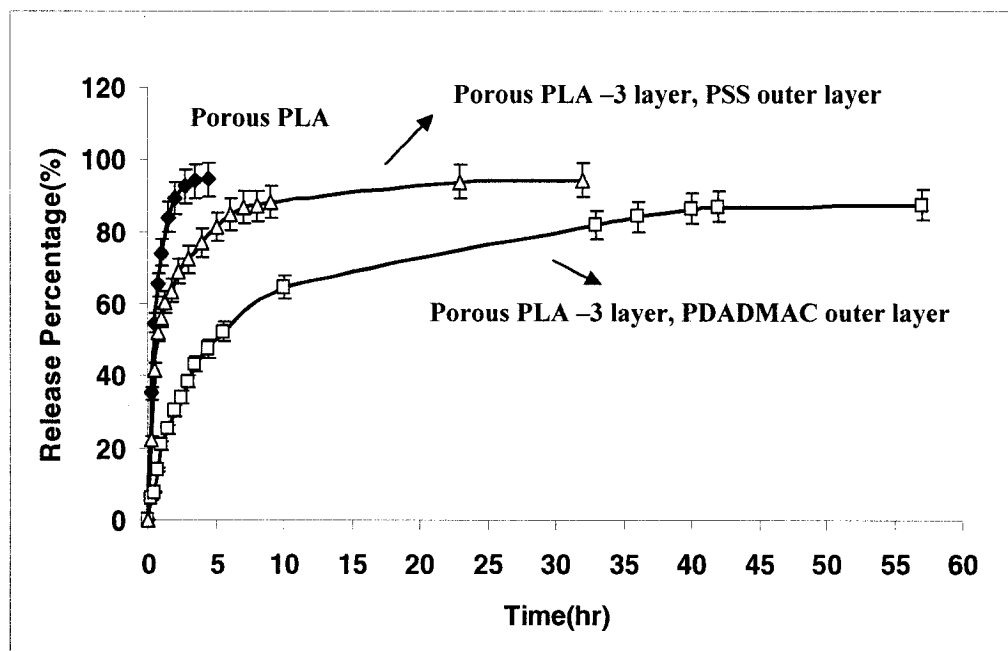


Figure 4.8 a) Porous HDPE of 0.63  $\mu\text{m}$  pore size, HDPE/BSA ( $\diamond$ ); HDPE/PSS/PDADMAC/PSS/BSA ( $\square$ );

b) Porous PLA of 1.56  $\mu\text{m}$  pore size, PLA/BSA ( $\diamond$ );  $\text{LbL}_1$  = PLA/PSS/PDADMAC/PSS/BSA( $\Delta$ );  $\text{LbL}_2$  = PLA/PDADMAC/PSS/PDADMAC/BSA ( $\square$ ).

For porous PLA using LbL, the release profile improves even more significantly; However, the second  $\text{LbL}_2$  series; PLA/PDADMAC/PSS/PDADMAC/BSA; seems to be more effective than the first  $\text{LbL}_1$  series PLA/PSS/PDADMAC/PSS/BSA. The PLA/PDADMAC/PSS/PDADMAC/BSA series decreased the initial burst 80% while PLA/PSS/PDADMAM/PSS/BSA series decreased it only by 38% as compared to the release profile of PLA/BSA. Moreover, the  $\text{LbL}_2$  surface modification approach results in a more sustained release, closer to the ideal profile. In the porous PLA  $\text{LbL}_2$  series, three stages for the release can be defined; burst release, steady state, and end release. The

observed differences between the release profile of LbL<sub>1</sub> and LbL<sub>2</sub> may be best explained by the surface charges. At pH 6.7-7.0, BSA with an isoelectric point<sup>1</sup> of 4.7 carries a net negative charge (Ladam et al, 2002). Therefore in LbL<sub>2</sub>, BSA and PDADMAC have different surface charges resulting in the stronger adhesion of BSA to the surface and consequently delayed burst release and slower release rate. Other groups (Kaibara et al, 2000, Xia et al, 1999) have reported that hydrophobic and electrostatic interactions are the main factors governing the adhesion between BSA and polyelectrolytes.

In Figure 4.8, although the PDADMAC outer layer in porous PLA clearly shows the lowest burst release of all, it is also interesting to note that when PSS is the outer layer the burst release is less for porous HDPE than for PLA. Hence, when a negatively charged outer surface contacts a negatively charged BSA, the dominant restriction to release returns to a pore size effect.

Increasing the number of layers leads to a more uniformly charged surface with higher charge density, which results in stronger adhesion between the BSA and the final polyelectrolyte layer. In order to investigate the effect of increasing polyelectrolyte layers on the release profile, Figure 4.9 compares the release profile of porous PLA for 3-layer (both PSS and PDADMAC outer layer) and a 7- layer formulation with PDADMAC as the outer layer.

---

<sup>1</sup> The isoelectric point (PI) is the pH at which a molecule or surface carries no charge. At pH above PI, proteins carry net negative charge.

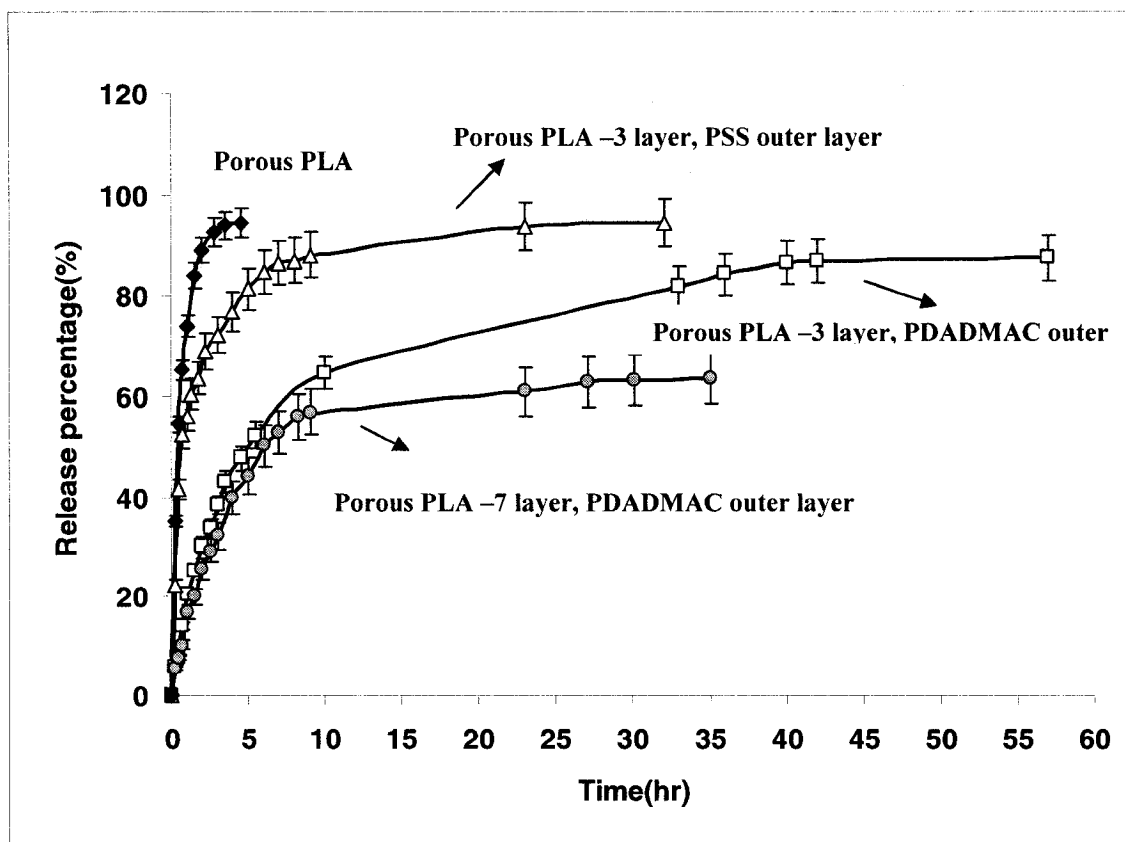


Figure 4.9 Drug release profile of Porous PLA of 1.56  $\mu\text{m}$  ( $\blacklozenge$ ); PLA/PSS/PDADMAC/PSS ( $\Delta$ ); PLA/PDADMAC/PSS/PDADMAC/BSA ( $\square$ ); PLA/PDADMAC/PSS/...PDADMAC 7layer/BSA ( $\bullet$ )

Figure 4.9 indicates that, increasing the number of polyelectrolyte layers from 3 to 7 leads to an incomplete release. These results are in line with explanation based on a more complete and uniformly charged surface. In 7-layer porous PLA, the burst release decreased 13% and only 63% of the total loaded BSA was released from the porous device. The incomplete release observed in the 7-layer porous PLA with a positively charged outer layer formulation is likely the result of highly immobilized BSA at the porous surface due to too much interaction of polyelectrolyte with BSA molecules.

In order to prepare porous HDPE with a positive outer layer (PDADMAC) and due to the restriction of using PSS as the first layer for HDPE (see Experimental), we tested porous HDPE with 4 layers and 8 layers. The results are shown in Figure 4.10.

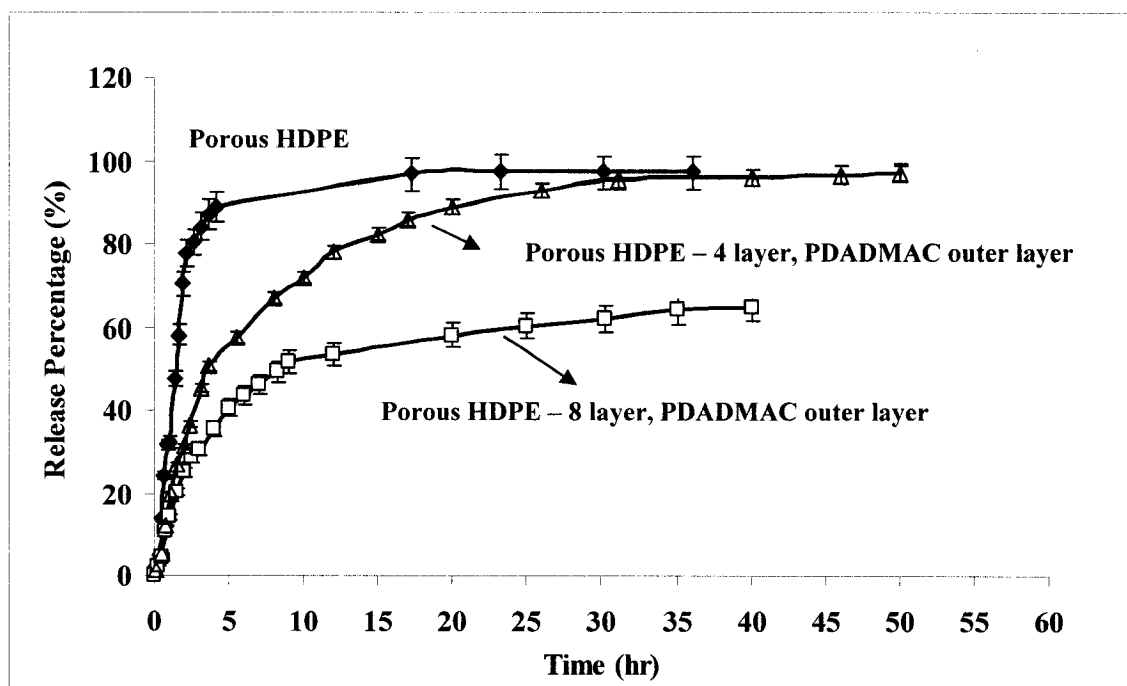


Figure 4.10 Drug release profile of porous HDPE of  $0.63\mu\text{m}$  ( $\blacklozenge$ ); HDPE/PSS/PDADMAC/PSS/PDADMAC ( $\blacktriangle$ ); HDPE/PSS/PDADMAC/...PDADMAC 8-layer ( $\square$ )

In porous HDPE treated with 4 and 8 layers of polyelectrolyte, the BSA release behavior shows similarities to the porous PLA treated with 3 and 7 layers of polyelectrolyte. Having four layers of polyelectrolyte evidently decreases the burst release and leads to a more controlled release behavior. A porous 8-layer HDPE, shows reduced a burst release followed by an incomplete release.

The above work shows that increasing the number of surface layers from 3 and 4 to 7 and 8 does not modify the burst release considerably, but does lead to an incomplete release of BSA. This strongly indicates that the burst release is a result of free BSA within the void volume of the porous device, whereas, the incomplete release is related to immobilized BSA inside the pores. As mentioned earlier, it is well known in the LbL process that increasing the number of layers results in a more organized and well defined charges associated with each layer. Since the BSA concentration is high, a multilayer BSA structure on the polyelectrolyte layers is expected. This protein buildup process can be repeated for several layers, but becomes less and less organized as BSA layers are added. Eventually the BSA is trapped in the pores of the device as free BSA.

Another potentially phenomenon, is the adsorption of multiple layers of polyelectrolyte and BSA that could be restricting the pore size of the channels in the device. The thickness of each polyelectrolyte layer was measured by ellipsometry on a silicon wafer film (flat model surface) and was found to be 1.75 nm. Although this is quite a small value when compared to the size of the pores, it is possible that the deposited layers are considerably larger when the LbL deposition is carried out within a co-continuous porous structure. The confinement of chains in small pores can significantly affect the growth mechanism of multilayers. In previous work from this laboratory on similar systems (Roy et al., 2006), it was shown that assembled polyelectrolytes and BSA formed a layer close to 100 nm in thickness. As a further support to this claim, the measurement of layer thicknesses in nanopores is provided by various other research groups (Alem et al., 2007; Lee et al., 2006; Liang et al., 2003). Alem et al. performed adsorption experiments for porous systems with pore diameters of 50-850 nm and claim that the thickness of layers in pores could, in some cases, be as high as 100 times greater as compared to flat surfaces. This aspect will be examined in more detail in future work.

Overall, at this stage in this pioneering study, it appears that the formulations of PLA with 3 layers of polyelectrolyte and HDPE with 4 layers of polyelectrolyte result in the best moderated release profile. These formulations have a low burst release followed by a more constant release rate and result in virtually all the loaded drug being released.

#### **4.2.4.7 Effect of a Closed-Cell Template on Drug Release**

All the porous substrates used so far in these experiments are open-cell structures. Open-cell structures possess a continuous porosity throughout from the core to the surface. However closed-cell systems possess continuous porous structures only in the core with a non-porous structure at the surface. Closed-cell structures have been examined in controlled release ( Matsumoto, A. et al, 2005; Rahman, N. A., et al, 2004) using terms such as multi-reservoir or double-wall formulation. However their preparation method is completely different from the approach in this paper. Closed-cell structures are interesting since they are an approach which can be used to prolong delivery times and also to eliminate the burst release effect. Typically, closed-cell systems are applicable only for biodegradable polymers since the wall needs to degrade over time to allow drug release.

For materials approach used in this study, open-cell porous PLA can be transformed into a closed-cell device by immersing the porous PLA (loaded with BSA) in chloroform for 2 seconds (Sarazin et al., 2006) as shown in Figure 4.11. Increasing the time that the device is immersed in chloroform, results in an increase of wall thickness.

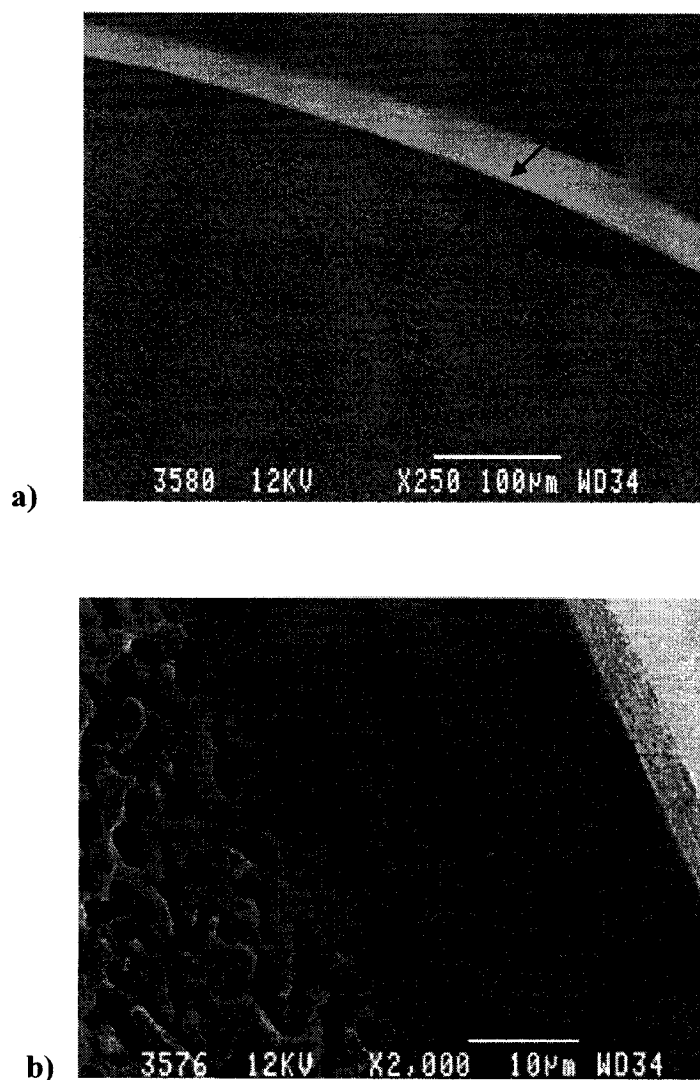


Figure 4.11 SEM micrographs of porous PLA with a closed-cell morphology, prepared from PLA/PS (50-50) (a)  $\times 250$  magnification, (b)  $\times 2000$  magnification (Sarazin et al., 2006)

A porous PLA cylinder with  $L = 6\text{mm}$ , and  $d = 3\text{mm}$  was selected for the *in vitro* drug release test. The cylinder was loaded with BSA solution (15%w/w) using the vacuum-pressure cycle protocol and dried overnight in a vacuum oven. The loaded cylinder was then immersed in chloroform for 2 seconds, washed with Milli-Q water for few seconds

and dried overnight at 40°C for 12 hours. The closed PLA capsule was then examined for drug release.

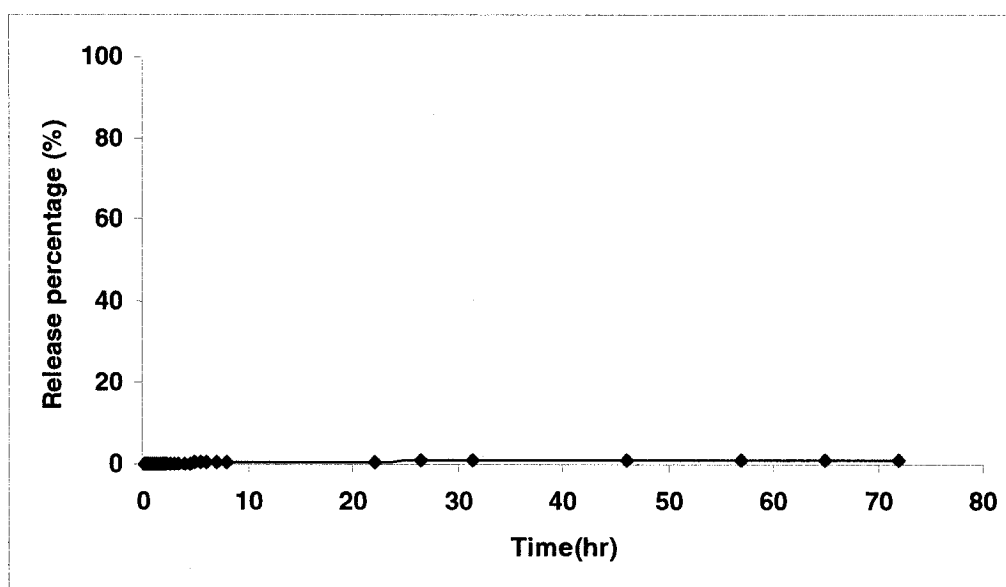


Figure 4.12 Drug release profile for closed –cell morphology. Porous PLA from PLA/PS (50-50)

As was shown in Figure 4.12, no BSA release was monitored by UV-Vis spectrophotometry. This confirms that the device is completely in a closed-cell configuration. Even continuing the experiment to 6 days showed no recorded diffusion. The PLA used in these experiments is 7% D-lactide and 93% L-lactide and due to its high molecular weight, degradation would be expected to initiate in a minimum of 6 -7 weeks.

The objective of this part of the work was not to initiate and track drug release after PLA degradation, but to demonstrate the ease and efficacy of closing the porous device used in this study. Future work will consider the use of amorphous PDLA, other biodegradable polymers and the effect of various wall thicknesses and partially closed-cell systems on BSA release rate using preparation approach presented in this paper.



#### 4.2.5 Conclusion

This is the first paper to report on the preparation of porous devices derived from co-continuous polymer blends for use in controlled drug release. In order to examine the effect of matrix pore size and surface area on the BSA release profile, substrates with three different pore sizes were used. Porous HDPE devices, derived from co-continuous HDPE/SEB as well as from HDPE/SEBS, were used as model substrates providing small pore sizes of 300 and 600 nm. Porous PLA derived from PLA/PS provided a system with a larger pore size of 1.5  $\mu\text{m}$ . A drug loading protocol involving alternating vacuum-pressure cycles was introduced as a method for the polymeric capsule preparation. It is shown that virtually all the porous network is accessible to water loading. However, BSA loads to a somewhat lesser level due to its higher viscosity. The release profile of BSA from the microporous structure was monitored by UV/Vis spectrophotometry. It is clearly shown that the larger pore sizes result in a significantly greater drug release rate. In order to extend the release rate to longer times, the surface modification of the porous polymer devices was carried out by layer by layer (LbL) deposition of polyelectrolytes unto the porous surface. This was undertaken so as to investigate the influence of surface charge on the adhesion of BSA molecules at the surface. In addition, the effect of the number of deposited layers on the BSA release rate was also examined by preparing porous PLA with 3 and 7 layers of polyelectrolyte and HDPE with 4 and 8 layers of polyelectrolyte. It was shown that the formulations of PLA with 3 layers of polyelectrolyte and HDPE with 4 layers of polyelectrolyte result in the best moderated release profile having a low burst release followed by a more constant release rate. Increasing the number of layers to 7 for PLA and 8 for HDPE, does not modify the burst release considerably, but does lead to an incomplete release of BSA. These effects are discussed in the paper in terms of free BSA within the pores and immobilized BSA at the surface. Finally, a porous PLA formulation with a closed-cell configuration at the surface was introduced as a technique to moderate the short-term burst release effect. No BSA release was recorded after 6 days which confirms that the device is completely in a closed-cell configuration and demonstrates the potential of this approach to extend the release of BSA to much longer times. In future

work, both partially closed-cell structures as well as structures with a rapidly degrading matrix polymer will be examined.

#### **4.2.6 Acknowledgment**

The authors would like to express their appreciation to Dr. M. Jolicoeur for useful discussions, to Dr. J. Kirchnerova for the use of BET and mercury porosimetry, to L. Jean for assistance with UV Spectrophotometry, to S. Ravati for providing the elipsometry data, and to J. Beausoliel for his assistance in cylindrical sample preparation. The authors gratefully acknowledge the Natural Sciences and Engineering Research Council of Canada for funding this work.

## CHAPTER 5

### GENERAL DISCUSSION AND CONCLUSIONS

#### 5.1. General Discussion

##### 5.1.1 Effect of Pore Size and Surface Area on BSA Loading and Release Rate

The polymeric substrates were made from HDPE/SEB, HDPE/SEBS, and HDPE/PLA blends, having average pore diameters of 0.32  $\mu\text{m}$  (porous HDPE from an HDPE/SEB blend), 0.63  $\mu\text{m}$  (porous HDPE from an HDPE/SEBS blend), and 1.56  $\mu\text{m}$  (porous PLA from a PLA/PS blend) respectively. The BSA solution was forced to penetrate the highly porous structure, following a vacuum-pressure cycle. In order to study the effect of pore size on loading efficiency, we performed loading experiments with three different pressures for devices with three different pore sizes. The results showed that at a constant pressure, larger pore sizes had higher loading efficacy, whereas smaller pore sizes showed a lower loading efficiency. This effect was due to the entrance port (pore size), as samples with smaller pore sizes had smaller channels within their structures and higher tortuosity.

BSA *in vitro* release tests were performed using UV-Vis spectrophotometry. The initial release tests were performed with samples of three pore sizes (0.32  $\mu\text{m}$ , 0.62  $\mu\text{m}$ , and 1.56  $\mu\text{m}$ ). The fastest release profile and largest burst release was observed for the sample with largest pore size (PLA, diameter = 1.56  $\mu\text{m}$ ). PLA showed a complete release in less than four hours, whereas HDPE samples released the BSA in 23-28 hours in a more controlled manner. This shows that a smaller pore size confers a larger surface area, which has a controlling effect on BSA release, whereas smaller interconnected

channels act as a barrier and limit the drug diffusion to some levels. Our observations strongly suggest that the hydrophobicity of HDPE and PLA substrates and the hydrophilicity of BSA are the main driving forces for the fast release of BSA from these polymer carriers. For this reason, using surface modification to improve the BSA attachment to the internal surface was examined as an option to improve the release behavior.

### **5.1.2 Effect of Modification on the BSA Release Profile**

In order to improve the BSA release profile, we investigated two methods of modification: internal surface modification by layer by layer deposition of polyelectrolytes and external surface modification using closed-cell morphology.

We conducted the release experiments on samples treated with three and seven layers of polyelectrolytes. The LbL technique was used for two pore diameters: 0.63  $\mu\text{m}$  (HDPE) and 1.56  $\mu\text{m}$  (PLA). Using three layers of LbL on HDPE improved the release profile by decreasing the initial burst by half, resulting in a more sustained release. For PLA templates using LbL treatment, the release profile was improved more significantly. With three layers of polyelectrolytes, the initial burst release decreased by 80%, which led to a more sustained release, and closer to the theoretically desired release profile.

The effect of the number of polyelectrolyte layers on the BSA release profile was also examined. We continued loading up to seven and eight polyelectrolyte layers. Results indicated that increasing the number of layers produces a uniformly charged surface with a stronger interaction to BSA. An increase in the number of layers may also occupy the void volume of the polymer, resulting in a porous structure with a smaller pore size than untreated templates or templates with three layers of treatment. The combination of these effects may lead to a slower release rate and an incomplete release for both HDPE and PLA substrates.

The effect of closing the capsule on controlled drug delivery was also investigated. A porous PLA closed-cell structure was prepared by dipping the loaded PLA cylinder into chloroform for two seconds. After closing the PLA capsule, the release experiment was performed in an aqueous medium. No BSA diffusion was recorded after 4–5 days, which confirms that the PLA exterior surface was completely closed. Further BSA diffusion can only take place when the PLA starts to biodegrade.

### 5.1.3 Future Work

Based on the literature and our results, we can conclude that various factors may affect the drug release profile during *in vitro* studies. Since we are in the preliminary stages of developing a novel drug delivery technology, more basic studies on these factors is essential. Our method may impose limitations in terms of size, amount, and nature of the loaded drug. From this point of view, we suggest future studies to complete our work:

- A high drug concentration may involve overloading and multilayer loading of the drug within our porous capsule, which may result in a very fast drug release from an open matrix. We know that concentration difference is a driving force for BSA to diffuse out from the matrix (high concentration) to the aqueous medium (low concentration). A higher BSA concentration in the polymer matrix may induce faster BSA diffusion which is not desirable. Therefore, lowering the BSA concentration may allow more control over BSA diffusion and slow down the migration of BSA molecules.
- The size of active agent molecules has an effect on their diffusion rate. Our porous matrix contains many pores of different sizes. The pores may have a selecting role, similar to column size exclusion chromatography. Since BSA is a very small protein with a small molecular weight, molecules pass readily through the pores to the surface during the diffusion test. However, for a protein with a larger molecular

weight, the pores and their internal walls may act as barriers and may slow down the protein diffusion from the polymer matrix to the aqueous medium.

- The closed-cell morphology is a promising technique. We showed that the porous PLA cell can be closed successfully. However, to monitor the BSA diffusion, the surface layer must start to degrade. We used PLA of 7% amorphous and 93% crystalline phase, for which the degradation of the holding layer may extend to over three months. Therefore, we suggest using PLGA or PDLLA, which has much faster degradation. By changing polymers, we can study the effect of the drug holding layer on the diffusion rate.
- So far we have discussed only fully closed-cell systems. A partially closed-cell technique may be another option for further investigation since it has the potential to control the BSA release.
- Along with the closed-cell technique, coating may be an option. If we can not find a suitable solvent for some of the fast degrading polymers, we can solve the problem by coating the loaded polymeric capsule with a layer of fast degradable biopolymer, or a layer of gelatin.
- Another option is to make a layer by layer formulation by loading layers of PLA on the protein layer. It is possible to deposit BSA and PLA solution in a multi-layer format. In this case, to see drug diffusion, the PLA layer must first degrade. When the outermost PLA layer starts to degrade, BSA starts to diffuse out by the time the PLA layer has degraded completely. Then, the next PLA layer must start to degrade. While waiting for PLA to start degrading, no diffusion would be observed. Using this method, we may be able to see a step-wise drug release.

- Using fluorescence labeled BSA may also be helpful. By labeling the BSA molecules, we could readily track their location in the matrix at different time interval, both after the loading and during the diffusion test. It would also be possible to film the BSA molecular migration during the release test.

## 5.2. Conclusions

- As a final word, it can be concluded that the combination of highly structured co-continuous morphologies with LbL self-assembly and cell-closing technology on a co-continuous template provides a novel basic method with the potential for generating novel surface-modified porous polymer as carriers for controlled drug release. Our investigation indicates how matrix pore size and internal surface area influence the release profile in both untreated and treated polymeric matrices, and how modifications to polymeric capsules (i.e. LbL method and closed-cell morphology) can improve the BSA release profile.
- Matrix pore size and surface area has an influence on the release profile. A smaller pore size confers a larger surface area and smaller interconnected channels which both have controlling effects on release.
- Modification of polymeric capsules i.e. LbL method and closed-cell morphology improve the BSA release profile.
- It was shown that the formulation of PLA with 3 layers of polyelectrolyte and HDPE with 4 layers of polyelectrolytes result in the best moderated release profile having a low burst release followed by a constant release rate.

- Increasing the number of layers to 7 for PLA and to 8 for HDPE do not modify the burst release considerably, but does lead to an incomplete release of BSA.
- Complete Closed-cell configuration demonstrates the potential of the approach to extend the release of BSA to much longer times.

Many factors may affect the drug release profile during in vitro studies, which have not yet been investigated. Our novel drug delivery device, which is currently in its preliminary stages, requires more extensive study.



## REFERENCES

- ABDEKHODAIE, M. J., CHENG, Y.-L. (1997). "Diffusional release of a dispersed solute from planar and spherical matrices into finite external volume." *Journal of Controlled Release* **43**: 175-182.
- ABOUBAKAR, M., PUISIEX, F., COUVREUR, P., DEYME, M., VAUTHIER, C. (1999). "Study of the mechanism of insulin encapsulation in poly (isobutylcyanoacrylate) nanocapsules obtained by interfacial polymerization." *Journal of biomedical materials research* **47**: 568-576.
- ADO, K., TAKEDA, N., KIKUCHI, M., TANIGUCHI, Y. (2006). "The pressure effect on the structure and functions of protein disulphide isomerase." *Biochimica et Biophysica Acta* **1764**: 586-592.
- AHMED, A. R., DASHEVSKY, A., BODMEIER, R. (2000). "Reduced burst effect in drug release with solvent-treatment microparticles prepared by the solvent evaporation method." *Proc. Int. Symp. Control. Release Bioact. Mater.* **27**: 6112.
- AI, H., JONES S. A., de VILLIERS, M. M., LVOV, Y. M. (2003). "Nano encapsulation of furosemide microcrystals for controlled drug release. " *Journal of Controlled Release* **86**:59-68
- AINAOUI, A., VERGNAUD, J. M. (2000). "Effect of nature of the polymer and the process of drug release (diffusion or erosion) for oral dosage forms." *Computational and Theoretical Polymer Science* **10**: 383-390.

ALEM, H., BLINDEAU, F., GLINEL, K., DEMOUSTRIER-CHAMPAGNE, S., JONAS, A. M. (2007). "Layer-by-layer assembly of polyelectrolyte in nanopores" *Macromolecules* **40**: 3366-3372

ARIGA, K., LVOV, Y., KUNITAKE, T. (1997). "Assembling alternate dye-polyion molecular films by electrostatic layer-by-layer adsorption." *Journal of American Chemical Society* **119**: 2224-2231.

ARSHADY, R. (1999). *Microspheres, microcapsules and liposomes*, Citus Books Publishers, London.

ARYS, X., LASCHEVSKY, A., JONAS, A. M. (2001). "Ordered polyelectrolyte multilayer. 1. mechanisms of growth and structure formation: a comparison with classical fuzzy multilayers." *Macromolecules* **34**: 3318-3330.

AVGEROPOULOS, G. N., WIESSERT, F. C., BIDDISSON, P. H., BOEHM, G. G. A. (1976). "Heterogeneous blends of polymers, Rheology and morphology." *Rubber Chemistry and Technology* **49**: 93-104.

BAKAN, J. A. (1975). "Microcapsule drug delivery systems." *polymer Science Technology* **8**: 213.

BAKAN, J. A., in Swarbrick and Boylan, J. C., eds., (1994). *Encyclopedia of controlled drug delivery*. Marcel Dekker, Inc, New York.

BERNAL, V., JELLEN, P. (1985). "thermal stability of whey proteins; A calorimetric study." *J. Dairy Sci.* **68**: 2847-2852.

BERTRAND, P., JONAS, A., LASCHEWSKY, A., LEGRAS, R. (2000). "Ultrathin polymer coatings by complexation of polyelectrolytes at interfaces: suitable material structure and properties." *Macromolecular Rapid Communications* **21**: 319-348.

BLANCO-PRIETO, M. J., BESSEGIR, K., ZERBE, O., ORSOLINI, P., HEIMGARTNER, F., DUESCHEL, C., MERKLE, H.P., GANDER, B. (1999). "Importance of test medium for the release kinetics of a somatostatin analogue from poly(D,L lactide-co-glycolide) microspheres." *Int. J. Pharm.* **184**: 243-250.

BLANCO-PRIETO, M. J., CAMPANERO, M. A., BESSEGHIR, K., HEIMGARTNER, F., GANDER, B. (2004). "Importance of single or blended polymer types for controlled in vitro release and plasma levels of a somatostatin analogue entrapped in PLA/PLGA microspheres." *Journal of Controlled Release* **96**: 437-448.

BOTTOM, C. B., MARIJO, C., CARSTENSEN, J. T. (1997). "Dissolution Testing Of Soft Shell Capsule - Acetaminofen And Nifedipine." *J. Pharm. Sci.* **86**: 1057-1061.

BOURRY, D., FAVIS, B.D. (1998). "Morphology development in a polyethylene/polystyrene binary blend during twin-screw extrusion." *Polymer* **39**: 1851-1856.

BRANDRUP, J., IMMERGUT, E.H., GRULKE, E.A. (1999). *Polymer handbook*. Wiley, New York.

BRANNON-PEPPAS, L. (1997). "Polymers in controlled drug delivery." *Medical plastics and biomaterials* **34**: 131-142

BRAZEL, C. S., PEPPAS, N. A. (1999). "Mechanisms of solute and drug transport in relaxing, swellable, hydrophilic glassy polymers." *Polymer* **40**: 3383-3398.

BRAZEL, C. S., PEPPAS, N. A. (1999). "Recent studies and molecular analysis of drug release from swelling- controlled devices." *STP Pharma. Sci.* **9**: 97-101.

BRIKETT , D. J. (1991). "Bioavailability and first pass clearance." *Australian prescriber* **14**: 14-16.

BUDNICK , M. O., FITZGERALD, R. S. (2003). "New life for a diagnostic reagent mainstay; improved manufacturing techniques enable bovine serum albumin to shed its low-tech image." *IVD Technology* **June 2003**: 45-51

CARRASQUILLO, K. G., STANLEY, A. M., APONTE-CARRO, J. C., DE JESUS, P., COSTANTINO, H. R., BOSQUES, C. J., GRIEBENOW, K. (2001). "Non- aqueous encapsulation of excipient - stabilized spray- freez dried BSA into poly (lactide- co - glycolide) microspheres results in release of native protein." *Journal of Controlled Release* **76**: 199-208.

CARTER, D. C., HO, J. X. (1994). "Structure of serum -Albumin." *Advances in protein chemistry* **45**: 153-203.

CARUSO, F., MOHWALD, H. (1999b). "Protein multilayer formation on colloids through a stepwise self-assembly technique." *Journal of American Chemical Society* **121**: 6039-6046.

Chaubal, M., Kumar, N. et al. (2002). "Controlled release technology." *Encyclopedia of polymer science and technology*, John Wiley & Sons inc, New York.

CHIA, H. H., CHUNG, T. S., YANG, Y. Y. (2000). "Effect of preparation temperature on the characteristics and release profiles of PLGA microspheres fabricated by double-

emulsion solvent extraction/ evaporation method." *Proc. Int. Symp. Control. Release Bioact. Mater* **27**: 8137.

CLARK, A. H., SAUNDERSON, D. H. P., SUGGETT, A. (1981b). "Infrared and laser-raman spectroscopic studies of thermally-induced globular protein." *Int. J. Peptide protein Res.* **17**: 353-364.

CLELAND, J. L., LIM, A., BARRON, L., DUENAS, E. T., POWELL, M. (1997). "Development of a single-shot subunit vaccine for HIV-1.4. Optimizing microencapsulation and pulsatile release of MN rgp 120 from biodegradable microspheres." *Journal of Controlled Release* **47**: 135-150.

COHEN, S., YOSHIOKA, T., LUCARELLI, M., HWANG, L. H., LANGER, R. (1991). "Controlled delivery systems for proteins based on poly(lactic/glycolic acid)microspheres." *Pharm. Res.* **8**: 713-720.

COLOMBO, P., BETTINI, R., MASSIMO, G., CATELLANI, P.L., SANTI, P., PEPPAS, N. A. (1995). "Drug diffusion front movement is important in drug release controll from swellable matrix tablets." *Journal of pharmaceutical science* **84**: 991-997.

COUVREUR, P., BLANCO-PRETO, M. J., PUISIEUX, F., ROQUES, B., FATTAL, E. (1997). "Multiple emulsion technology for the desin of microspheres containing peptides and oligopeptides." *Advanced drug delivery reviews* **28**: 85-96.

DECHER, G., HONG, J. D., SCHMITT, J. (1992). "Builtup of ultrathin multilayerfilms by a self-assembly process: III Consequently alternating adsorption onionic and cationic polyelectrolytes on charged surfaces." *Thin Solid Films* **210/211**: 831-835.

DECHER, G. (1997). "Fuzzy nanoassemblies: Toward layered polymeric multicomposites." *Science* **277**: 1232-1237.

DESAI, K. G. (2007). "Properties of tableted high-amylose corn starch-pectin blend microparticles intended for controlled delivery of diclofenac sodium." *Journal of Biomaterials Applications* **21**: 217-233.

DESAI, S. J., SIMINELLI, A. P., HIGUCHI, W. I. (1965). "Investigation of factors influencing release of solid drug dispersed in inert matrix." *J. Pharm. Sci.* **54**: 1459-1464.

DICKINSON, E., PAWLOWSKY, K. (1996). "Effect of high pressure treatment of protein on the rheology of flocculated emulsions containing protein and polysaccharide." *J. Agric. Food Chem.* **44**: 2992-3000.

DOMGMING, L., KALACHANDRA, S., (2002). "Controlled drug release for oral condition by a novel device based on ethylene vinyl acetate (EVA) copolymer." *Journal of Materials Science: Materials in Medicine* **13**: 53-58.

DUBAS, S. T., SCHLENDOFF, J. B. (1999). "Factors controlling the growth of polyelectrolyte multilayer." *Macromolecules* **32**: 8153-8160.

DUBAS, S. T., SCHLENDOFF, J. B. (2001). "Swelling and smoothing of polyelectrolyte multilayers by salt." *Langmuir* **17**: 7725-7727.

DUMITRIU, S. (2002). *Polymeric Biomaterials*, Dekker Inc., New York

DUNCAN, R., RINGSDORF, H., SATCHI-FAINARO, R. (2006). "Polymer therapeutics: polymers as drugs, drug and protein conjugates and gene delivery systems: past, present and future opportunities." *Advances in Polymer Science* **192**: 1-8.

EDLUND, U., ALBERTSSON, A. C. (2002). "Deradable polymer microspheres for controlled drug delivery." *Advances in polymer science* **157**: 67-112.

ELEMANS, P. H. M., JANSSEN, J.M.H., et MEIJER H.E.H. (1990). "The measurement of interfacial tension in polymer/polymer system: the breaking thread method." *J. Rheology* **34**: 1311-1325.

ERMIS, D., YUKSEL, A. (1999). "Preparation of sprayed -dried microspheres of indomethacin and examination of the effects of coating on dissolution rates." *Journal of Microencapsulation* **16**: 315-324.

FALDT, P., BERGENSTAH, B. (1996). "Spray- dried whey protein/ lactose/ soybean oil emulsion .1. Surface composition and particle structure." *Food Hydrocolloids* **10**: 421-429.

FAVIS, B. D., CHALIFOUX, J. P. (1987). "The effect of viscosity ratio on the morphology of polypropylene/polycarbonate blends during processing." *Polymer Engineering Science* **27**: 1591-1600.

FAVIS, B. D., CHALIFOUX, J. P. (1988). "Influence of composition on the morphology of polypropylene/polycarbonate blends." *Polymer* **29**: 1761-1767.

FAVIS, B. D., WILLIS, J. M. (1990). "Phase size/composition dependence in immiscible blends: experimental and theoretical consideration." *Journal of Polymer Science Part B - Polymer Physics* **28**: 2259-2269.

FERREIRA, M., RUBNER, M. F. (1995). "Molecular-level processing of conjugated polymers. 1. layer-by-layer manipulation of conjugated polyions." *Macromolecules* **28**: 7107-7114.

FERRY, J. D. (1948). "Protein gels." *Adv. protein Chem.* **4**: 1-82.

FICEK, B. J., PEPPAS, N. A. (1993). "Novel preparation of poly(vinyl alcohol) microparticles without crosslinking agent for controlled drug delivery of proteins." *Journal of Controlled Release* **27**: 259-264.

FOLKMAN, J., LONG, D. M. (1964). "The use of silicone rubber as a carrier for prolonged drug therapy." *J. Surg., Res.* **4**: 139.

FOSTER, J. F., (1977). *Albumin structure, function and uses*. Pergamon, Oxford.

FRIEDLI, G.-L. (1996). "PhD thesis; Interaction of de-amidated soluble wheat protein with other food proteins and metals." Retrieved April 2007, from <http://www.friedli.com/research/PhD/chapter5a.html#bsa1>.

FREIBERG, S., ZHU, X. X. (2004). "Polymer microspheres for controlled drug release." *International Journal of Pharmaceutical* **282**: 1-18

GLASEL, J. A. (1995). "Validity of nucleic acid purities monitored by 260nm/280nm absorbance ratios." *Biotechniques* **18**: 62-65.

GLINEL, K., MOUSSA, A., JONAS, A. M., LASCHEWSKY, A. (2002). "Influence of polyelectrolyte charge density on the formation of multilayers of strong polyelectrolytes at low ionic strenght." *Langmuir* **18**: 1408-1412.



GREGEN, W. P., LUTZ, R. G., DAVISON, S. (1996). "*Hydrogenated block copolymers in thermoplastic elastomer interpenetrating polymer networks*". Hanser publication, Munich,

GROSS, M., JAENICKE, A. (1994). "Proteins under pressure - The influence of high hydrostatic -pressure on structure, function and assembly of proteins and protein complexes." *European Journal of Biochemistry* **221**: 617-630.

GRUNDY, J. S., ANDERSON, K. E., ROGERS, J. A. FOSTER, R. T. (1997). "Studies On Dissolution testing Of The Nifedipine Gastro-Intestinal Therapeutic System " *Journal of Controlled Release* **48**: 1-8.

GUBBLES, F., JEROME, R., TEYSSIE, Ph. (1994). "Selective localization of carbon black in immiscible polymer blends: a useful tool to design electrical conductive composites." *Macromolecules* **27**: 1972-1974.

GUPTA, K. C., KUMAR, N. M. V. R. (2001). "pH dependent hydrolysis and drug release behavior of chitosan/poly(ethylene glycol) polymer network microspheres." *J. Mater. Sci. Mater. Med.* **12**: 753-759.

HARRIS, D. C. (2003). *Quantitative chemical analysis, 6th edition*. Freeman W.H.Publication, New York

HARRIS, J. J., BRUENING, M. L. (2000). "Electrochemical and in situ ellipsometric investigation of the permeability and stability of layered polyelectrolyte films." *Langmuir* **16**: 2006-2013.

HE, X. M., CARTER, D. C. (1992). "Atomic structure and chemistry of human serum albumin." *Nature* **358**: 209-214.

HIGUCHI, T. (1963). "Mechanism Of Sustained -Action Medication : Theoretical Analysis Of Rate Of release Of Solid Drugs DispersedIn Solid Matrices." *J. Pharm. Sci.* **52**: 1145-1149.

HINO, T., SHIMABAYASHI, S., TANAKA, M., NAKANO, M., OKOCHI, H. (2000). "Improvement of encapsulation efficiency of water- in- oil- in- water emulsion with hypertonic inner aqueous phase." *Journal of Microencapsulation* **18**: 19-28.

HO, R. M., WU, C.H., SU, A.C. (1990). "Morphology of plastic/rubber blend." *Polymer Engineering and Science* **30**: 511-519.

HSU, Y.-Y., GRESSER, J. D., STEWART, R. R., TRANTOLO, D.J., LYONS, C. M., SIMONS, G. A., GANGADHARAM, P. R. J., WISE, D. L. (1996). "Mechanism of ionized release from poly (d,l-lactide-co-glycolide) matrices prepared by dry mixing." *Journal of pharmaceutical science* **85**: 706-713.

HUANG, X., BRAZEL, C. S. (2001). "On the importance and mechanisms of burst release in matrix-controlled drug delivery systems." *Journal of Controlled Release* **73**: 121-136.

HUANG, Y.-Y., CHUNG T.-W., TZNEG, T.-W. (1999). "A method using biodegradable polylactides/polyethylene glycole for drug release with reduced initial burst." *Int. J. Pharm.* **182**: 93-100.

- HUH, K. M., LEE, S. C., CHO, Y. W., LEE, J., JEONG, J. H., PARK, K. (2005). "Hydrotropic polymer micelle system for delivery of paclitaxel." *Journal of Controlled Release* **101**: 50-68.
- HUNTER, S. K., ANDRACHI, M. E., KREIG, A. M. (2001). "Biodegradable microspheres containing group B Streptococcus vaccine: Immune response in mice." *American Journal of Obstetrics and Gynecology* **185**: 1174-1179.
- INOUE, K., YAMADA, H., IMOTO, T., AKASAKA, K. (1998). "High pressure NMR study of small proteins." *Journal of Biomolecular NMR* **12**: 525-541.
- IBRAZ, G., DAHNE, L., DONATH, E., MOHWALD, H. (2001). "Smart micro and nanocontainer for storage, transport and release. " *Advanced Materials* **13**: 1324-1327
- JABER, J. A., SCHLENOFF, J. B. (2006). "Recent developments in the properties and applications of polyelectrolyte multilayers. " *Current Opinion in Colloid & Interface Science* **11**: 324-329
- JALIL, R., NIXON J. R., (1990). "Biodegradable poly(lactide acid) and poly (lactide - co- glycolide) microcapsules - Problems associated with preparative techniques and release properties." *Journal of Microencapsulation* **7**: 297-325.
- JEONG, B., BAE, Y. H., KIM, S. W. (2000). "Drug release from biodegradable injectable thermosensitive hydrogel of PEG-PLGA-PEG triblock copolymer." *J. Control. Release* **63**: 155-163.
- JEONG, Y. I., CHEON, J. B., KIM, S. H., NAH, J. W., LEE, Y. M., SUNG, Y. K., AKAIKE, T., CHO, C. S. (1998). "Clonazepam release from core shell type nanoparticles in vitro." *Journal of Controlled Release* **51**: 169-178.

JONES, C. D., LYON, L. A. (2000). "Synthesis and characterization of multiresponsive core-shell microgels." *Macromolecules* **33**: 8301-8306.

JORDHAMO, G. M., MANSON, J. A., SPERLING, L. H. (1986). "Phase continuity and inversion in polymer blends and simultaneous interpenetrating networks." *Polymer Engineering Science* **26**: 517-524.

JU, R. T. C., NICON, P. R., PATEL, M.V. (1997). "Diffusion coefficient of polymer chains in the diffusion layer adjacent to a swollen hydrophilic matrix." *Journal of Pharmaceutical Science* **43**: 175-182.

KADER, A., JALIL, R. (1998). "In vitro release of theophylline from poly (lactide acid) sustained- release pellets prepared by direct compression. " *Drug Development and Industrial Pharmacy*. **24**: 527-534

KAKISH, H. F., TASHTOUSH, B., IBRAHIM, H. G., NAJIB, N. M. (2002). "A novel approach for the preparation of highly loaded polymeric controlled release dosage forms of diltiazem HCl and diclofenac sodium." *Eur. J. Biopharm.* **54**: 75-81.

KAIBARA, K., OKAZAKI, T., BOHIDAR H.B., DUBIN, P.L., (2000). "pH-induced coacervation in complexes of bovine serum albumin and cationic polyelectrolytes." *Biomacromolecules* **1**: 100-107

KHAN, M. Y., SALAHUDDIN, A. (1990). "Isolation , characterization and effect of pH on the unfolding-refolding mechanism of serum albumin " *Journal of Biosciences* **15**: 361 - 376.

KIM , C.-J. (2000). *Controlled release dosage form design*. Technomic published company Inc, Pensylvania, USA

KIM, H. K., PARK, T. G. (2001). "Microencapsulation of dissociable human growth hormone aggregates within poly (D,L-lactide-co-glycolide) microparticles for sustained release." *Int. J. Pharm.* **229**: 107-116.

KIM, J.-H., TALUJA, A., KNUTSON, K., HAN BAE, Y. (2005). "Stability of bovine serum albumin complexed with PEG-poly (L-histidine) diblock copolymer in PLGA microspheres." *Journal of Controlled Release* **109**: 86-100.

KISHIDA, A., MURAKAMI, K., GOTO, H., AKASHI, M., KUBITA, H., ENDO, T. (1998). "Polymer drugs and polymeric drugs ; slow release of 5-fluorouracil from biodegradable poly(gama- glutamic acid) and its benzyl ester matrices." *J. Bioact. Compat. Polym.* **13**: 270-278.

KOLHE, P., KHANDARE, J., PILLAI, O., KANNAN, S., LIEH-LAI, M., KANNAN, R. (2004). "Hyperbranched polymer-drug conjugates with high drug payload for enhanced cellular delivery." *Pharm. Res.* **21**: 2185-2195.

KWON, G. S., KATAOKA, K. (1995). "Block copolymer micelles as long-circulating drug vehicles." *Advanced Drug Delivery Reviews* **16**: 295-309.

LAIDLER, K. J. (1965). *Chemical kinetics, 2nd ed.* McGraw – Hill, New York.

LADAM, G., SCHAAF, P., DECHER, G., VOEGEL, J.C., CUISINIER J.C. (2002). "Protein adsorption onto auto-assembled polyelectrolyte. " *Biomolecular Engineering* **19**: 273-280

LANGER, R., (1998). "Drug delivery and targeting. " *Nature* **392**: 5-10

LANGNER, M., UGORSKI, M. (2000). "The macromolecular aggregate as a drug carrier." *Cellular and Molecular Biology Letters* **5**: 433-440.

LECOMTE, F., SIEPMANN, J., WALTHER, M., MACRACE, R.J., BODMEIER, R. (2005). "pH sensitive polymer blends used as a coating material to control drug release from spherical beads: Elucidation of the underlying mass transport mechanisms. " *Pharmaceutical Research* **22**: 1129-1140

LEE, T. H., WANG, J., WANG, C.-H. (2002). "Double-walled microspheres for sustained release of a highly water soluble drug: characterization and irradiation studies." *Journal of Controlled Release* **83**: 437-452.

LEO, E., SCATTURIN, A., VIGHI, E., DALPIAZ, A. (2006). "Polymeric nanoparticles as drug controlled release systems: a new formulation strategy for drugs with small or large molecular weight." *Journal of Nanoscience and Nanotechnology* **6**: 3070-3079.

LEVON, K., MARGOLINA, A., PATASHINSKY A. Z. (1993). "Multiple percolation in conducting polymer blends." *Macromolecules* **26**: 4061-4063.

LI, J., FAVIS, B. D. (2001). "Characterizing co-continuity high density polyethylene/polystyrene blends." *Polymer* **42**: 5047-5053.

LI, J. (2001). Co-continuous polymer blends.: These de Doctorat, Ecole polytechnique. Montreal

LI, J., MA, P. L., FAVIS, B. D. (2002). "The role of the blend interface type on morphology in co-continuous polymer blends." *Macromolecules* **35**: 2005-2016.

LI, S., QIAN, Z. Y., LIU, X. L., LIU, X. B. (2003). "Preparation and in vitro release of poly( butylecyanoacrylate) nanocapsules with an aqueous core containing bovine serum albumin." *ACTA Polymerica Sinica* **5**: 679-682.

LIAO, Y. C., LEE, D. J. (1997). "Slow release from coated sphere with slight deformations of coating film and drug matrix." *Journal of Pharmaceutical Science* **86**: 92-100.

LIANG, Z., SUSHA, A.S., YU, A., CARUSO, F. (2003). "Nanotubes prepared by layer-by-layer coating of porous membrane templates. " *Journal of Advanced Material* **15**: 1849-1853

LIN, D. M., KALACHANDRA, S., VALIAPARAMBI, J., OFFENBACHER, S. (2003). "A polymeric device for delivery of anti-fungal drugs in oral environment: effect of temperature and medium on the rate of drug release." *Dental Materials* **19**: 589-596.

LORENZA-LAMOSA, M. L., REMUNAN-LOPEZ, C., VILA-JATO, J. L., ALONSO, M. J. (1998). "Design of microencapsulated chitosan microspheres for clonic drug delivery." *Journal of Controlled Release* **52**: 109-118.

LOWELL, S., SHIELDS, J. E. (1991). *Powder surface area and porosity, 3rd ed.* Champman and Hall, NewYork.

LU, S., RAMIREZ, W. F., ANSETH, K. S. (1998). "Modeling and optimization of drug release from laminated polymer matrix devices." *AIChE J.* **44**: 1689-1696.

LVOV, Y. M., DECHER, G., MOHWALD, H. (2003). "Assembly, structural characterization and thermal behavior of layer-by-layer deposited ultrathin films. " *Langmuir* **9**: 481-486

LYNGAAE-JORGENSEN, J., Utracki, L. A. (1991). "Dual phase continuity in polymer blends." *Makromolekular Chemie-Macromolecular Symposia* **48/49**: 189-209.

LYNGAAE-JORGENSEN, J., RASMUSSEN, K. L., CHTCHERBAKOVA, E. A. , UTRACHI, L. A. (1999). "Flow induced deformation of dual-phase continuity in polymer blends and alloys. part 1." *Polymer Engineering and Science* **39**: 1060-1071.

MACGREGOR, R. B. (1998). "Effect of hydrostatic pressure on Nucleic Acids." *Biopolymers (Nucleic Acid Sciences)* **48**: 253-263.

MAEDA, H., OHASHI, E., SANO, A., KAWASKI, H., KUROSAKI, Y. (2003). "Investigation of the release behavior of a covered-rod-type formulation using silicon. " *Journal of controlled release* **90**: 59-70

MAHATO, R. I. (2005). *Biomaterials for delivery and targeting of proteins and nucleic acids*, CRC press, USA.

MARABOTTI, A., HERMAN, P., STAIANO, M., VARRIALE, A., CHAMPDORE, M., ROSSI, M., GRZYCZYNSKI, Z., D'AURIA, S. (2006). "Pressure effect on the stability and conformational dynamics of the D-Glucose/D Glucose binding protein." *Proteins: Structure, Function, and Bioinformatics* **62**: 193-201.

MARININA, J., SHENDEROVA, A., MALLERY, S.R., SCHWENDEMAN, S. P. (2000). "Stabilization of vinca alkaloids encapsulated in poly (lactide-co-glycolide) microspheres." *Pharm. Res.* **17**: 677-683.



MARTINI, L. G., COLES, M., GRAVELL, K., STEPHENSON, S., THOMSON, C. M. (2000). "The use of hydrophobic matrix for the sustained release of a highly water soluble drug." *Drug Development and Industrial Pharmacy* **26**: 79-83.

MASON, N., THIES, C., CICERO, T. J. (1976). "In-vivo and in vitro evaluation of microencapsulated narcotic antagonist." *J. Pharm. Sci.* **65**: 847-850.

MATHIEWWITZ, E., AMATO, C., DOR, P., LANGER, R. (1990). "Polyanhydride microspheres .3. morphology and characterization of systems made by solvent removal." *Polymer* **31**: 547-555.

MATHIOWWITZ, E., KREITZ, M. R., BRANNON-PEPPAS, L. (1999). *Encyclopedia of controlled drug delivery* John Wiley & Sons, Inc. New York,

MATOS, M., FAVIS, B. D. (1995). "Interfacial modification of polymer blends- the emulsification curve: 1. Influence of molecular weight and chemical composition of the interfacial modifier." *Polymer* **36**: 3899-3907.

MATSUDOMI, N., OSHITA, T., KOBAYASHI, K., KINSELLA, J. E. (1993). "Alpha – lactalbumin enhances the gelation properties of bovine serum albumin." *J. Agric. Food Chem.* **41**: 1053-1057.

MATSUMOTO A., MATSUKAWA, Y., SUZUKI, T., YOSHINO, H. (2005). "Drug release characteristics of multi-reservoir type microspheres with poly (DL-lactide-co-glycolide) and poly (DL-lactide). " *Journal of Controlled Release* **106**: 172-180

MCALONEY, R. A., SINYOR, M., DUDNIC, V., GOH, C. (2001). "Atomic force microscopy studies of salt effects on polyelectrolyte multilayer film morphology." *Langmuir* **17**: 6655-6663.

MCCARTHY, A. N., GRIGERA, J. R. (2006). "Effect of pressure on the conformation of proteins. A molecular dynamics simulation of lysozyme." *Journal of Molecular Graphics and Modelling* **24**: 254-261.

MEKHILEF, N., VERHOOGT, H. (1996). "Phase inversion and dual-phase continuity in polymer blends: theoretical prediction and experimental results." *Polymer* **37**: 4069-4077.

MEKHILEF, N., FAVIS, B. D., CARREAU, P. J. (1997). "Morphological stability, interfacial tension, and dual- phase continuity in polystyrene-polyethylene blends." *Journal of Polymer Science Part B - Polymer Physics* **35**: 293-308.

Miles, I. S., Zurek, A. (1988). "Preparation, structure and properties of two-phase co-continuous polymer blends." *Polymer Engineering and Science* **28**: 796-805.

MOZHAEV, V. V., HEREMANS, A., FRANK, J., MASSON, P., BALNY, C. (1996). "High pressure effects on protein structure and function." *Proteins: Structure, Function, and Genetics* **24**: 81-91.

NARA, E., MASEGI, M., HATONO, T., HASHIDA, M. (1992). "Pharmacokinetics analysis of drug adsorption from muscle based on a physiological diffusion model: effect of molecular size on absorption." *Pharmaceutical Research* **9**: 161-168.

NARASIMHAM, B., LANGER, R. (1997). "On the importance of the burst effect during drug release from polymer films." *Polym. Mater. Sci. Eng. Proc.* **76**: 558-569.

NARASIMHUN, B. (2001). "Mathematical models describing polymer dissolution: consequences for drug delivery." *Advanced drug delivery reviews* **48**: 195-210.

NUWAYSER, E. S., NUSEFORA, W. A. (1986). US patent

OKADA, H. (1997). "One- and three-month release injectable microspheres of LH-RH superagonist leuporelin acetate", *Adv. Drug Delivery Rev.* **28**: 43-70

OKUMURA, K., MIYAKE, Y., TAGUCHI, H., SHIMABAYASHI, Y. (1990). "Formation of stable protein foam by intermolecular disulfide cross-linkages in thiolated  $\alpha$ , $\beta$ -Casein as a Model." *J. Agric. Food Chem.* **38**: 1303-1306.

OTSUKA, M., TOKUMITSU, K., MATSUDA, Y. (2000). "Solid dosage form preparations from oily medicines and their drug release. Effect of degree of surface-modification of silica gel on the drug release from phytonadione-loaded silica gels. " *Journal of Controlled Release* **67**: 369-384

OWUSUABABIO, G., ROGERS, J. A. (1996). "Formulation and release of ciprofloxacin from poly (L-lactic acid) microparticles. " *European Journal of Pharmaceutics and Biopharmaceutics* **42**: 188-192

PARK, T. G., COHEN, S., LANGER, R. (1992). "Controlled protein release from polyethyleneimine-coated poly(L-lactide acid)/pluronic blends matrices." *Pharm. Res.* **9**: 37-39.

PEKAREK, K. J., JACOB, J. S., MATHIOWITZ, E. (1994b). "Double-walled polymer microspheres for controlled drug release." *Nature* **367**: 258-260.

PEKAREK, K. J., JACOB, J. S., MATHIOWITZ, E. (1994a). "One step preparation of double-walled microspheres." *Adv. Mater.* **6**: 684-686.

- PEREZ-RODRIGUEZ, C., MONTANO, N., GONZALEK, K., GRIBENOW, K. (2003). "Stabilization of alfa-chymotrypsin at the CH<sub>2</sub>Cl<sub>2</sub>/water interface and upon water- in-oil- in- water encapsulation in PLGA microspheres." *Journal of Controlled Release* **89**: 71-85.
- PETERS, T. J. (1985). "Serum Albumin." *Adv. protein Chem.* **37**: 161-245.
- PILLAY, V., FASSIHI, R. (1998). "Evaluation And Comparison Of Dissolution Data Derived From Different Modified Release Dosage Forms: An Alternative Method." *Journal of Controlled Release* **55**: 45-55.
- PISTEL, K.-F., KISSEL, T. (1999). "Effects of salt addition on the microencapsulation of proteins using W/O/W double emulsion technique." *Journal of Microencapsulation* **17**: 467-483.
- POLISHCHUK, A. Y., ZAIKOV, G. E., (1997). *Multicomponent transport in polymer systems for controlled release*. Publishers Association, Amesterdam.
- POOLE, S., WEST, S. I., FRY, J. C. (1987). "Effects of basic proteins on the denaturation and heat-gelation of acidic proteins." *Food Hydrocolloids* **1**: 301-316.
- POTSCHKE, P., PAUL, D. R. (2003). "Formation of co-continuous structures in melt-mixed immiscible polymer blends." *Journal of Macromolecular Science* **C43**: 87-141.
- QUI, L. Y., BAE, Y. H. (2006). "Polymer architecture and drug delivery." *Pharm. Res.* **23**: 1-30.
- RAHMAN, N. A., MATHIOWITZ, E. (2004). "Localization of bovine serum albumin in double-walled microspheres." *Journal of Controlled Release* **94**: 163-175.

- RE, M. I. (1998). "Microencapsulation by spray drying." *Drying Technology* **16**: 1195-1236.
- ROBINSON , J. R. (1997). *Controlled drug delivery; challenges and strategies*. Oxford University Press, England.
- ROY, X. (2004). Fabrication de substrats ultra-poreux a partir de melanges de polymeres. Montreal: These de Maitrise, Ecole polytechnique.
- ROY, X., SARAZIN, P., FAVIS, D. B. (2006). "Ultraporous nanosheath materials by layer-by-layer deposition onto co-continuous polymer blend templates." *Advanced Materials* **18**: 1015-1019.
- RUEGG, M., MOOR, U., BLANC, B. (1977). "A calorimetric study of thermal denaturation of whey proteins in simulated milk ultrafiltrate." *J. Dairy Res.* **44**: 509-520.
- SAH, H. K., TODDYWALA, R., CHIEN, Y.W. (1994). "The influence of biodegradable microcapsule formulations on the controlled release of a protein." *Journal of Controlled Release* **30**: 201-211.
- SANDOR, M., ENSCORE, D., WESTON, P., MATHIOWITZ, E. (2001). "Effect of protein molecular weight on release from micron-sized PLGA microspheres." *Journal of Controlled Release* **76**: 297-311.
- SARAZIN, P., FAVIS, B. D. (2003). "Morphology control in co-continuous poly (L-lactide)/polystyrene blends: a route towards highly structured and interconnected porosity in poly (L-lactide) materials." *Biomacromolecules* **4**: 1669-1679.

SARAZIN, P. (2003). Substrats poreux biodégradables préparés à partir de phase co-continues dans les mélanges de polymères immiscibles. Montréal: Thèse de Doctorat, Ecole Polytechnique.

SARAZIN, P., ROY, X., FAVIS, B. D. (2004). "Controlled preparation and properties of porous poly (L-lactide) obtained from co-continuous blend of two biodegradable polymers." *Biomaterials* **25**: 5965-5978.

SCHLENOFF, J. B., LY, H., LI, M. (1998). "Charge and mass balance in polyelectrolyte multilayer." *Journal of American Chemical Society* **120**: 7626-7634.

SCHLENOFF, J. B., DUBAS, S. (2001). "Mechanism of polyelectrolyte multilayer growth: charge overcompensation and distribution." *Macromolecules* **34**: 592-598.

SCHLENOFF, L., H., LI, M. (1998). "Charge and mass balance in polyelectrolyte multilayers." *Journal of American Chemical Society* **120**: 7626-7634.

SCHOELER, B., KUMARASWAMY, G., CARUSO, F. (2002). "Investigation of the influence of polyelectrolyte charge density on the growth of multilayer thin films prepared by the layer-by-layer technique." *Macromolecules* **35**: 889-897.

SEOW, W. Y., XUE, J. M., (2007). "Targeted and intracellular delivery of paclitaxel using multi-functional polymeric micelles." *Biomaterials* **28**: 1730-1740.

SHAHIDI, F., HAN, X. Q. (1993). "Encapsulation of food ingredients." *Critical Reviews in Food Science and Nutrition* **33**: 501-547.

SHENEY, D. B., SUKHORUKOV, G. B. (2004). " Engineered microcrystals for direct surface modification with layer-by-layer technique for optimized dissolution. " *Eur. J. Phar. Biopharm* **58**: 521-527.

SIEPMANN, J., LECOMTE, F., BODMEIER, R. (1999). "Diffusion- controlled drug delivery systems: calculation of the required composition to achieve desired release profiles." *Journal of Controlled Release* **60**: 379-389.

SIGMA-ALDRICH. "Sigma-Aldrich product information sheet (A 7248)." from [http://www.sigmaaldrich.com/sigma-aldrich/product\\_information\\_sheet/a7284pis.pdf](http://www.sigmaaldrich.com/sigma-aldrich/product_information_sheet/a7284pis.pdf).

SILVA, J. L., SILVERIA, C. F., CORREIA, A., PONTES, L. (1992). "Dissociation of a native dimer to molten globule monomer -effects of pressure and dilution on the association equilibrium " *Journal of Molecular Biology* **223**: 545-555.

SILVA, J. L., FOGUEL D., ROYER C. A. (2001). "Pressure provides new insights into protein folding, dynamics and structure." *Trends in Biochemical Sciences* **26**: 612-618.

SINHA, V. R., KUMRIA, R. (2001). "Colonic drug delivery: Prodrug approach" *Pharmaceutical Research* **18**: 557-564.

SKOOG, D. A., HOLLER, N. (2004). *Principals of instrumental analysis*. Brooks/cole, Stanford.

SOOD, A., PANCHAGNULA, R. (1999). "Role of dissolution studies in controlled release drug delivery systems." *STP Pharma. Sci.* **9**: 157-168.

SPARKS, R. E., JACOBS, I. C., MASON, N. S., in AVIS, K. E., SHUKLA, A. J., CHANG, R.-K., eds (1999). *Pharmaceutical unit operations: Coating*. Buffalo Grove, Interpharm Press, USA.

SPARNACCI, K., LAUS, M., TONDELLI, L., MAGNANI, L., BERNARDI, C. (2002). "Core-shell microspheres by dispersion polymerizations drug delivery system." *Macromol. Chem. Phys.* **203**: 1364-1369.

STAMLER, J. S., SINGEL, D. J., LOSCALZO, J. (1992). "Biochemistry of nitric oxide and its redox -activated forms." *Science* **258**: 1898-1902.

SUKHORUKOV, G. B., DONATH, E., LICHTENFELD, H., KNIPPLE, E., KNIPPLE, M., BUDDE, A., MOHWALD, H. (1998b). "Layer-by-Layer self-assembly of polyelectrolytes on colloidal particles." *Colloids and Surfaces A: Physiochemical and Engineering Aspects* **137**: 253-266.

SUKHORUKOV, G. B., DONATH, E., LICHTENFELD, H., CARUSO, F., POPV, V. I., MOHWALD, H. (1998a). "Stepwise polyelectrolyte assembly on particle surfaces: a novel approach to colloid design." *Polymer for Advanced Technologies* **9**: 759-767.

SUNDARARAJ, U., MACOSKO, C. W. (1995). "Drop breakup and coalescence in polymer blends: the effects of concentration and compatibilization." *Macromolecules* **28**: 2647-2657.

SUTTON, D., DURANT, R., SHUAI, X., GAO, J. (2006). "Poly (L-lactide-co-glycolide)/ poly (ethylenimine) blend matrix systems for pH sensitive drug delivery. " *Applied Polymer Science* **100**: 89-96



TAI, H. C. (2004). X-ray crystallographic studies of bovine serum albumin and Helicobacter Pylori Thioredoxin-2. Department of Chemistry, University of Saskatchewan.

TAN, W.-C., WU, W.-Y., YAN, Z.-Y., WEN, G.-B. (2001). "Moving Boundary Problem For Diffusion Release of Drug From A Cylinder Polymeric Matrix." *Applied Mathematics and Mechanics* **22**: 379-384.

TCHOUDAVOC, R., BREUER, O., NARKIS, M., SIEGMANN, A. (1996). "Conductive polymer blends with low carbon black loading: polypropylene/polyamide." *Polymer Engineering and Science* **36**: 1336-1346.

THIES, C., in DONBROW, M. ed. (1992). Microcapsules and Nanoparticles in medicine and pharmacy. CRC Press, Boca Raton, Fla.

THOMASIN, C., CORRADIN, G., MEN, Y., MERKLE, H. P., GANDER, B. (1996). "Tetanus toxoid and synthetic malaria antigen containing poly (lactide)/poly (lactide-co-glycolide) microspheres: importance of polymer degradation and antigen release for immune response." *Journal of Controlled Release* **41**: 131-145.

TILTON, R. F., DEWAN J.C., PETSKE, G.A. (1992). "Effects of temperature on protein structure and dynamics: x-ray crystallographic studies of the protein at nine different temperatures from 98 to 320 K." *Biochemistry* **31**: 2469-2481.

TOJO, K., NAKAGAWA, K., MORITA, Y., OHTORI, A. (1999). "A pharmacokinetics model of intravitreal delivery of ganciclovir." *European Journal of Pharmaceutics and Biopharmaceutics* **47**: 99-104.

TOJO, K., ISOWAKA, A. (2001). "Pharmacokinetics model for in vivo/in vitro correlation of intravitreal drug delivery." *Adv. Drug Delivery Rev.* **52**: 17-24.

TORCHILIN, V. P., (200). "Block copolymer micelles as a solution for drug delivery problems." *Expert Opinion on Therapeutic Patents* **15**: 63-75

TU, R. S., BREESVELD, V. (2005). "Microrheological detection of protein unfolding." *Physical Review E*. **72**(041914).

TUOVINEN, L., PELTONEN, S., LIIKOLA, M., HOTAKAINEN, M., LAHTELA-KAKKONEN, M., POSO, A., JARVINEN, K. (2004). "Drug release from starch-acetate microparticles and films with and without incorporated alpha-amylase." *Biomaterials* **25**: 4355-4362

UNIVERSITY, M. A. (Winter 2005). *Protein biochemistry*. Biochemistry program, Department of biology, Access year: 2006.

UTRACKI, L. A. (1991). "On the viscosity - concentration dependance of immiscible polymer blends." *Journal of Rheology* **35**: 1615-1637.

VASIR, J. K., TAMBWEKAR, K., GARG, S. (2003). "Bioadhesive microspheres as controlled drug delivery systems." *International Journal of Pharmaceutics* **255**: 13-32.

VASUDEV, S. C., CHANDY, T., SHARMA, C. P. (1997). "Development of chitosan/polyethylene vinyl acetate co-matrix : controlled release of aspirin- heparin of preventing cardiovascular thrombosis." *Biomaterials* **18**: 375-381.

VERHOOGT, H., VAN DAM, J., POSTHUMA DE BOER, A. (1994). "*Morphology-processing relationship in interpenetrating polymer blends*". American Chemical Society Washington.

VYAS S. P., SIHORKAR, V., MISHRA, V. (2000). "Controlled and targeted drug delivery strategies toward intraperiodontal pochet disease. " *Journal of clinical pharmacy and therapeutics*, **25**: 21-42

WANG, J. J., CHUA, K. M., WANG, C. H. (2004). " stabilization and encapsulation of human immunoglobulin G into biodegradable microspheres." *Journal of colloid and interface science* **271**: 92-101.

WANG, Q., DU, Y.-M., FAN, L.-H. (2005). "Properties of chitosan/poly(vinyl alcohol) films for drug controlled release. " *Journal of Applied Polymer Science* **96**: 808-813

WASHBURN, E. W. (1921). "Note on a method of determining pore size in a porous material." *Proc. Nat. Acad. Sci.* **7**: 115-116.

WATTS, P. J., DAVIES, M.C., MELIA, C.D. (1990). "Microencapsulation using emulsification solvent evaporation - a review of techniques and applications." *Critical Reviews in Therapeutic Drug Carrier Systems* **7**: 235-259.

WENDEL, S., CELIK, M. (1997). "An overview of spray-srying applications Pharmaceutical. " *Technology* **21**: 124-156

WETZEL, R., BECKER, M., BEHLKE, J., BILLWITZ, H., BOHM, S., EBERT, B., HAMANN, H., KRUMBIEGEL, J., and LASMANN, G. (1980). "Temperature behavior of human serum albumin." *Eur. J. Biochem.* **104**: 469-478.

WHEATLEY, M. A., CHANG, M., PARK, E., LANGER, R. (1991). "Coated alginate microspheres: factors influencing the controlled delivery of macromolecules." *Pharm. Res.* **9**: 37-39.

WILLEMSE, R. C., POSTHUMA DE BOER, A., VAN DAM, J., et GOTSIS, A.D. (1998). "Co-continuous morphologies in polymer blends: a new model." *Polymer* **39**: 5879-5887.

WILLEMSE, R. C., POSTHUMA DE BOER, A., VAN DAM, J., et GOTSIS, A.D. (1999). "Co-continuous morphologies in polymer blends: the influence of interfacial tension." *Polymer* **40**: 827-834.

WILLIS, J. M., FAVIS, B.D. (1988). "Processing morphology relationship of compatibilized polyolefin/polyamide blends. part1: the effect of an ionomer compatibilizer on blend morphology." *Polymer Engineering and Science* **28**: 1416-1426.

XIA, J., DUBLIN, P.L., KOKUFUTA, E., HAVEL, H., MUHOBERAC, B.B. (1999). "Light scattering, Cd, and ligand binding studies of ferrihemoglobin-polyelectrolyte complexes." *Biopolymers* **2**: 153-161

YANG, K., HAN, C. D. (1996). "Effects of shear flow and annealing on the morphology of rapidly precipitated immiscible blends of polystyrene and polyisoprene." *Polymer* **37**: 5795-5805.

YANG, Y.-Y., CHING, T.-S., BAI, X.-L., CHAN, W.-K. (2000). "Effect of preparation condition on morphology and release profiles of biodegradable polymeric microspheres containing protein fabricated by double-emulsion method." *Chem. Eng. Sci.* **55**: 2223-2236.

YANG, Y.-Y., SHI, M., GOH, S.-H., MOOCHHALA S.-M., NG, S., HELLER, J. (2003). "PEO/PLGA microspheres: formation and in vitro behavior of double -walled microspheres." *Journal of Controlled Release* **88**: 201-213.

YU, M.-A., DAMODARAN, S. (1991). "Kinetics of protein foam destabilization: evaluation of a method using bovine serum albumin." *J. Agric. Food Chem.* **39**: 1555-1562.

YUAN, Z., FAVIS, B. D. (2004). "Macroporous poly (L-lactide) of controlled pore size derived from the annealing of co-continuous polystyrene/poly (L-lactide) blends." *Biomaterials* **25**: 2161-2170.

ZHU, G., SCHWENDEMAN, S. P. (2000). "Stabilization of proteins encapsulated in cylindrical poly (lactide-co-glycolide) implants: mechanism of stabilization by basic additives." *Pharm. Res.* **17**: 351-357.

ZHU, G., MALLERY, S. R., SCHWENDEMAN, S. P. (2000). "Stabilization of proteins encapsulation in injectable poly (lactide-co-glycolide)." *Nature Biotechnology* **18**: 52-57.

ZHU, Y. F. SHI, J. L. LI, Y. S. CHEN, H., R., SHEN, W. H. DONG, X. P. (2005). "Storage and release of ibuprofen drug molecules in hollow mesoporous silica spheres with modified pore surface. " *Microporous and Mesoporous Materials* **85**: 75-81

ZHANG, H., KIM, Y., DUTTA, P. K. (2006). "Controlled release of paraquat from surface modified zeolite Y. " *Microporous and Mesoporous Materials* **88**: 312-318

## **APPENDIX A**

### **LOADING THE POROUS POLYMER WITH BSA**

#### **Loading Protocol**

- Wash the test tubes completely and dry them
- Weigh the capsules of porous polymer
- Fill the test tubes with BSA at desired concentration (15%)
- Immerse each capsule into the BSA
- Apply the vacuum for 30 minutes
- Release the vacuum and keep the system at room pressure for few minutes
- Stir and mix the samples inside BSA
- Put the samples under pressure (40-60-80 atm) for 15 minutes
- Release the pressure and keep the system at room pressure for few minutes
- Stir and mix the samples inside BSA
- Put the samples under the same pressure as before, for 15 minutes
- Release the pressure and keep the system at room pressure for few minutes
- Stir and mix the samples inside BSA
- Apply the vacuum on the samples for 45 minutes
- Release the vacuum and keep the system at room pressure for few minutes
- Stir and mix the samples inside BSA
- Put the samples under pressure for 15 minutes
- Release the pressure and keep the system at room pressure for few minutes
- Stir and mix the samples inside BSA
- Again apply the pressure on the samples for 15 minutes
- Release the pressure and keep the system at room pressure for few minutes
- Stir and mix the samples inside BSA

- Apply the vacuum on the samples this time for 60 minutes
- Release the vacuum and keep the system at room pressure for few minutes
- Stir and mix the samples inside BSA
- Put the samples under pressure for 15 minutes
- Release the pressure and keep the system at room pressure for few minutes
- Stir and mix the samples inside BSA
- Apply the final vacuum on the samples for 30 minutes
- Release the pressure and keep the system at room pressure for few minutes
- Bring out the polymer capsules from test tubes
- Wash the surface of the capsules with Milli-Q water
- Dry the capsules under vacuum oven at 40-45 °C since the weight of samples become constant
- Weight the final mass of the capsules
- Calculate the loading percentage of BSA

## **APPENDIX B**

### **LOADING THE POROUS POLYMER WITH POLYELECTROLYTE**

#### **Loading Protocol**

- Wash the test tubes completely and dry them
- Weigh the capsules of porous polymer
- Fill the test tubes with polyelectrolyte solution at desired concentration (10 mg/ml)
- Immerse each capsule into the polyelectrolyte
- Apply the vacuum for 30 minutes
- Release the vacuum and keep the system at room pressure for few minutes
- Stir and mix the samples inside polyelectrolyte
- Put the samples under pressure (60 atm) for 15 minutes
- Release the pressure and keep the system at room pressure for few minutes
- Stir and mix the samples inside polyelectrolyte
- Put the samples under the same pressure as before, for 15 minutes
- Release the pressure and keep the system at room pressure for few minutes
- Stir and mix the samples inside polyelectrolyte
- Apply the vacuum on the samples for 45 minutes
- Release the vacuum and keep the system at room pressure for few minutes
- Stir and mix the samples inside polyelectrolyte
- Put the samples under pressure for 15 minutes
- Release the pressure and keep the system at room pressure for few minutes
- Stir and mix the samples inside polyelectrolyte
- Again apply the pressure on the samples for 15 minutes
- Release the pressure and keep the system at room pressure for few minutes
- Stir and mix the samples inside polyelectrolyte



- Apply the vacuum on the samples this time for 60 minutes
- Release the vacuum and keep the system at room pressure for few minutes
- Stir and mix the samples inside polyelectrolyte
- Put the samples under pressure for 15 minutes
- Release the pressure and keep the system at room pressure for few minutes
- Stir and mix the samples inside polyelectrolyte
- Apply the final vacuum on the samples for 30 minutes
- Release the pressure and keep the system at room pressure for few minutes
- Bring out the polymer capsules from test tubes
- Wash the capsules with Milli-Q water for 4 hours under constant shaking (refresh water each hour)
- Dry the capsules under vacuum oven at 50-60 °C since the weight of samples become constant
- Weigh the final mass of the capsules
- Calculate the loading percentage of polyelectrolyte
- Start loading another polyelectrolyte layer following the same procedure
- After loading sufficient layers, load BSA following the same protocol

## APPENDIX C

### “F” FACTOR ESTIMATION TABLE

Table A.1. Estimation table of protein concentration by UV absorbance (Mount Allison University, 2002).

<b>R (280/260)</b>	<b>Nucleic Acid , %</b>	<b>F</b>
1.75	0.00	1.116
1.63	0.25	1.081
1.52	0.50	1.054
1.40	0.75	1.023
1.36	1.00	0.994
1.30	1.25	0.970
1.25	1.50	0.944
1.16	1.75	0.809
1.09	2.00	0.852
1.03	2.50	0.814
0.979	3.00	0.776
0.939	3.50	0.743
0.874	4.00	0.682
0.846	5.00	0.656
0.822	6.00	0.632
0.784	7.00	0.585
0.753	8.00	0.545
0.730	9.00	0.508
0.705	10.00	0.478
0.644	14.00	0.377
0.595	20.00	0.278

## APPENDIX D

### BSA INSTABILITY DURING THE RELEASE TESTS

Figure A.1 shows the BSA instabilities within the BSA release experiments. As we came closer to the end of the experiment, a fluctuation in the BSA concentration can be observed. This fluctuation results from BSA instabilities in the release medium caused by the very small amount of release compared to the water evaporation from the cell.

BSA instability makes it difficult to have an accurate final point for the release curve. In order to know the final concentration of BSA in the release medium, the indirect method (weighing dry sample before and after release test) was used.

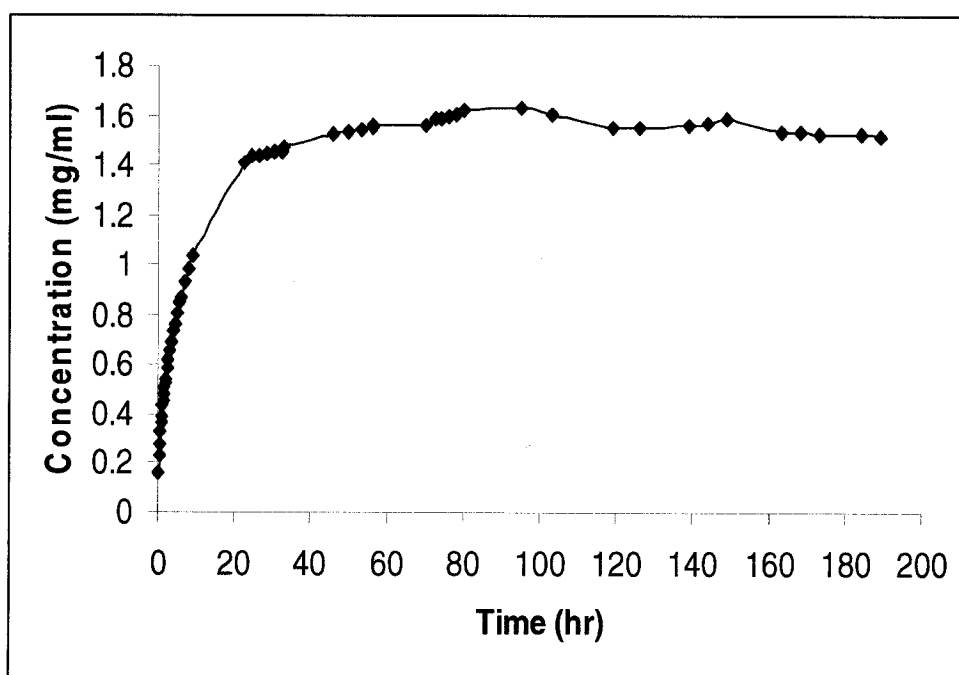


Figure A.1 Instability in BSA release profile

## APPENDIX E

### EFFECT OF CHARGE ON BSA RELEASE

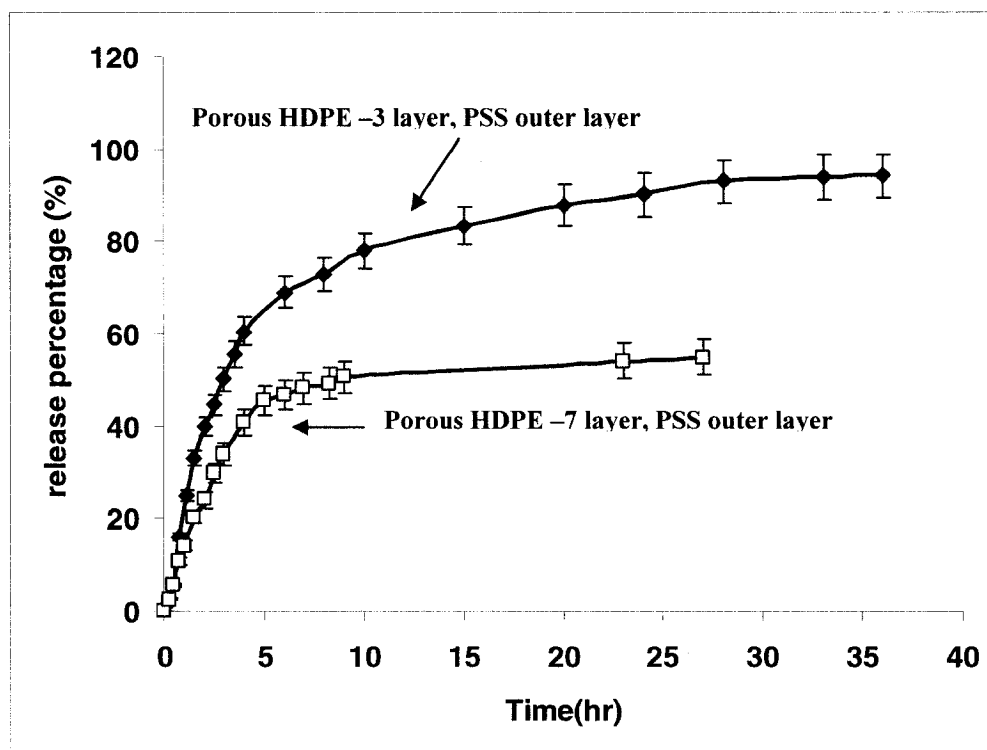
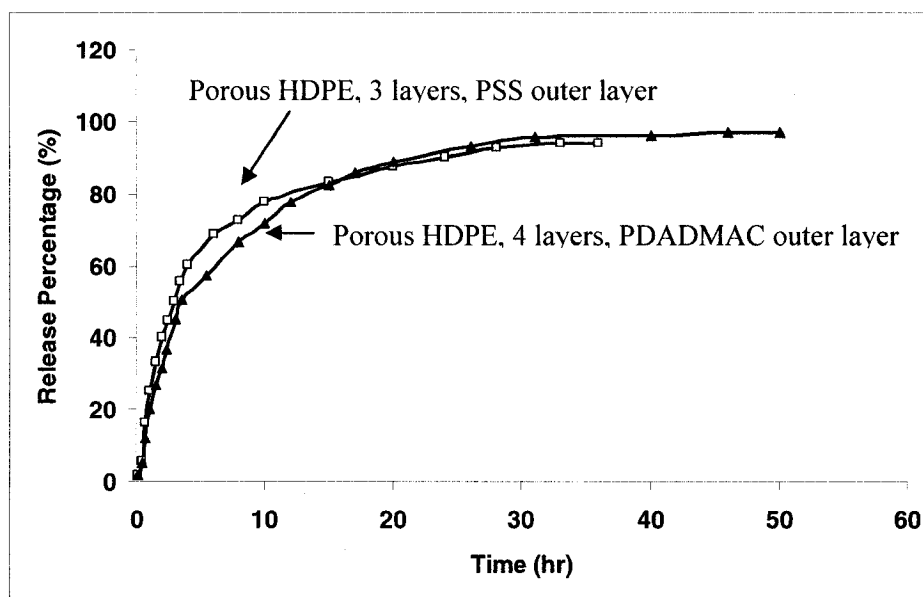


Figure A.2 Drug release profile a) Porous HDPE of 0.63  $\mu\text{m}$ , HDPE/PSS/PDADMAC/PSS/BSA (♦), HDPE/PSS/PDADMAC/...7layer/BSA (□)

Porous HDPE carriers of 3 and 4 layers polyelectrolyte and 7 and 8 layers of polyelectrolyte were compared to each other. Results are shown in the following diagrams. No considerable differences in release profile can be observed between 3-layer and 4-layer treatment and 7 and 8 layers of treatment especially in burst release. Slower release rate for a positive outermost layer, are shown. It is known that last layer's charge have control over the organization of multilayer buildup of BSA. Having a positively charged polyelectrolyte in last layer is responsible for thicker and more organized multilayer of BSA and therefore more stable attachment of BSA to the polyelectrolyte surface which finally leads to a delayed BSA diffusion. However this assumption requires more thoroughly investigation in case of porous carriers.

a)



b)

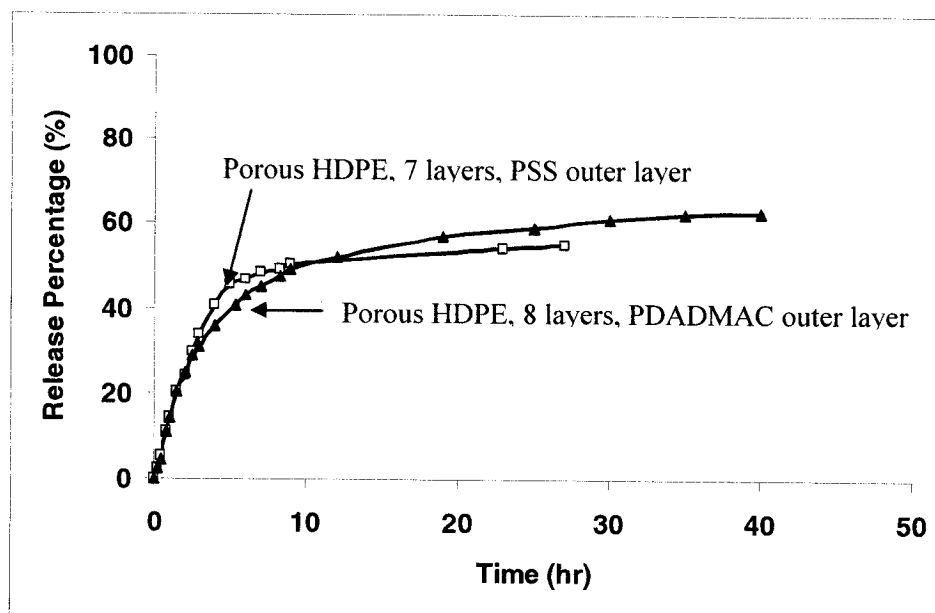


Figure A.3 Release behavior comparison of Porous HDPE samples with  $0.63\mu\text{m}$  a) Release behavior comparison between 3 layers of treatment and negative outermost layer ( $\square$ ), and 4 layers of polyelectrolyte treatment with positive outermost layer ( $\blacktriangle$ ). b) Release comparison between 7 layers of treatment with negative outermost layer ( $\square$ ) and 8 layers of polyelectrolyte with positive outermost layer ( $\blacktriangle$ ).